Diss. ETH No. 18846

High pressure crystal growth, thermodynamics and physical properties of $Al_xGa_{1-x}N$ semiconductors

A dissertation submitted to the

EIDGENÖSSISCHE TECHNISCHE HOCHSCHULE ZÜRICH

for the degree of

Doctor of Sciences

presented by

ANDREY BELOUSOV

Master of Physics, State Technological University

"Moscow Institute of Steel and Alloys" (MISIS), Moscow

Dipl. -Ing, TU Bergakademie Freiberg, Germany

born November 23, 1979

citizen of Barvikha, Russia

accepted on the recommendation of

Prof. Dr. Bertram Batlogg, examiner

Dr. Janusz Karpinski, co-examiner

Dr. hab. Izabella Grzegory, co-examiner

Zurich, 2010

This work is dedicated to Violeta and my parents, Alexander and Nadezhda.

Contents

Summary

The rapid development in the field of nitrides, particularly (Al,Ga)N system, in the past decade has become of technical significant due to their optical and electrical properties. (Al,Ga)N is characterized by its wide band gap, which can be tuned by the Al content, from 3.4 eV to 6.2 eV. Despite the technical applications of (Al,Ga)N in thin film form, only a few studies dealing with the synthesis of bulk (Al,Ga)N crystals have been reported because of some significant challenges. The target of the research in this work is mainly the synthesis of (Al,Ga)N bulk crystals under high nitrogen pressure as well as the investigation of their properties in relation to the growth conditions.

This thesis work addresses and answers the question of how to grow (Al,Ga)N bulk single crystals from solution. As a main result, we demonstrated reproducible (Al,Ga)N growth using high pressure solution growth method (HPSG) in a self-constructed gas autoclave. After a general introduction of the basic aspects of III-nitride synthesis from solution, we briefly present our high pressure techniques used in this study: a high nitrogen pressure gas autoclave and a cubic anvil cell.

From the solution in Al/Ga melt under high nitrogen pressure (2.5-10 kbar) und at high temperature (1425-1780 °C), we have been able to grow (Al,Ga)N bulk single crystals with an Al content in the range from 0.22 to 0.91. We have used Ga metal as the solvent and we have introduced an appropriate amount of Al in the form of pre-reacted polycrystalline (Al,Ga)N or AlN pellets. The growth process was optimized, yielding (Al,Ga)N crystals up to 0.8x0.8x0.8 mm^3. We found that (Al,Ga)N crystals could be grown by choosing the appropriate pressure and temperature conditions, selected below the GaN equilibrium line. Moreover, the Al composition in the growing crystals can be selected by the proper choice of p-T conditions. Further studies with different Al sources such as Al metal, pre-reacted polycrystalline (Al,Ga)N or AlN tablets showed that using (Al,Ga)N helps to avoid the formation of an AlN capping layer on the melt surface and the AlN combustion reaction. By contrast, by adding Al metal into the melt (up to 0.4 at%) resulted in a growth of very small (Al,Ga)N crystals and Al_2O_3 crystals as by-product. Larger amount of Al (up to 30 at%) leads to AlN combustion. The crystals were mainly characterized by laser ablation inductively coupled plasma mass spectrometry (LA-ICP-MS) and X-ray diffraction. We pay an essential attention to the composition homogeneity of the crystals and its crystallographic analysis. Importantly, it was

demonstrated that an about 1-μm-thick, inhomogenously substituted (Al,Ga)N capping layer with various Al content was formed on the crystal surface. It was noted that the Al composition of this layer depends on the cooling profile.

The growth results allowed us to study the thermodynamics and the p-T-x equilibrium phase diagram of (Al,Ga)N system. Based on the experimental p-T growth conditions the standard Gibbs free energy, the enthalpy and entropy of formation of the (Al,Ga)N system were estimated for temperatures of up to 1800 °C and up to 30 kbar pressure. Furthermore, knowing the thermodynamic functions allowed us to determine the p-T and x-T phase diagrams for extended parameter ranges. For instance, in the p-T phase diagram, the equilibrium lines between (Al,Ga)N(s) and Al/Ga(l) + N_2(g) for various Al composition in the crystals were calculated.

Zusammenfassung

Die rasante Entwicklung auf dem Gebiet der Nitride, insbesondere der (Al,Ga)N Verbindung, in den letzten Jahrzehnten gewann dank ihrer optischen und elektrischen Eigenschaften eine technische Bedeutung. (Al,Ga)N zeichnet sich durch eine breite Bandlücke aus, die je nach Al-Gehalt von 3.4 eV bis 6.2 eV variiert werden kann. Trotz den interessanten Anwendungen wurden bisher nur wenige Studien über die Synthese von (Al,Ga)N Kristallen publiziert, weil diese einige bedeutende Herausforderungen stellt. Das Ziel der Forschung in dieser Arbeit ist vor allem die Synthese von (Al,Ga)N Kristallen unter hohem Stickstoffdruck sowie die Untersuchung ihrer Eigenschaften in Bezug auf die Wachstumsbedingungen.

Diese Dissertationsarbeit stellt und beantwortet die Frage, wie (Al,Ga)N Einkristalle aus der Schmelze gezüchtet werden können. Als ein Hauptresultat haben wir ein reproduzierbares Züchten von (Al,Ga)N Kristallen aus einer Schmelze unter hohem Druck (HPSG) in einem selbst konstruierten Gasautoklav demonstriert. Nach einer allgemeinen Einführung zu den grundlegenden Aspekten der III-Nitriden Synthese aus der Schmelze, beschreiben wir kurz die Hochdruckanlagen, die in dieser Arbeit verwendet wurden: den Stickstoff Hochdruck Gasautoklav und die kubische Druckzelle.

Aus der Al/Ga Schmelze konnten wir (Al,Ga)N Einkristalle mit einem Al-Gehalt im Bereich von 0.22 bis 0.91 unter hohem Stickstoffdruck (2.5-10 kbar) und bei hoher Temperatur (1425-1780 °C) synthetisieren. Wir haben Ga Metall als Schmelze verwendet und die entsprechende Al Menge in der Form vom vorsynthetisierten polykristallinen (Al,Ga)N oder AlN Tabletten eingebracht. Die Optimierung des Wachstumsprozesses ermöglichte die Synthese von (Al,Ga)N Einkristallen mit einer maximalen Größe von bis zu 0.8x0.8x0.8 mm^3. Wir haben festgestellt, dass (Al,Ga)N Einkristalle durch die Auswahl der entsprechenden Druck- und Temperaturbedingungen unterhalb der GaN Gleichgewichtslinie gezüchtet werden können. Darüber hinaus kann der Al-Gehalt in den wachsenden Kristallen durch geeignete Wahl der Druck- bzw. Temperaturbedingungen gewählt werden. Weitere Studien mit verschiedenen Al-Quellen wie Al Metall, vorsynthetisierten polykristallinen (Al,Ga)N oder AlN Pellets zeigten, dass die Verwendung von (Al,Ga)N die AlN Schichtbildung auf der Schmelzoberfläche und die AlN Verbrennungsreaktion vermeiden lässt. Im Gegensatz dazu hat die Verwendung von Al Metall in der Schmelze (bis zu 0,4 at%)

das Wachstum von sehr kleinen (Al,Ga)N Einkristallen und von Al_2O_3 Kristallen als Nebenprodukt zur Folge. Grössere Al Mengen (bis zu 30 at%) führen zu der AlN Verbrennungsreaktion. Die Kristalle wurden hauptsächlich mit Hilfe von Laserablation induktiv gekoppelter Plasma Massenspektrometrie (LA-ICP-MS) und X-ray Diffraktion analysiert. Dabei fokussierten wir hauptsächlich auf die Homogenität der Zusammensetzung in den Kristallen und auf ihre kristallographischen Eigenschaften. Es wurde gezeigt, dass sich eine etwa 1-µm dicke inhomogene (Al,Ga)N Schicht mit verschiedenem Al-Gehalt auf der Kristalloberfläche bildet. Dabei hängt die Al Zusammensetzung dieser Schicht überwiegend vom Abkühlungsprofil ab.

Die Ergebnisse haben uns erlaubt, die Thermodynamik und die *p-T-x* Gleichgewichts-phasendiagramm vom (Al,Ga)N System zu studieren. Basierend auf den experimentellen Druck- und Temperaturwachstumsbedingungen wurden die Standard Gibbs Freie Energie, die Bildungsenthalpie und die Bildungsentropie von (Al,Ga)N für Temperaturen von bis zu 1800 °C und bis zu 30 kbar Druck kalkuliert. Darüber hinaus ermöglichte uns die Kenntnis der thermodynamischen Funktionen die *p-T* und *x-T* Phasendiagramme zu bestimmen. Beispielsweise wurden die Gleichgewichtskurven zwischen (Al,Ga)N(s) und Al/Ga(l) + N_2(g) für verschiedenen Al-Gehalt in den Kristallen im *p-T* Phasendiagramm berechnet.

Chapter 1

Introduction

The research of III-nitrides, such as GaN and AlN, from their synthesis to characterisation to device manufacturing is continuously developing since Lirman and Zhdanov synthesized the first GaN in 1930 [1] and AlN by Briegleb and Geuther in 1842 [2]. The interest in III-nitride materials and their solid solutions have become of technical significant due to their optical and electrical properties [3]. They are characterized not only with their wide band gap, covering the near and middle UV range, but also by the good thermal stability, thermo-electrical properties as well as mechanical strength. This has, over the years, resulted in significant advances in the synthesis of such compounds, as well as in much progress in understanding and control of their thermodynamic stability, physical properties and employment in increasingly sophisticated device architectures.

There is currently a great need of solid-state light emitters with wavelength in the blue-UV range that have a promising application in the detection of chemical and biological agents, in the ventilation system for bacteria disinfection, optical storage of data, high power-high frequency transistors for radars and communication as well as for general lighting. Many nitride-based devices include heterostructures involving binary or ternary alloys of GaN, AlN and InN. In particular, ternary layers such as (Al,Ga)N is one of the key material and conductive n-type and p-type (Al,Ga)N alloys with high Al contents are especially important for applications. Such ternary (Al,Ga)N alloys are mainly used as electron barriers in power-switching HEMTs [4], as an active zone in light-emitting structures [5], or as cladding layers in lasers [6] since the band gap energy can be tuned from 3.4 to 6.2 eV depending on the atomic composition, or as quantum wells in UV LEDs [7].
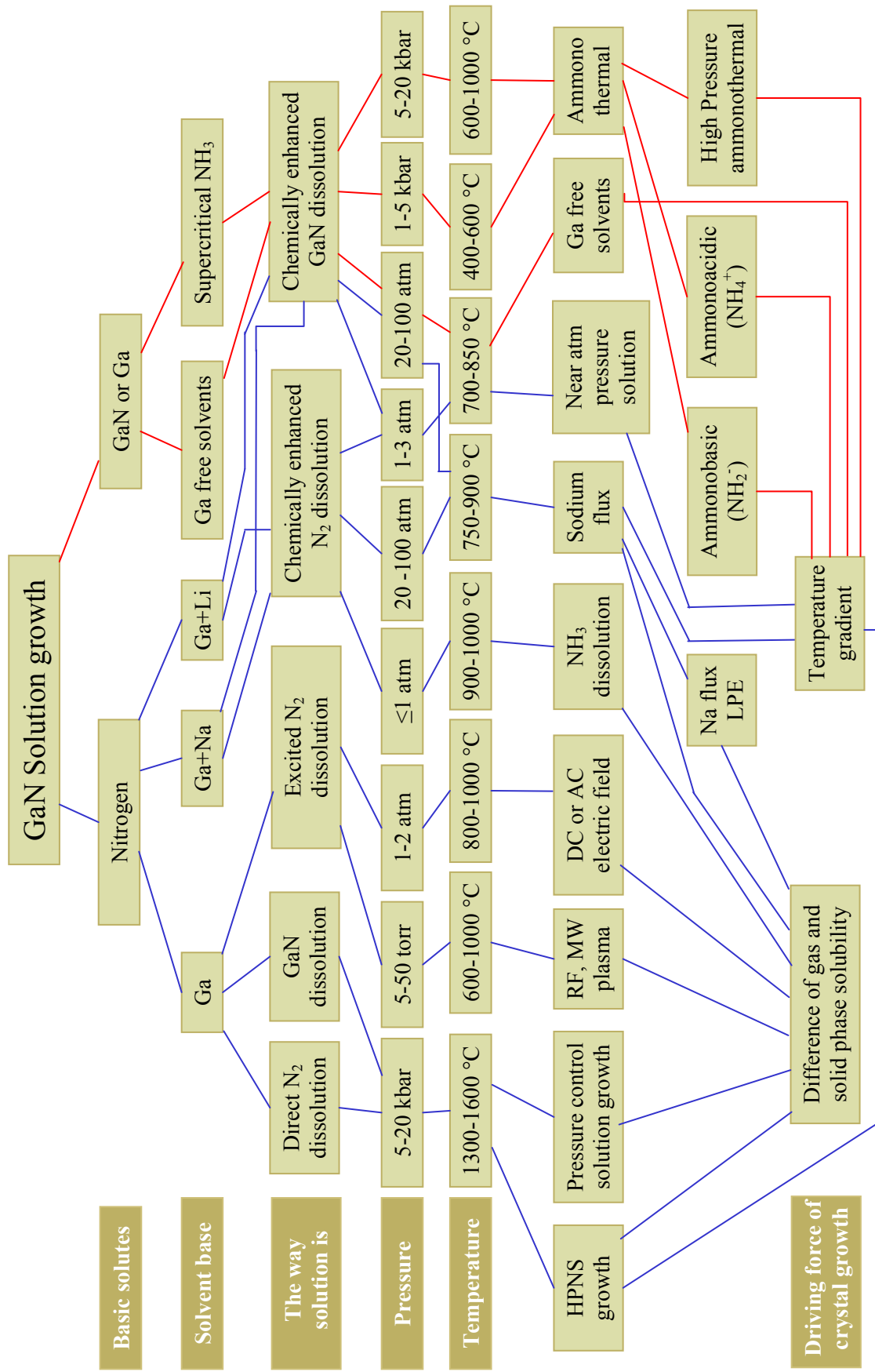
In commercially available devices (Al,Ga)N is mainly deposited by epitaxy techniques such as MBE [8-10], MOVPE [11-13] and HVPE [14-17] on different substrates, e.g. on sapphire or silicon carbide because of the lack of native substrates. The resulting thin films exhibit large defects concentrations (e.g. high dislocation density up to 10^9 cm^{-2}), mainly due

to the difference of thermal expansion coefficient between such substrates and nitride. Homoepitaxy is strongly preferred and some attempts are reported for GaN thin-film deposited on bulk GaN crystals grown by solution method at high nitrogen pressure [18,19].

There are two ways of growing high quality nitride crystals: solution or vapour growth methods. Due to the high Al vapour pressure the vapour growth method (sublimation method) is more suitable for the bulk AlN crystal growth and is mostly used [20-22]. The AlN crystals with up to 25 mm in diameter and up to 15 mm thickness are currently reported by B. Epelbaum *et al.* [23]. Despite the relatively low dislocation density of about 10^3 cm^{-2} in AlN grown by sublimation method, control of voids and point defects remains an issue. GaN single crystals are basically synthesized by solution growth method. In *Table I* the bulk GaN solution growth methods are summarized. Generally, large GaN bulk crystals can be grown by high pressure nitrogen solution growth (HPSG), by a Na flux method or by the using ammonothermal method. The Na flux method was first introduced by Yamane et. [24] and leads to GaN crystals (with maximum size of about 6x4x0.25 mm^3 [25]), slightly smaller then crystals grown by the HPSG method (platelets with a surface exceeding 100 mm^2 [26]). This method is characterized by low growth temperature (750-900 °C) and pressure (20-50 atm). The nitrogen dissolution will be enhanced by sodium acting as a catalyst. The most promising method for synthesis of GaN substrates in a commercial and industrial scale is the ammonothermal crystal growth, where the synthesis is realized in supercritical ammonia, from metallic gallium, at a temperature of about 400-600 °C and pressures of 1-5 kbar. This method was invented by Dwilinski et al [27] in the middle of the 1990s. The low solubility of nitrogen in the melt and slow mass transport result in very low growth rates. Thermal decomposition of NH$_3$ is so fast that the ammonia method can not be extended to the temperatures higher than 1150 °C. To increase the solubility of GaN in ammonia, a mineralizer, acidic (ammonium halogenide NH$_4$X) or basic (lithium or potassium amide XNH$_2$:NH$_3$) is used. Currently, high quality 2-inch c-plane GaN substrates grown by ammonothermal method have been reported [28] and 1 and 1.5-inch substrates are already available on the market. However, the crystal quality, for example, the dislocation density is still quite higher (order of 10^4 cm^{-2} [29]) than by GaN grown by HPSG method (order of 10^2 cm^{-2} [30]).

The first attempt of GaN high pressure growth from solution at temperature about 1200 °C and pressure up to 10 kbar was done by Madar et al [31]. This work was specified by Karpinski *et al.* [32] and lately developed by UNIPRESS in Warsaw, Poland [33]. The GaN

Table I. *Bulk GaN Growth from solution [36]*

GaN Solution growth

Basic solutes

Solvent base

The way solution is

Pressure

Temperature

Driving force of crystal growth

GaN or Ga

Nitrogen

Ga

Supercritical NH_3

Ga free solvents

Ga+Li

Ga+Na

GaN dissolution

Direct N_2 dissolution

Chemically enhanced GaN dissolution

Chemically enhanced N_2 dissolution

Excited N_2 dissolution

5-20 kbar

1-5 kbar

20-100 atm

1-3 atm

20-100 atm

≤1 atm

1-2 atm

5-50 torr

5-20 kbar

600-1000 °C

400-600 °C

700-850 °C

750-900 °C

900-1000 °C

800-1000 °C

600-1000 °C

1300-1600 °C

Ammono thermal

Ga free solvents

Near atm pressure solution

Sodium flux

NH_3 dissolution

DC or AC electric field

RF, MW plasma

Pressure control solution growth

HPNS growth

Na flux LPE

High Pressure ammonothermal

Ammonoacidic (NH_4^+)

Ammonobasic (NH_2^-)

Temperature gradient

Difference of gas and solid phase solubility

high pressure crystal growth is characterized by low solubility of nitrogen in Ga liquid and high equilibrium temperature and pressure that make this method technically difficult. Nevertheless, the modern HPSG method leads to the synthesis of excellent quality GaN near dislocation free crystals. However, the size of those crystals still needs to be improved.

Inoue et al [34] proposed recently another process based on HPSG method. By applying the controlled nitrogen overpressure that supports the N supersaturation in Ga melt GaN single crystals with the size up to 25 mm were synthesized. However, such crystals exhibit higher defects density ($\sim 10^5 \, cm^{-2}$ dislocations) than by HPSG.

The thin film deposition methods of (Al,Ga)N alloy need some improvements, in particular due to the structural defects and the inhomogeneities in the Al concentration in obtained films. Thus, improving the material quality of (Al,Ga)N alloys is of crucial importance for the device fabrication. Moreover, there is some variance in the properties of (Al,Ga)N alloys, e.g. the compositional dependence of the lattice constants, the direct energy gap, produced by different methods and groups. A relatively little is known about the growth of bulk ternary (Al,Ga)N alloys from solution [35]. The major difficulties are the equilibrium conditions required to thermodynamically stabilize the (Al,Ga)N alloy at certain temperature and pressure. The growing (Al,Ga)N crystals poses significant challenges; two of which have been successfully addressed in this work: control of the thermodynamic conditions and proper choice of the solvent.

Scope and overview of this thesis

The principal objective of the present thesis is to explore the understanding of the synthesis of (Al,Ga)N compound using the high pressure techniques. Two methods have been applied: synthesis of the polycrystalline $Al_xGa_{1-x}N$ by solid-state reaction [37] and of $Al_xGa_{1-x}N$ bulk single crystals from solution in Ga melt.

Driven by the previously reported pioneer study [35,38] and a disappointing poor availability of the information on the crystal growth of bulk (Al,Ga)N compound in general, in this thesis, the synthesis of $Al_xGa_{1-x}N$ bulk single crystals in gas autoclave is intensively investigated and discussed. Crystal growth results involving the control of the chemical composition in the crystals and the reproducibility of the experiments are reported.

The research presented in this thesis is focused on synthesis and thermodynamic aspects as well as characterisation of (Al,Ga)N system. In particular, we pay an essential attention on the investigation of the stability of the compound and its crystallographic analysis. Among other things, the *p-T-x* diagram, which is the basis for crystal growth experiments, thermal annealing and for the device application in general, has been determinated.

In *Chapter 2*, the basics of the thermodynamic and kinetic aspects of the III-nitride synthesis from solution are discussed. The most essential studies on GaN, AlN and (Al,Ga)N crystal growth under high pressure are overviewed. The high pressure growth technique used in this thesis for the synthesis of the polycrystalline as well as bulk single (Al,Ga)N crystals is described in *Chapter 3*.

In *Chapter 4*, the synthesis of the $Al_xGa_{1-x}N$ bulk single crystals with $0.22 \leq x \leq 0.91$ from solution in Ga melt under high nitrogen pressure and high temperature is discussed. Moreover, the measurements of the bandgap of $Al_{0.86}Ga_{0.14}N$ crystals and some preliminary studies on *p-T* phase diagram are addressed. The detailed study of the crystal growth as well as the crystallographic characterisation of the obtained crystals and extended *p-T* phase diagram is described in *Chapter 5*.

Finally, in *Chapter 6*, the essential and pioneer results obtained from the studying the thermodynamics of the stability of ternary (Al,Ga)N up to 10 kbar and 1800 °C are demonstrated.

In order to validate the applicability of our high pressure technique and to overcome technical hurdles a numerous work was carried out in tremendously fruitful collaborations with Dr. Jan Jun, who, at the time, engaged himself for this proposal and who is currently working at the Institute of High Pressure Physics of the Polish Academy of Sciences. The optical bandgap studies using a femtosecond, pump-probe spectrometry technique were done in fruitful collaboration with Jie Zhang, who is currently conducting research for his PhD on this topic under the supervision of Prof. Roman Sobolewski at the Department of Electrical and Computer Engineering and Laboratory for Laser Energetics at the University of Rochester, USA (*Chapter 4*). Most compositional characterisations were carried out using laser ablation inductively coupled plasma mass spectrometry in collaboration with Kathrin Hametner, who is working in the group of Prof. Detlef Günther at the Laboratory of Inorganic Chemistry,

ETH Zurich (*Chapter 4* and *5*). Furthermore, substantial contributions were made by Dr. Sergiy Katrych, who conducted the numerous X-ray diffraction measurements on our single crystals (*Chapter 4* and *5*); by Peter Wägli from the Electron Microscopy Center at ETH Zurich, who did a series of essential EDX measurements and recorded a numerous of EDX spectra of our crystals.

This dissertation is reproduced from a collection of papers, which have been published or have been submitted for publication:

Chapter 4. A. Belousov, S. Katrych, J. Jun, J. Zhang, D. Günther, R. Sobolewski, J. Karpinski, and B. Batlogg, J. Cryst. Growth, **311** (2009) 3971-3974.

Chapter 5. A. Belousov, S. Katrych, K. Hametner, D. Günther, J. Karpinski and B. Batlogg, $Al_xGa_{1-x}N$ bulk crystal growth: crystallographic properties and *p-T* phase diagram, (2010) submitted to J. Cryst. Growth.

Chapter 6. A. Belousov, J. Karpinski and B. Batlogg, Thermodynamics of the $Al-Ga-N_2$ system, (2010) submitted to J. Cryst. Growth.

In addition, the publications related to this work are listed on page 99.

References:

[1]   J. V. Lirman, H.S. Zhdanov, Acta Physicochim. USSR **6** (1930) 306.

[2]   F. Briegleb and A. Geuther, Ann. Chem. **123** (1862) 228.

[3]   S. Nakamura, G. Fasol, The Blue Laser Diodes, Springer Verlag, Berlin (1997).

[4]   W. Saito, Y. Takada, M. Kuraguchi, K. Tsuda, I. Omura, T. Ogura, and H. Ohashi, in IEEE Transaction on electron devices **50** (2003) 2528-2531.

[5]   T. J. Schmidt, X. H. Yang, W. Shan, J. J. Song, A. Salvador, W. Kim, O. Aktas, A. Botchkarev, and H. Morkoc, App. Phys. Lett. **68** (1996) 1820-1822.

[6]   S. Nakamura, M. Senoh, S. Nagahama, N. Iwasa, T. Yamada, T. Matsushita, H. Kiyoku, Y. Sugimoto, T. Kozaki, H. Umemoto, M. Sano, and K. Chocho, Appl. Phys. Lett. **72** (1998) 211-213.

[7]   H. X. Jiang and J. Y. Lin, Opto-electronics Rev. **10** (2002) 271-286.

[8]   Y. Cordier, F. Semond, M. Hugues, F. Natali, P. Lorenzini, H. Haas, S. Chenot, M. Laügt, O. Tottereau, P. Vennegues, J. Massies, J. Cryst. Growth **278** (2005) 393-396.

[9]   W. Kim, Oe. Akta, A. Botchkarev, H. Morkoc, J. Appl. Physiology **79** (1996) 7657-7666.

[10]   E. Iliopoulos, K. F. Ludwig, T. D: Moustakas, and S. N. G. Chu, Appl. Phys. Lett. **78** (2001) 463-465.

[11]   M. Matloubian, M. Gershenzon, J. Electro. Mater. **14** (1985) 633-644.

[12]   M. Migoshi, M. Sakai, H. Ishikawa, T. Egawa, T. Jimbo, M. Tonaka, O. Oda, J. Cryst. Growth **272** (2004) 293-299.

[13]   H. Amano, M. Imura, M. Iwaya, S. Kamiyama and I. Akasaki, Materials Science Forum **590** (2008) 175-210.

[14]   L. Liu, J. H. Edgar, Materials Science and Engineering R: Reports **37** (2002) 61-127.

[15]   S. S. Park, I. W. Park, S. H. Choh, Jpn. J. Appl. Physics **39** (2000) L1141-1142.

[16]   J. Hagen, R. D. Metacalfe, D. Wickenden, W. Clark, J. Phys. C **11** (1978) L143-146.

[17]   B. Baranov, L. Daweritz, V. B. Gutan, G. Jungk, H. Neumann, H. Raidt, Phys. Status Solidi (a) **49** (1978) 629-636.

[18]   P. R. Hageman, V. Kirilyuk, W. H. M. Corbeek, J. L. Weyher, B. Lucznik, M. Bochkowski, S. Porowski, S. Muller, J. Cryst. Growth **255** (2003) 241-249.

[19]   C. Krichner, V. Schwegler, F. Eberhard, M. Kamp, K. J. Ebeling, P. Pystawko, M. Leszczynski, I. Grzegory, and S. Porowski, Prog. Cryst. Growth. Charact. **41** (2000)

57-83.

[20]   J. H. Edgar, L. Liu, B. Liu, D. Zhuang, J. Chaudhuri, M. Kuball, S. Rajasinggam, J. Crystal growth **246** (2002) 187-193.

[21]   R. Schlesser, R. Dalmau, Z. Sitar, J. Crystal Growth **241** (2002) 416-420.

[22]   B. M. Epelbaum, C. Seitz, A. Magerl, M. Bickermann, A. Winnacker, J. Crystal growth **265** (2004) 577-581.

[23]   B.M. Epelbaum, O. Filip, M. Bickermann, P. Heimann and A. Winnacker, „Growth direction and polarity on properties of bulk AlN crystals", 6th International Workshop on Bulk Nitride Semiconductors", August 23-28 (2009), Galindia, Poland.

[24]   H. Yamane, M. Shimada, S. J. Clarke, F. J. Disalvo, Chem. Mater. **9** (1997) 413-416.

[25]   M. Aoki, H. Yamane, M. Shimada, S. Sarayama, F. J. DiSalvo, J. Cryst. Growth **242** (2001) 70-76.

[26]   S. Krukowski, C. Skierbiszewski, P. Perlin, M. Leszczyński, M. Bockowski, S Porowski, Acta Physica Polonia B **37** (2006) 1265-1312.

[27]   R. Dwilinski, A. Wysmolek, J. Baronowski, M. Kaminska, R. Doradzinski, J. Garczynski, L. Sierzputowski, Acta Physica Polonica **88** (5) (1995) 833-836.

[28]   R. Dwilinski *et al.*, „Growth of GaN crystals by the ammonothermal method", International Workshop on Nitride Semiconductors, October 6-10 (2008), Montreux, Switzerland.

[29]   R. Dwilinski, R. Doradzinski, J. Garczynski, L. Sierzputowski, M. Zajac, „Recent achievements in AMMONO bulk method", 6th International Workshop on Bulk Nitride Semiconductors", August 23-28 (2009), Galindia, Poland.

[30]   Z. Liliental-Weber, J. Jasinsk, J. Washburn, J. Cryst. Growth **246** (2002) 259-270.

[31]   R. Madar, G. Jacob, J. Hallais and R. Fruchart, J. Cryst. Growth **31** (1975) 197-203.

[32]   J. Karpinski, S. Porowski, J. Cryst. Growth **66** (1986) 1-10.

[33]   S. Porowski, Acta Physica Polonica **87** (2) (1995) 295.

[34]   T. Inoue, Y. Seki, O. Oda, S. Kurai, Y. Hamada, T. Taguchi, Phys. Stat. Sol. B **223** (2001) 15-27.

[35]   P. Geiser, J. Jun, S. M. Kazakov, P. Wägli, L. Klemm, J. Karpinski, and B. Batlogg, Appl. Phys. Lett. **86** (2005) 081908.

[36]   The table is demonstrated with kind permission from Dr. Boris Feigelson, Naval Research Laboratory, USA (Email: borisf@estd.nrl.navy.mil).

[37]   H. Saitoh, W. Utsumi, H. Kaneko, and K. Aoki, Jpn. J. Appl. Phys. **43** (2004) L981.

[38]   P. Geiser, Dissertation №16126, ETH Zurich (2005).

Chapter 2

III-nitride synthesis from solution

This chapter describes the thermodynamic and kinetic aspects of the III-nitride synthesis from solution under high nitrogen pressure. The thermal stability of the compounds and its dependence on the nitrogen pressure are discussed. We also present a comprehensive overview of a GaN, AlN and $Al_xGa_{1-x}N$ growth from solution under high nitrogen pressure.

2.1 Basic thermodynamic and kinetic aspects

It is known that III-nitrides are compounds of high bonding energy compared to other III-V compounds. The bonding energy in III nitrides are 11.52 and 8.92 eV/atom for AlN and GaN respectively, whereas for GaAs this energy is only 6.52 eV/atom [1]. Therefore, nitrides melt at very high temperatures and are good thermally stable. The synthesis/decomposition reaction of one mole of metal nitride MeN is simply:

$$Me + \frac{1}{2}N_2 \Leftrightarrow MeN \tag{1}$$

However, the strong triple bond in the N_2 molecule (4.38 eV/atom) lowers the thermodynamical potential (Gibbs free energy G) of the system of nitrides constituents, Me + ½ N_2, approaching that of the nitrides [2]. Moreover, the free energy of constituents decreases faster with the temperature than G(T) for the compound, and therefore the stability of the nitride is shifted towards metal and nitrogen at high temperature as illustrated in *Figure 1*. In *Figure 1* the Gibbs free energy of nitride (1 mol) and the Gibbs free energy of the sum of its constituents (Ga+½ N_2) are shown as a function of temperature and nitrogen pressure (adapted from [2]). The free energy change ΔG for the considered reaction is:

$$\Delta G = G_{MeN} - (G_{Me} + \frac{1}{2}G_{N_2}) \qquad (2)$$

or for ternary $Al_xGa_{1-x}N$:

$$\Delta G = G_{Al_xGa_{1-x}N} - (xGa_{Al} + (1-x)G_{Ga} + \frac{1}{2}G_{N_2}) \qquad (3)$$

In equilibrium, $\Delta G=0$. If $\Delta G<0$, the nitride compound is stable. We will describe this reaction (3) in more detail in *Chapter 6*.

The data for the constituents in *Figure 1* were taken from the thermodynamic tables [3,4]. Since the enthalpy and entropy of formation of GaN [5] are known, we can evaluate the G(T) dependence for GaN shown in *Figure 1a*. For AlN, in *Figure 1b*, the data were used according to Slack and McNelly [6]. *Figures 1a* and *1b* illustrate the large difference in the thermal stability between GaN and AlN. At 1 bar pressure GaN becomes thermodynamically unstable at high temperatures and decomposes around 850 °C, whereas AlN is stable up to 2494 °C [6]. Similar consideration can be made for ternary $Al_xGa_{1-x}N$. Based on the experimental data and thermodynamic calculations described in *Chapter 5* and *Chapter 6* the Gibbs free energy of e.g. $Al_{0.86}Ga_{0.14}N$ as a function of temperature was evaluated as indicated in *Figure 1c* and *1d*. $Al_xGa_{1-x}N$ with high Al content has as predicted higher thermal stability as for GaN. $Al_{0.86}Ga_{0.14}N$ decomposes at ∼942 °C at 1 bar nitrogen pressure. However, the Gibbs free energy of $Al_{0.86}Ga_{0.14}N$ is much lower than of AlN and is comparable with GaN. The reasons of this fact will be discussed in *Chapter 6*. More importantly, it means that $Al_xGa_{1-x}N$, even with high Al content, becomes unstable at the temperatures comparable to the GaN decomposition temperature. In particular, for the synthesis of $Al_xGa_{1-x}N$ the decomposition temperature is one of the key issues. Considering the solution growth of nitrides, where the kinetics of the growth strongly depends on the process temperature, knowing the decomposition temperature is very important.

Figure 1d shows the influence of the nitrogen pressure on the stability of the nitrides. It can be seen that the application of the pressure increases the Gibbs free energy of the constituents more than G(T) of the nitride, which causes the equilibrium point to shift to higher temperatures, increasing the range of nitride stability. Thus, at 5 kbar $Al_{0.86}Ga_{0.14}N$ decomposes at 1675 °C, compared to 942 °C at 1 bar nitrogen pressure.
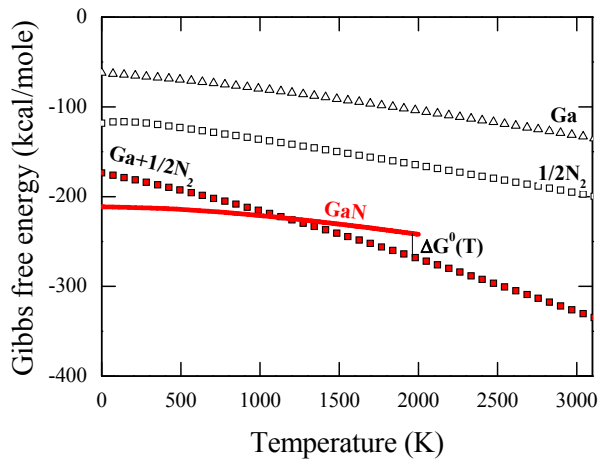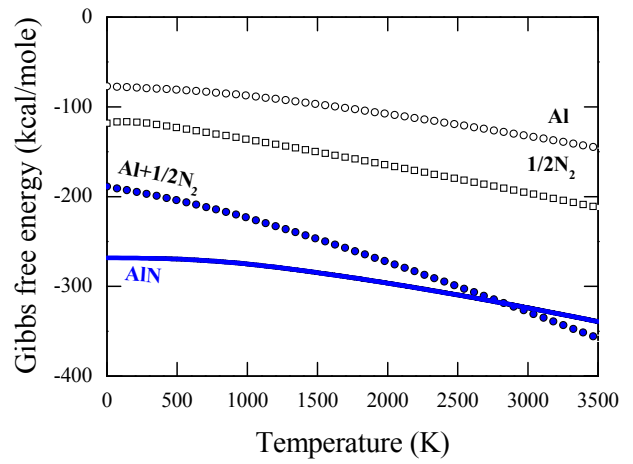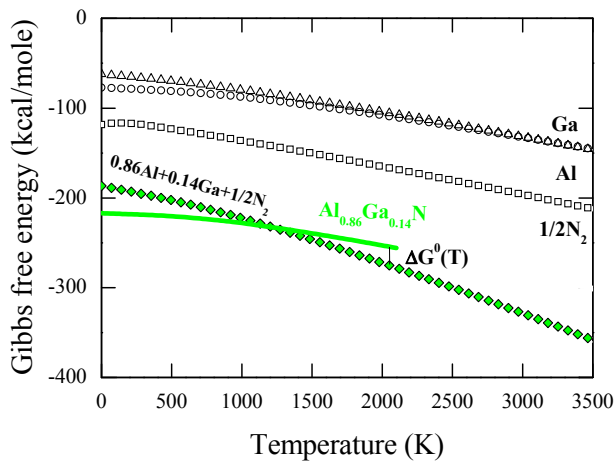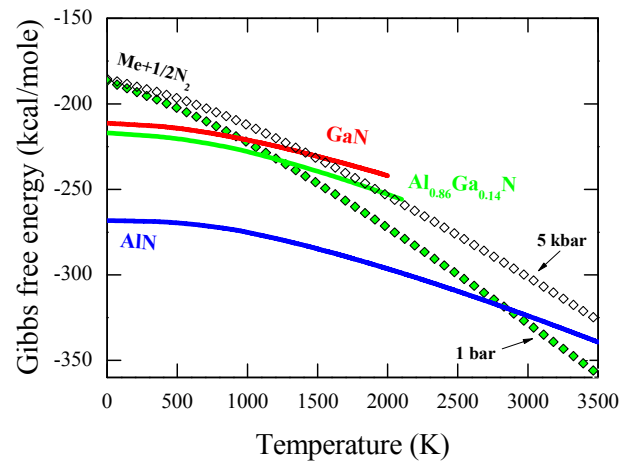
Fig. 1. *Gibbs free energy change with temperature for III nitrides and their constituents: (a)-(c) for N_2 pressure 1 bar; (d) - G(T) for the constituents is the sum of averaged energy of the metal and the free energy of nitrogen at pressures of 1 bar and 5 kbar.*

The results of the analysis agree well with the experimental equilibrium data obtained in this study (*Chapter 5 Figure 3*).

Figure 2 shows the equilibrium nitrogen pressure curves for GaN and AlN. The curve for AlN was calculated by Slack and McNelly [6] using the available thermodynamical data of the constituents of the AlN formation reaction. On the basis of the GaN decomposition and crystal growth experiments, Karpinski and Porowski [5] evaluated the equilibrium curve for GaN (*Figure 2*). In short, under certain conditions of temperature and pressure lying above the equilibrium curve the binary nitride is stable. For example, at 10 kbar GaN starts to decompose at temperatures higher than 1490 °C. Compared to AlN, the GaN equilibrium curve deviates from a linear dependence. This is mainly due to the non-ideal behaviour of nitrogen gas at high temperature and pressure. For AlN, the high nitrogen pressure is not necessary to extend the thermal stability range.
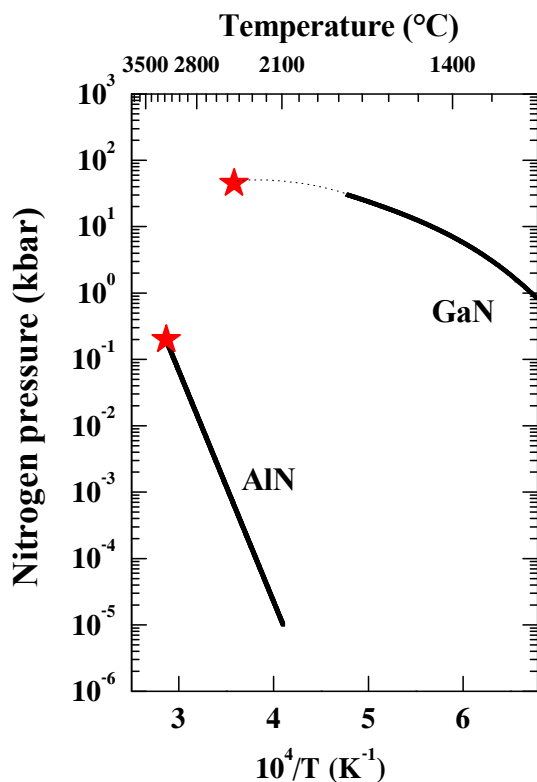
Fig. 2. *Equilibrium nitrogen pressure over GaN and AlN corresponding to the curves reported by Slack and McNelly. [6] and Karpinski and Porowski [5]. The melting points of the two binary compounds are indicated by stars.*

The stars in the *Figure 2* indicate the melting points of AlN and GaN (*Table I*). These points were calculated by the use of Quantum Dielectric Theory of Chemical Bonding proposed by Van Vechten [7]. According to his estimations, the melting temperatures of GaN

and AlN are much higher than the temperatures ever reached in the gas autoclave. For example, in a gas pressure chamber used in this study the maximum temperature is 1900 °C.

Table I. *Melting temperatures and decomposition nitrogen pressures for AlN and GaN [2].*

Nitride	T^m (K)	$P_{N_2}^*$ (kbar)	$P_{N_2}^{**}$ exp (kbar)
GaN	2488 [8]	60	>55 [8]
AlN	3487 [7]	0.2	>0.1 [9]

* - extrapolation of the experimental equilibrium data

** - the highest pressure at which decomposition was observed.

For pressures above the equilibrium curve at a given temperature, the decomposition occurs at a slow and apparently constant rate suggesting a diffusion-controlled process of decomposition as reported by Karpinski and Porowski [5].

In the solution growth the behaviour of nitrogen at high pressure is not a trivial problem. The nitrogen gas is absorbed on the Ga surface and then dissolved in liquid gallium. Therefore, adsorption of nitrogen N_2 molecules leads to its disintegration. This process required energy not higher than 4.8 eV. According to the quantum mechanical calculations [10] penetration of the disintegrated single N atoms into Ga liquid leads to the dissolution of nitrogen N in liquid Ga. For AlN the barrier of this process is 3.2 eV. In addition, the dissolution of nitrogen in liquid Ga is limited. The solubility of nitrogen in gallium was reported by Logan and Thurmond [11], Karpinski and Porowski [12] and Grzegory *et al.* [2].
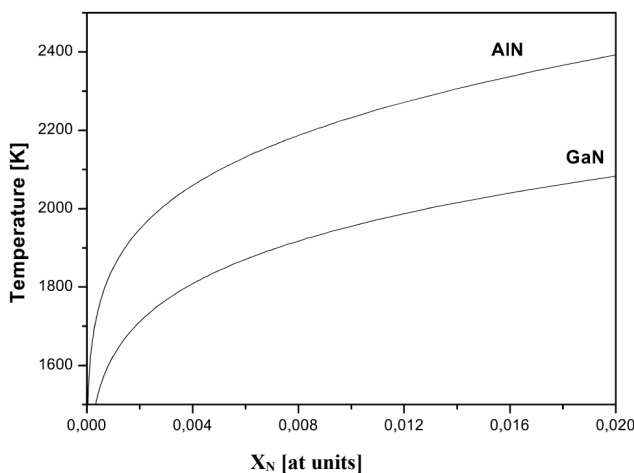
Fig. 3. *Liquidus lines for Ga-GaN and Al-AlN [13].*

In *Figure 3* the liquidus curves for Ga-GaN and Al-AlN calculated for ideal solution approximation with the use of melting parameters estimated by Van Vechten [7] are shown. The nitrogen solubility is higher for Ga-GaN than for Al-AlN. At 2000 K for Ga-GaN the solubility of nitrogen can reach 1.5 at% and for Al-AlN only 0.3 at%. Accordingly, for Al-Ga-AlGaN, adding Al into the Ga melt should decrease the solubility of nitrogen in Al-Ga melt. However, it is expected that the solubility of nitrogen in Al should have a strong negative deviation from the ideal solution behaviour and the higher concentration of nitrogen than predicted by the ideal solution model can be dissolve in the Al liquid [13].

As we discussed, the dissociation of nitrogen in liquid Ga or Al is a kinetically controlled process dependent on the temperature. Since the barrier for AlN is lower than for GaN, the efficiency of the nitrogen dissociation by AlN does not require high temperatures (*Figure 4*). *Figure 4* represent the rate of the nitrogen dissociation estimated for nitrogen pressure of 20 kbar. The horizontal dotted line is the experimental limit for the effective synthesis of GaN and AlN. In this case, it is 10 mg of nitride at 1 cm^3 during 100 hours [13]. As it can be seen, at low temperature the dissociation rate for GaN is relatively slow. Only at temperatures higher than 1500 K the effective synthesis of GaN becomes possible. If we take into account the *p-T* phase diagram (*Figure 2*), then we can also conclude that the growth of GaN from the Ga solution is only possible by application of the high nitrogen pressure.
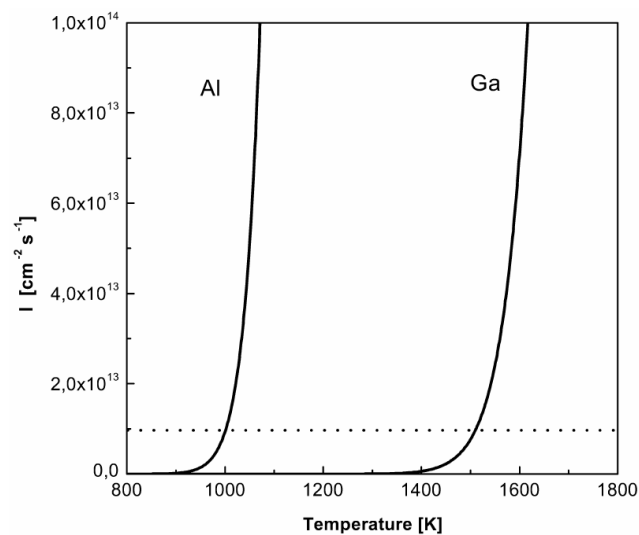
Fig. 4. *Nitrogen dissociation rate I on Al and Ga surface as a function of temperature [14].*

2.2 GaN crystal growth

The first attempt at high pressure crystal growth of GaN from the solution was reported by Madar *et al.* [15]. They could grow the GaN single crystal of the needle, platelets and prism type at 1200 °C and pressures up to 10 kbar. The growth at 1000 °C led to very thin GaN films on the gallium surface. It was concluded that an increase of the temperature to 1250 °C enhances the solubility of nitrogen to 10^{-3} mole fraction. Karpinski and Porowski [5,12] continued the study of GaN crystal growth. They constructed a high pressure gas autoclave that allowed to work up to 1700 °C and 20 kbar. In their experiments, a study of the equilibrium nitrogen pressure by decomposition of GaN was done: up to 1700 °C and 20 kbar using gas autoclave and from 1500 to 2300 °C und pressures from 20 to 70 kbar using an anvil apparatus. For the crystal growth two methods were used: thermal gradient solution growth and cooling an isothermal solution. They reported the growth of small single crystals up to 100 µm by thermal gradient method in 4h experiments with the growth rate of about 10 µm/h. This growth rate was significantly higher than reported by Madar et al [15]. The layers grown at 1250 °C under 16 kbar pressure had a resistivity higher than 10^8 Ωcm. At the temperature of 1400-1500 °C under the same pressure, n-type layers of resistivity 10^{-2}-10^{-4} Ωcm were obtained. It was assumed that nitrogen vacancies developed at the conditions closer to the equilibrium curve are the source of free electrons. Afterwards, the GaN crystal growth was investigated at the UNIPRESS Institute of High Pressure in Warsaw [16, 17, 18]. This Institute is the leading research center on GaN bulk crystal growth with and without intentional seeding, on the thermodynamic and kinetic of the GaN growth under high nitrogen pressure. Most thermodynamic aspects of GaN growth from solution described in this chapter are reviewed from the numerous papers published by UNIPRESS. In our High Pressure Materials Synthesis Group we investigated the GaN growth from solution using 30 and 40 mm interner diameter chambers. The high pressure gas autoclave is described in *Chapter 3*. Boron nitride and graphite were used as a crucible material. The inner diameter of the crucible is 8 or 14 mm.

Single crystals of GaN have been grown in our lab without initial seeding at nitrogen pressure of about 8-12 kbar at temperature of about 1500 °C. The size of the crystals scaled up to a size of 3x4 mm^2 (*Figure 5b*). The morphology of such crystals strongly depends on the process pressure, temperature range and nitrogen supersaturation. The low temperature gradient promotes the growth of hexagonal platelets into the $\{10\bar{1}0\}$ direction (perpendicular

to the c-axis). Such crystals are colourless, transparent, with a flat face and perfect morphology. Larger thermal gradients as well as limited size of crucible support the high supersaturation of nitrogen what leads to the growth of dendrites or needles into the {0001} direction parallel to the c-axis. We succeeded in the growth of large GaN crystals using a seeding crystal. The crystals are up to $\approx$ 5x3 mm^2 in size (*Figure 5*).

a)   b)
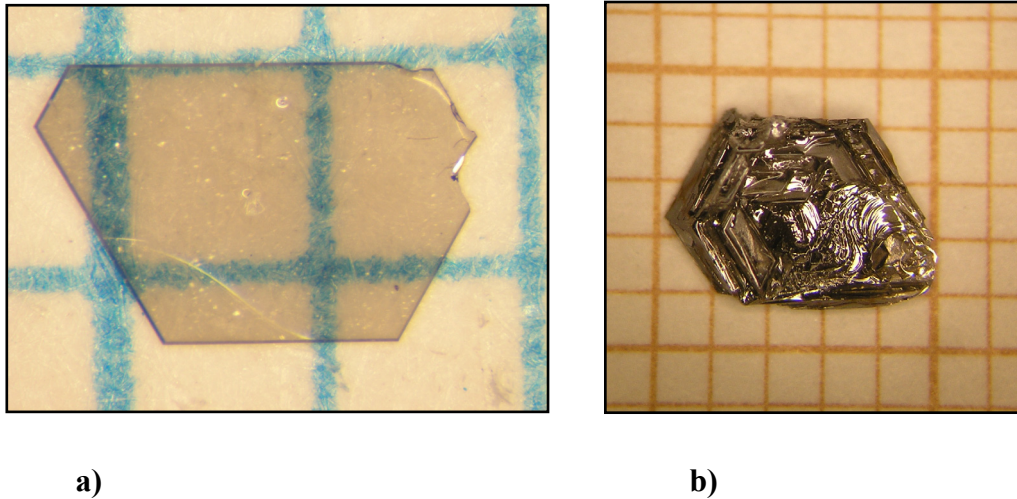
Fig. 5. GaN crystals grown in 40 mm chamber using high nitrogen pressure: (a)- without initial seeding; (b) with seeding. The grid is 1 mm.

Without initial seeding the GaN crystals typically grow spontaneously as it can be seen in *Figure 6*. At first, the wall of the crucible will be covered with GaN polycrystalline layer, on which the GaN crystals then start to grow.

The experiments showed that the size of the crystals can be extended by using a larger pressure chambers. At UNIPRESS, GaN can be crystallized in gas pressure chambers with volume up to 5000 cm^3, which allow the use of crucibles with a working volume up to 50-100 cm^3.

Fig. 6. Spontaneous growth of GaN crystals in the BN crucible.

The internal diameter of the chamber is up to 100 mm. The crystals are typically synthesized in the range of 5-20 kbar and temperatures of 1400-1720 °C. The supersaturation in the growth solution is created by the application of the temperature gradient

of 2-20 °C/cm along the axis of the crucible. Typical duration of the growth process is 120-200 hours. The GaN crystals grown from the solution under high nitrogen pressure are typically of wurtzite structure, mainly in the form of hexagonal planes.

The two polar faces of the crystal are observed: N-side polar denoted as $\{000\overline{1}\}$ and Ga-side polar as $\{0001\}$. The growth rate for the platelets without intentional seeding is below 0.1 mm/h along $[10\overline{1}0]$ direction (perpendicular to the c-axis), suggesting stable layer-by-layer growth by low supersaturation. The size of the platelets grown without intentional seeding is usually about 2-3 cm^2. The dislocation density in the GaN crystals is lower than 10^2 cm^{-2}. Usually, the crystals are strongly n-type with free electron concentration of 10^{19}-10^{20} cm^{-3} and mobility of about 60 cm^2/Vs [19]. The source of free electrons is the oxygen impurity in the growth system. These free carriers can be eliminated by adding Mg acceptor into the growth solution. In *Figure 7*, GaN crystals grown using high nitrogen pressure at UNIPRESS with 0.2-0.5 at% Mg or Be are shown [20].
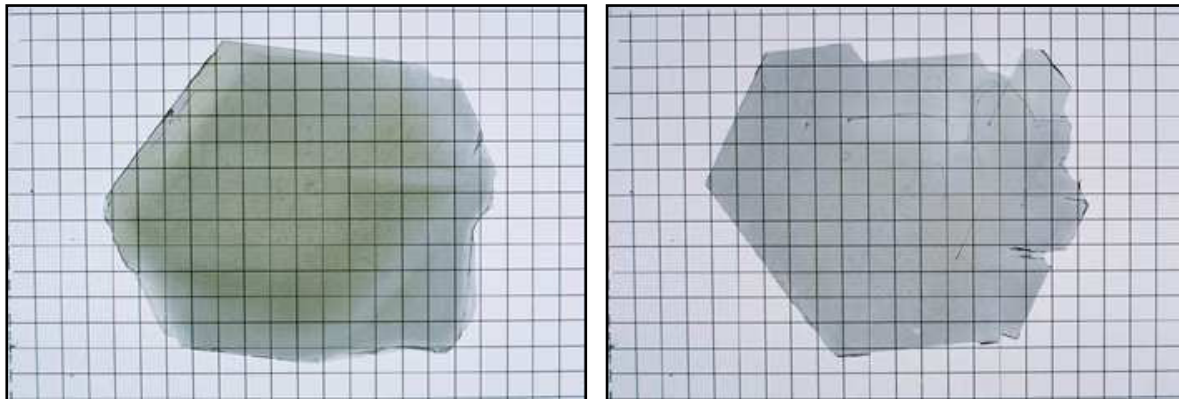
Fig. 7. *GaN crystals with 0.2-0.5 at% of Mg or Be grown at UNIPRESS using high nitrogen pressure. The grid is 1 mm [20].*

The resistivity of the GaN:Mg becomes as high as 10^4-10^6 Ωcm at 300 K. More detailed analysis of electrical properties of pressure grown Mg doped GaN was reported by Litwin-Staszewska *et al.* [21]. It should be mentioned that p-type doping is very important for the technology of all nitride based devices. However, the high ionization energy (200 meV for GaN) of Mg limits the fraction of ionized acceptors to 1% at room temperature. This affects the electrical properties of GaN and Al$_x$Ga$_{1-x}$N layers and causes intensive heat generation,

which is a serious problem in high power devices [20]. The GaN crystals grown under high nitrogen pressure have a high concentration of Ga vacancies as shown by positron annihilation measurements [22]. In GaN:Mg crystals no gallium vacancies could be observed. The difference in the Photoluminescence (PL) spectra of the conductive (strong yellow luminescence) and Mg-doped crystals (no yellow luminescence, but blue Mg-related signal) supported the view that gallium vacancies are involved in the yellow luminescence in GaN. The later studies showed that the oxygen impurities and gallium vacancies are both involved in the yellow luminescence [23]. In case of GaN without doping, the full width at half maximum (FWHM) is 20-30 arcsec for 1 mm crystals and 30-40 arcsec for 1-3 mm ones. For large platelets the rocking curve often splits into a few 30-40 arcsec peaks showing a presence of low angle (1-3 arcsec) boundaries separating grains of a few mm in size. The structural studies of pressure grown GaN and their dependence on the Ga/N face polarity can be found here, for X-ray Diffraction [24], transmission electron microscopy (TEM) [25, 26, 27], defect selective etching (DSE) [28] and atomic force microscopy (AFM) [29].

In this section, we should also shortly mention the method PCSG (Pressure-Controlled Solution Growth) recently proposed by Inoue et al [30, 31]. In fact, this is similar to HPSG method. In this method, an over-pressure instead of the temperature decrease is used to induce the supersaturation of the Ga melt. Inoue *et al.* constructed high-pressure system with an inner diameter up to 130 mm which alloys the use of the crucibles with up to 52 mm diameter. Temperatures up to 1600 °C and pressures up to 10 kbar can be achieved. For crystal growth the furnace was heated up to the growth temperature of 1475 °C, with pressurizing by nitrogen. The nitrogen pressure was tentatively increased to 10 kbar at a rate up to 3 kbar/h, lasting from 0.5 to 16 h. GaN crystal growth was performed without thermal gradient and initial seeding. Several BN crucibles were simultaneously placed into the furnace. The largest GaN crystals with a size up to 25 mm were synthesized at 1475 °C and 10 kbar with a rate of pressure increase about 690 bar/h. Experiments with different rates showed that at lower rates the growth of larger GaN crystal with a good morphology was preferred. The crystals are yellowish transparent hexagonal platelets with macro steps and cracks. The reported dislocation density of these crystals is below 10^5 cm^{-2}, which is still higher than by HPSG process.

2.3 AlN crystal growth

The main method used to grow AlN bulk crystals is the sublimation technique as mentioned in *Chapter 1* [6, 32, 33]. Only few attempts at growing AlN bulk crystals using high pressure were made [13, 34]. As we discussed, from the thermodynamic point of view the high nitrogen pressure is not necessary for AlN crystal growth. AlN is stable at 1 bar up to 2494 °C [6]. However, at the high temperature and at few mbar nitrogen pressure the vapour pressure of aluminium is high enough that evaporated aluminium destroys the furnace elements. This can be avoided by increasing the nitrogen pressure, whereas at higher pressure the self-propagating combustion of AlN is observed [34]. In this case, only low-oxygen content AlN sintered powder can be obtained. This reaction under nitrogen and nitrogen-argon mixtures was investigated by M. Bockowski *et al.* [35]. They proposed a model of AlN combustion. Accordingly, due to the high enthalpy of AlN formation (see *Chapter 6*) the heat released during the creation of nitride warms the sample and the flame starts to propagate through the liquid aluminium initiating the spontaneous AlN formation. The flame temperature can reach locally a very high level (~2500 °C). The combustion process strongly depends on pressure. According to M. Bockowski *et al.* [34] at pressure higher than 6.5 kbar the AlN combustion can be suppressed. However, in our experiments in Ga melt the AlN combustion reaction was observed even up to 10 kbar nitrogen pressure (see *Chapter 4*). In those experiments the pressure was applied at first and then the temperature was increased to the desired value. The understanding of combustion reaction is very important for the growth of ternary (Al,Ga)N crystals from solution, since the Al metal can be considered as a source of aluminum in the Ga melt. The growth of $Al_xGa_{1-x}N$ crystals by this combustion reaction is impossible. In case of AlN, only whiskers can be obtained during the combustion reaction according to Guojian et al [36]. Even if the combustion reaction is suppressed, a thin AlN layer forms on the liquid aluminum surface and prevents the diffusion of nitrogen into the melt.

However, this layer can be dissolved into the melt at high temperature. The AlN needle-like and irregularly shaped crystals were obtained from solution in aluminum at the nitrogen pressure of ~10 kbar and in temperature range of ~1525-1725 °C (*Figure 8*) [34]. In a typical experiment, the bulk aluminum, contained in a BN crucible, located in the furnace inside the high-pressure chamber with 40 mm internal diameter, was heated at a constant rate of 10 °C/h

to the given temperature. Then, the metal sample was annealed at high temperature for 120 hours.
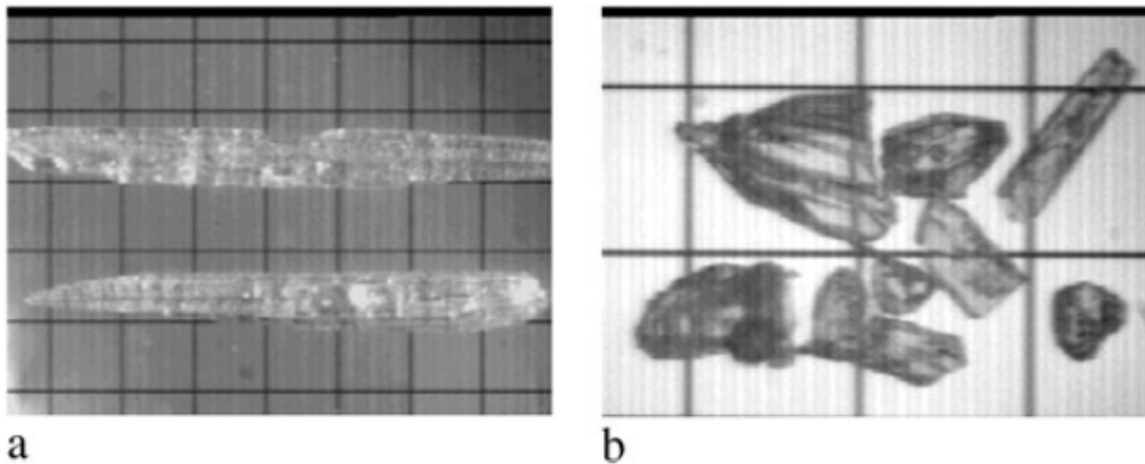

Fig. 8. Typical AlN crystals grown from a liquid solution of nitrogen in aluminium: (a) need-like crystals; (b) irregular bulk [34]. The grid spacing is 1mm.

The temperature gradient, comparable with that used for GaN, was in order of 5-25 °C/cm along the axis of the crucible. The crystals were white in colour and had a wurtzite structure. They grew spontaneously at the cooler end of the crucible from the polycrystalline AlN layer created on the surface of liquid aluminium. At high temperature this AlN layer was dissolved in the Al melt and subsequently serves as a nitrogen source for the crystal growth. The need-like crystals were grown in a large thermal gradient, greater than 10 °C/cm, and the bulk crystal with lower than 10 °C/cm. The chemical or physical characterisation of these AlN crystals was not reported until now.

2.4 AlGaN crystal growth

AlN and GaN were successfully synthesized in a high nitrogen pressure gas autoclave at high temperature and under nitrogen atmosphere [5,12,16,17,34]. However, no reports were available on the growth of ternary (Al,Ga)N alloy in gas autoclave. The first attempts to grow (Al,Ga)N under nitrogen atmosphere were made by Peter Geiser in our group [37, 38]. He looked for a possibility to synthesize the ternary nitride from solution in Al/Ga melt using 30

mm interner diameter gas autoclave. It was found that if the concentration of Al dissolved in the Ga melt is higher than ~1% at 1475 °C, the $Al_xGa_{1-x}N$ crystal growth is suppressed. After the crucible with the Ga melt was cooled down to room temperature, a very dense AlN layer forms on the Al/Ga melt surface. This layer probably prevents dissolving of nitrogen gas in the melt. For higher Al concentration (>10%), a strong AlN combustion reaction, similar as it is described in [34] for AlN solution growth, occurred, yielding fine-grained material. Though at higher temperatures around 1550 °C and by adding small amount of Al into the melt (<1%) the AlN layer did not form; nevertheless $Al_xGa_{1-x}N$ crystal growth was not possible [37]. It was expected that growth of (Al,Ga)N would be possible at higher temperatures, since the AlN layer can be dissolved in the melt as reported by Bockowski for AlN layer in the Al melt [34]. However, due to the temperature limitations in the gas autoclave at that time, the growth experiments were pursued in a cubic anvil cell, allowing to operate the temperature up to 2100 °C and pressure up to 35 kbar. $Al_xGa_{1-x}N$ bulk single crystals up to x=0.3 were synthesized from solution in Ga/Al melt using a cubic anvil cell [38]. The cubic anvil cell itself is described in the *Chapter 3*. For the crystal growth, annealed GaN powder was placed in the middle of the gold capsule, whereas on the top and the bottom of the capsule liquid Ga and small pieces of Al were added. Then, the gold capsule was placed into the BN crucible, which was introduced into the pressure cell. The gold capsule prevented the liquid Ga from being pressed out of the BN crucible. GaN powder served as a source of nitrogen. The crystals were typically synthesized at 30 kbar and 1750 °C during annealing for 12-60 h. The shape of the crystal varies from needle-like to platelets. The largest platelets-shaped crystal up to 0.6x0.4x0.2 mm^3 is shown in *Figure 9*. The crystals are colourless or slightly brown.
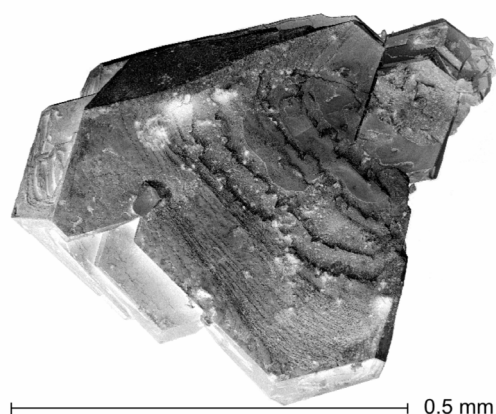
Fig. 9. $Al_{0.3}Ga_{0.7}N$ single crystal grown at 1750 °C and 30 kbar for 45h [38].

According to the laser ablation mass spectrometry gold was not incorporated into the $Al_xGa_{1-x}N$ crystals. Only Si was detected as a significant trace element, with concentrations in the range of 10^3 ppm. However, a thin GaN capping layer in range of few µm was observed on the surface of $Al_xGa_{1-x}N$ crystals [37]. Room-temperature photoluminescence measurements showed the blue shift of the near-band gap luminescence of GaN up to 0.45 eV for Al-substituted samples.

Since a single-stage heater was used that produces temperature gradient along the c-axis of the crucible, the various shapes of crystals thus reflect the local temperature gradient. The temperature and therefore the temperate gradient is controlled by the applied power according to the calibration made using B-type thermocouples. As a result the temperature error may reach ±50 °C. In addition, the pressure is controlled in a range of 0.5 kbar. Misalignment of the starting materials, mainly GaN pellet, in the BN crucible is possible during built-up of the pressure. All considered factors make it difficult to precisely control the crystal growth conditions and therefore to provide the reproducibility of the crystal growth and Al content in the crystals.

However, small $Al_xGa_{1-x}N$ crystals can be grown from Al/Ga melt with a low Al content (1-3 %Al) using a gas pressure autoclave [37]. If GaN powder is used as a nitrogen source small crystals with 3 to 6 %Al were obtained. Unfortunately, since the *p-T* conditions for those experiments were chosen above the GaN equilibrium line, at which GaN is stable (see *Figure 2*), GaN crystals with diffused Al were probably synthesized. This is also supported by the fact that Al content in the GaN crystals varies from the cold to hot zone of the crucible, depending on the temperature.

The key question here concerns the equilibrium conditions required to thermodynamically stabilize the (Al,Ga)N phase. As it will be shown in *Chapter 4-6*, the reproducible $Al_xGa_{1-x}N$ crystal growth in a nitrogen gas pressure autoclave is possible. The use of the pre-reacted $Al_xGa_{1-x}N$ precursor as a source of aluminium and nitrogen in the melt (as proposed by Peter Geiser [37]), allows to overcome the problem with formation of AlN layer on the Ga/Al surface. Such $Al_xGa_{1-x}N$ precursors were synthesized using a cubic anvil cell. Knowing the proper *p-T* conditions one can synthesize the crystals even at lower temperature such 1426 °C. As we found, the *p-T* conditions for the $Al_xGa_{1-x}N$ growth should be selected below the GaN equilibrium curve. Moreover, the composition *x* in the growing $Al_xGa_{1-x}N$ crystals can be selected by the proper chose of *p-T* conditions according to the estimated $Al_xGa_{1-x}N$ equilibrium phase diagram.

References:

[1]   W. A. Harrison, Electronic Structure and Properties of Solids, San Francisco (1980).

[2]   I. Grzegory, J. Jun, M. Bockowski, S. Krukowski, M. Wróblewski, B. Lucznik, and S. Porowski, J. Phys. Chem. Solids **56** (1995) 639-647.

[3]   L. V. Gurvich, I. V. Veyts and C. B. Alcock, Thermodynamic properties of individual substances, 4th edition, V. 1, part 2, Hemisphere Publishing Corp., 1989.

[4]   L. V. Gurvich, I. V. Veyts and C. B. Alcock, Thermodynamic properties of individual substances, 3rd edition, V. 3, part 1-2, Begell House, Inc., 1996.

[5]   J. Karpinski, S. Porowski, J. Cryst. Growth **66** (1986) 11-20.

[6]   G. A. Slack, T. F. McNelly, J. Cryst. Growth **34** (1976) 263-279.

[7]   J. A. Van Vechten, Phys. Rev. B **7** (1973) 1479-1507.

[8]   W. Utsumi, H. Saitoh, H. Kaneko, T. Watanuki, K. Aoki and O. Shimomura, Nature Materials **2** (2003) 735-737.

[9]   W. Class., Contract Rep., NASA-Cr-1171 (1968).

[10]   S. Krukowski, Cryst. Res. Technol. **34** (1999) 785-795.

[11]   R. A. Logan, C. D. Thurmond, J. Electrochem. Soc. **125** (1976) 1161.

[12]   J. Karpinski and S. Porowski, J. Cryst. Growth **66** (1986) 1-10.

[13]   M. Bockowski, Cryst. Res. Technol. **36** (2001) 771-787.

[14]   S. Krukowski, Z. Romanowski, I. Grzegory, S. Porowski, J. Cryst. Growth **175** (1998) 159-162.

[15]   R. Madar, G. Jacob, J. Hallais and R. Fruchart, J. Cryst. Growth **31** (1975) 197-203.

[16]   I. Grzegory, J. Jun, S. Krukowski, Proceedings of XI AIRAPT Conference, Naukowa Dumka, Kijev (1989).

[17]   J. Prywer, S. Krukowski, MRS Internet J. Nitride Semicond. Res. **3** (1998) 47.

[18]   I. Grzegory, J. Phys. Condens. Matt. **13** (2001) 6875-6892.

[19]   P. Perlin, J. Camassel, W. Knap, T. Talercio, J. C. Chervin, T. Suski, I. Grzegory, S. Porowski, Appl. Phys. Lett. **67** (1995) 2524-2526.

[20]   S. Krukowski, C. Skierbiszewski, P. Perlin, M. Leszczyński, M. Bockowski, S. Porowski, Acta Physica Polonica B **37** (2006) 1265-1312.

[21]   E. Litwin-Staszewska, T. Suski, R. Piotrkowski, I. Grzegory, M. Bockowski, L. Robert, J. Knczewcz, D. Wasik, E. Kaminska, D. Cote, B. Clerjaud, J. Appl. Phys. **89** (2001) 7960-7965.

[22] K. Saarinen, T. Laine, S. Kuisma, P. Hautojarvi, L. Dobrzynski, J. M. Baranowski, K. Pakula, R. Stepniewski, M. Wojdak, A. Wysmolek, T. Suski, M. Leszczynski, I. Grzegory, S. Porowski, Phys. Rev. Lett. **79** (1997) 3030.

[23] G. Slack, L. J. Schowalter, D. Morelli, J. A. Freitas, J. Cryst. Growth **246** (2002) 287-298.

[24] M. Leszczynski, I. Grzegory, H. Teisseyre, T. Suski, M. Bockowski, J. Jun, J. M. Baronowski, S. Porowski, J. Domagala, J. Crystal Growth **169** (1996) 235-242.

[25] Z. Liliental-Weber, EMIS Data review Series No23, Published by INSPEC, The Institution of Electrical Engineers, London (1999) 230.

[26] S. H. Christiansen, M. Albrecht, H. P. Strunk, C. T. Foxon, D. Korakakis, I. Grzegory, S. Porowski, Phys. Stat. Solidi (a) **176** (1999) 285-290.

[27] J. L. Weyher, P. D. Brown, J. L Rouviere, T. Wosinski, A. R. A. Zauner, I. Grzegory, J. Cryst. Growth **210** (2000) 151-156.

[28] J. L. Weyher, S. Müller, I. Grzegory, S. Porowski, J. Cryst. Growth **182** (1997) 17-22.

[29] P. Prystawko, R. Czernecki, M. Leszczyński, P. Perlin, P. Wiśniewski, L. Dmowski, H. Teisseyre, T. Suski, I. Grzegory, M. Bockowski, G. Nowak, S. Porowski, Phys. Stat. Solidi (a) **192** (2002) 320-324.

[30] T. Inoue, Y. Seki, O. Oda, S. Kurai, Y. Hamada and T. Taguchi, Phys. Stat. Sol. (b) **223** (2001) 15-27.

[31] T. Inoue, Seki, O. Oda, S. Kurai, Y. Hamada and T. Taguchi, Jpn. J. Appl. Phys. Part 1 **39** (2000) 2394-2398.

[32] B. M. Epelbaum, C. Seitz, A. Megerl, M. Bickermann, A. Winnacker, J. Cryst. Growth. **265** (2004) 577-581.

[33] R. Schlesser, R. Dalmau, Z. Sitar, J. Cryst. Growth **241** (2002) 416-420.

[34] M. Bockowski, B. Lucznik, I. Grzegory, S. Krukowski, M. Wróblewski and S. Porowski., J. Phys. Condens. Mat. **14** (2002) 11237-11242.

[35] M. Bockowski, A. Witek, S. Krukowski, M. Wróblewski, S. Porowski, R. M. Marin-Ayral, and J. C. Tedenac, J. Mat. Synth. Proc. **5** (1997) 449-458.

[36] J. Guojian, Z. Hanrui, Z. Jiong, R. Meiling, L. Wenlan, W. Fengying, Z. Baolin, J. Mater. Sci. **35** (2000) 63-69.

[37] P. Geiser, Dissertation №16126, ETH Zurich (2005)

[38] P. Geiser, J. Jun, S. M. Kazakov, P. Wägli, J. Karpinski, and B. Batlogg, Appl. Phys. Lett. **86** (2005) 081908.

Chapter 3

High pressure growth technique

As mentioned in *Chapter 1*, effective ways to grow high quality III-nitrides bulk crystals is the use of solution or vapour growth methods. The solution method applied in this work is based on the growth from nitrogen dissolved in liquid Ga/Al under high nitrogen pressure. In this chapter we describe the high pressure technique used for the synthesis of the polycrystalline samples as well as $Al_xGa_{1-x}N$ bulk single crystals.

3.1 High nitrogen pressure gas autoclave

Originally, the gas autoclave for the growth from solution in a gas atmosphere was applied in the beginning of the 1980s by Karpinski et al [1,2] at UNIPRESS in Poland. They could work with pressures up to 20 kbar and temperatures up to 1700 °C. Similar equipment was used in our laboratory and was continuously modified and improved. For crystal growth crucial system parameters are the crucible size, pressure and the maximum temperature. To increase the size of crucible chambers with larger interner diameter are needed. If a higher maximum operating temperature is required, the isolation of the furnace plays an important role. This required again a larger volume of the pressure chamber. To increase the interner diameter of the chamber and at the same time to be able to operate with high pressure is not a trivial problem. The pressure-induced stress and strain distribution in the chamber is important. According to the elastic equilibrium theory the highest stress occurs at the bore surface of the chamber [3]. And for the most part of the cross section, only a small part is loaded with a maximum stress. It means that increasing the outer diameter will bring only a small advantage for the maximum pressure inside. The most suitable solution is the use of two cylinders mounted together with pre-stress. The outer cylinder applies a compressive stress on the inner one in opposite direction to the internal gas pressure, yielding the reducing of

material fatigue and therefore increasing the maximum operational pressure by up to approximately a factor of 2. Such compressive stress is built up by pressing an outer cylinder on top of the inner cylinder. For that reason the inner diameter of that outer cylinder is smaller than the outer diameter of inner one. The contact surface between two cylinders is designed as a slight cone (0.2°). Another possibility is to cool the inner cylinder and simultaneously heat the outer one. As a result, the outer cylinder will thermally expand in comparison to the inner one and the necessary compressive stress will be produced. However, the latter method is quite difficult to handle and therefore the solution with the slightly conical cylinders is used more often. In the beginning the 30 mm interner diameter chamber was used in our laboratory for the growth of GaN crystals. The maximum pressure that could be safety operated is 15 kbar. By using the BN ceramics and alumina isolation the temperature up to 1600 °C can be achieved. Later, in order to grow larger crystals the new chamber with 40 mm interner diameter was designed by Jan Jun in our lab [4].
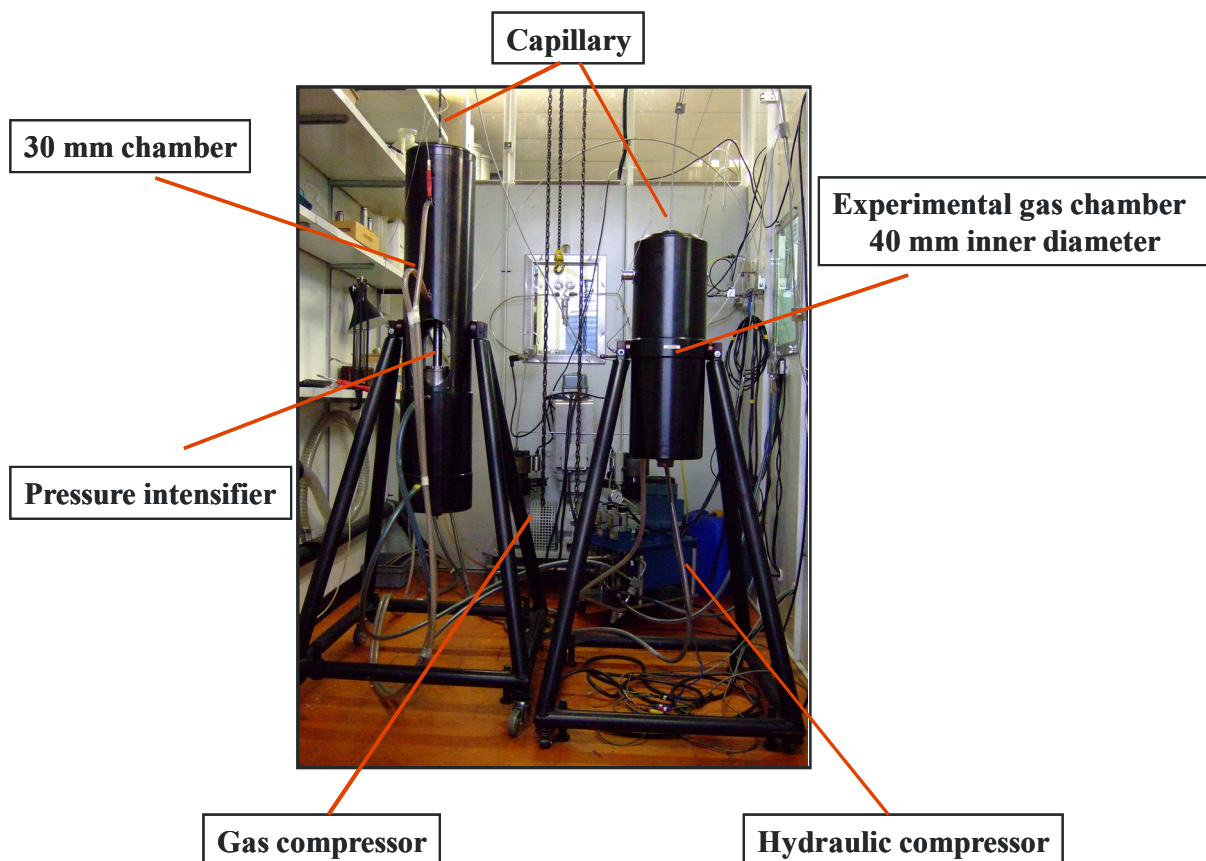

Fig. 1. Nitrogen high pressure growth system used for the synthesis of binary and ternary III nitrides.

A state of art high pressure equipment, constructed in our lab and suitable for the crystal growth experiments at high gas pressure and high temperature is shown in *Figure 1*. By using a 40 mm interner diameter chamber, we can operate up to 12 kbar pressure and temperature around 1800 °C. The 30 mm chamber is used as a pressure intensifier and the 40 mm chamber is used for the crystal growth. Both chambers are connected through a thin capillary (0.3 mm inner diameter). The capillary are fixed in a plug, which closes the chambers from one side. On the other side the piston and the plug with a furnace are placed for the 30 mm and 40 mm chamber respectively. At first, the high purity nitrogen gas (99,9999 %) is pumped up to 3 kbar in the 30 mm and 40 mm chambers using a commercial gas compressor by "Nova Swiss". Then, the inlet into 30 mm chamber will be closed with a piston operated by an oil hydraulic compressor with a maximum oil pressure of 630 bar. Thus, by moving the piston into the 30 mm chamber the gas inside is compressed to desired value. For safety reasons, the free volume in the 30 mm chamber is reduced by filling free space with an aluminium spacer. Only the space required to move the piston is left free. The diameter of the oil hydraulic cylinder and the autoclave bore yield a multiplication factor of about 30 for the pressure intensifier. The gas pressure can be kept constant by using specially constructed sealing rings on the piston. Depending on the required pressure range the rubber ring and $CuBe_2$ alloy rings with different hardness are used as seals. The same type of sealing is also used for the plugs of both chambers. More details about construction and description of the sealing rings can be found in Peter Geiser`s thesis [4]. Finally, the 40 mm chamber is shut off from the system by a high pressure valve. When the temperature is ramped up, the gas pressure increases accordingly. On the basis of previous experiments one can select the starting pressure so, that the desired pressure can be achieved after establishing of the growth temperature. Several gauges are used for pressure measurements. One unit is attached to the 3 kbar compressor to monitor the pressure during operation of the first compressor. The second one is connected to the oil hydraulics. The measured oil pressure can be converted to the pressure inside the chamber. Due to the friction forces between autoclave walls, metal seal and piston some significant uncertainty in determining of the pressure can occur. For that reason, another pressure sensor, a manganese coil, is placed on the capillary plug inside the chamber for precise pressure monitoring. In order to control the pressure in the 40 mm chamber after all valves were closed, another additional pressure gauge is installed. Thus, the pressure in both chambers can be monitored with a good accuracy ~±50 bar.

In our construction the heater is placed inside the pressure chamber. In comparison to another pressure technique, where the pressurized volume is heated externally, this is more

advantageous. There is no heating of the walls of the mechanically stressed chamber that encloses the gas of very high pressure.

As discussed, the second important aspect in the growth from solution is the temperature and temperature control. The previous experiments for the growth of crystals in the Al-Ga-N ternary system have shown that the temperature was too low [4]. For that reason the heater system has been improved. At high temperature the typically used platinum or tungsten wires recrystallize and become brittle, decreasing the lifetime of the heater and the heater fails during the experiment. This problem was solved in that we have now used W/Re wires. The heater now operates up to about 200-300 hours. For experiments at high temperature the new furnace with BN isolation and W/Re wires for the 40 mm chamber was constructed (*Figure 2*). With it temperature of about 1900 °C can be reached. At this condition increase diffusion of nitrogen through AlN films formed on the surface of Ga/Al melt or/and their solubility in Ga/Al melt.
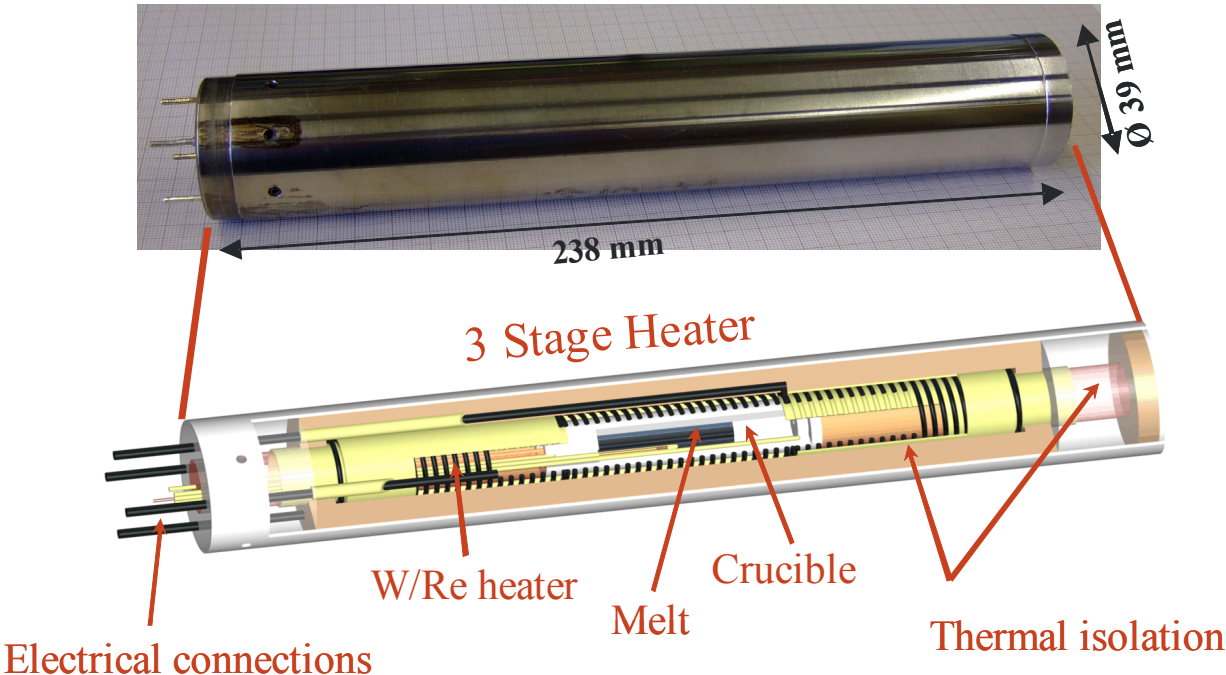
Fig. 2. Three stage furnace and its cut open view with crucible and thermal isolation.

A schematic cross-section of this high temperature furnace is shown in *Figure 3*. For the construction of this furnace, the W/Re are wrapped around the BN tube with a small spacing.

The heater wires are protected by BN and, in addition, with alumina sleeve cylinders (*Figure 3*).
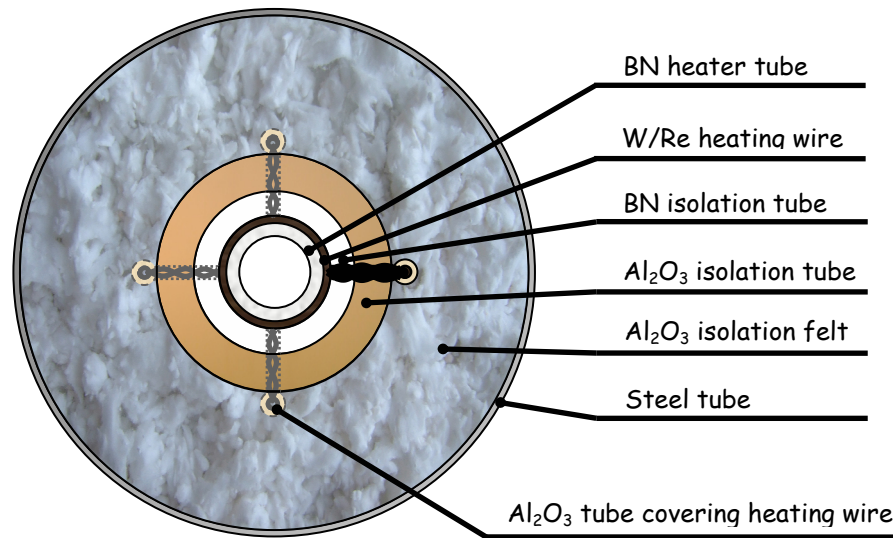
Fig. 3. *Schematic cross-section of the high temperature furnace.*

Afterwards, alumina felt is placed between the alumina protection and the outer steel mantel of the furnace serves as a thermal isolation. Each isolation tube has a small aperture for the heating wires that will be additionally protected by an alumina tube in isolation felt. At higher temperature due to the temperature gradients and different thermal expansion coefficients of the construction materials large forces can occur along the heater axis. The thermal isolation, an alumina felt, provides space for the core tube to expand as needed. The thermal isolation is previously heated at 800 °C for 8-9 hours in air for removing the water and organic inclusions. The furnace has a three stage heater for precise controlling the temperature gradient along the crucible axis. The temperature is controlled by a programmable unit, Eurotherm 2704, with independent feedback loops for all three stages. The temperature can be stabilized within ±0.5 °C at gradients as large as 20 °C/cm.

The output signal controls thyristors for each heater stage. The applied current and voltage on each stage are measured separately. In case of a short connection in the furnace the current is switched off by the monitoring device that is adjusted for certain values of the current threshold. Too high current can damage the electrical connections. The temperature is

measured with W/Re thermocouples Type C in every furnace stage. This type of thermocouples delivers a temperature accuracy of about ±1%. In addition, the temperature of electrical connections will be also measured with a thermocouple Type T (copper-constantan) as a reference for the cold point of the three thermocouples placed inside the furnace. The furnace can have two different internal diameters depending on the desired temperature. For the temperatures up to 1600 °C the furnace with the alumina tube and isolation can be used. This furnace has a 19 mm internal diameter in which a crucible of 14 mm interner diameter (*Figure 4*) can be inserted. At higher temperatures, the inner wall of the steel chamber will be heated and causes degradation of its mechanical properties due to the embittlement. For higher temperatures the furnace with BN ceramics is suitable as described above. Subsequently, the thermal isolation of this furnace is much thicker and the internal diameters of the furnace and therefore of the growth crucible are reduced to 12.5 mm and 8 mm respectively. In *Figure 4* two kind of aforementioned crucibles with inner diameter 8 mm and 14 mm are shown. In this work graphite was used as crucible material. The graphite crucible is 70 mm long and has 3 slots on the side for thermocouples. For safe operation, the inner wall of the steel chamber must not be hotter than 200 °C. To prevent overheating the chamber is equipped with a steel mantel that is cooled by water.
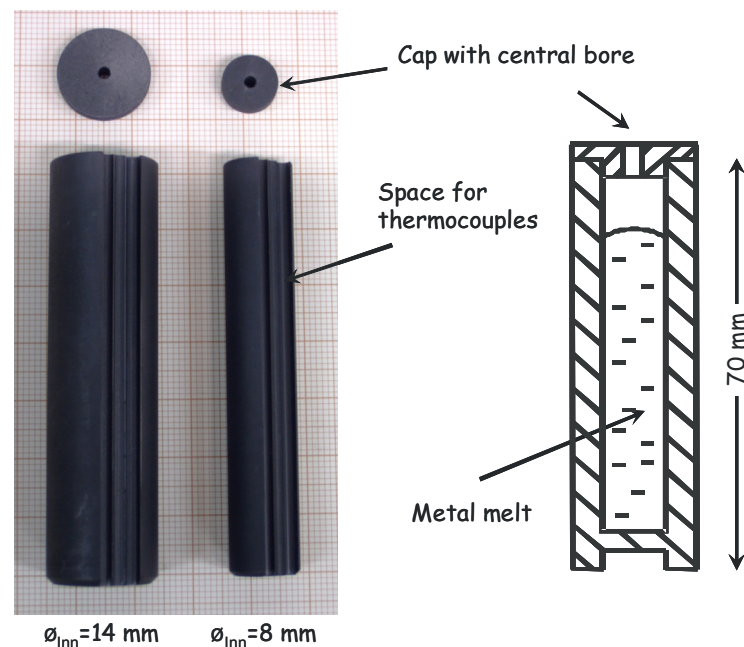
Fig. 4. Side- and schematic view of graphite crucibles.

There is a failsafe system that was built in the cooling water supply. In case of problems with the water supply all heater stages are turned off. All acquired data such as temperatures and pressures are monitored and logged in a computer.

The experimental procedure for the crystal synthesis will be described in *Chapter 4* in the crystal growth part. However, here we would like to give addition information on the operating of the high pressure equipment. After the crucible is loaded with the starting materials, it is placed into the middle of the furnace. Afterwards, the whole bore of the furnace is covered from the top and bottom with alumina ceramics. It is important for ensuring of a good thermal isolation and for preventing heat convection inside the furnace. Especially for the growth experiment in a vertical autoclave position the heat convection plays a crucial role. If heat convection is too strong, the loss of heat for the certain heater stage will be so big that the temperature can not be controlled anymore properly. All free volume in the furnace must be well filled. The heat convection can be reduced by slightly tilting the gas autoclave. The furnace is connected to the plug equipped with electrical feed-through and is placed into the experimental chamber. A high purity of the system is achieved by an initial evacuation of the whole high pressure equipment (30 and 40 mm chambers and capillary) to 10^{-6} mbar. Subsequently, the furnace is annealed in vacuum in order to remove the water adsorbed on the surface of the crucible and the thermal isolation of the furnace. The bake-out is done at around 300 °C for 4-5 hours. After the furnace is cooled to the 50 °C, nitrogen gas is introduced into the system and pumped to the desired value. From this stage the system is ready for the experiment.

In order to test the high pressure system, the furnace is pre-heated to 300 °C under high nitrogen pressure. After this the experiment run can begin according to the desired time-temperature program. A typical growth run follows the temperature program steps listed in *Table I*.

At first, the temperature is slowly increased to 1000 °C during 2 hours and then to the growth temperature. The duration of the second heating stage is selected depending on the desired growth temperature. It is also advisable to heat up slowly at temperatures higher than 1000 °C. Too quicker heating or cooling of the furnace may cause its failure. Then, the temperature gradient is set and the crystal growth dwell starts. As we observed in this study, the crystal with a particular composition x can be synthesised at the p-T conditions lying on the equilibrium line for a particular $Al_xGa_{1-x}N$ composition (see *Chapter 5* and *Chapter 6*). If the temperature or pressure are shifted from this characteristic equilibrium line, another $Al_xGa_{1-x}N$ compound with different composition x will grow. This is a very important during

the cooling process after the growth dwell. For that reason, during the cooling down to 1000 °C the pressure of the system is simultaneously reduced following a particular $Al_xGa_{1-x}N$ equilibrium line. This stage is usually quicker and takes about 1 hour. However, changing temperature and pressure at the same time is difficult and as a result a thin layer of GaN or $Al_xGa_{1-x}N$ with different Al content may form on the crystal surface during the cooling (see *Chapter 4*).

Table I. *Standard temperature program for $Al_xGa_{1-x}N$ growth experiments in gas pressure autoclave. Duration of the crystal growth is 168 hours. The temperature gradient is 80 °C between top and bottom of the crucible.*

Step	Description	Stage temperature, °C			Duration, min	Comments
		bottom	middle	top		
1	Start	50	50	50	-	Pressure is pumped
2	Ramp up	300	300	300	15	Testing the system
3	Dwell	300	300	300	10	Stabilisation
4	Ramp up	1000	1000	1000	120	No gradient
5	Ramp up	1700	1700	1700	120	No gradient
6	Dwell	1700	1700	1700	10	Stabilisation
7	Ramp up	1700	1740	1780	10	Set gradient
8	Dwell	1700	1740	1780	10080	Crystal growth
9	Ramp down	1700	1700	1700	10	Close gradient
10	Ramp down	1000	1000	1000	60	No gradient, reducing the pressure, if it is needed
11	Ramp down	50	50	50	120	No gradient
12	Dwell	50	50	50	-	Hold till stopped

Finally, the temperature is slowly decreased from 1000 °C to 50 °C without intentional decreasing of the pressure. At such low temperatures, the growth kinetics of $Al_xGa_{1-x}N$ is too slow for the effective growth and thus there is no need to control the pressure.

After the cooling, the pressure is reduced to the atmospheric pressure and the autoclave can be opened. At the end of experiment, the heater is kept at 50 °C. Hot water is pumped

through the cooling jacket. This prevents the condensation of water on the wall of the crucible after exposing the cooled system to the air. The steel used for the pressure autoclave may corrode and therefore the mechanical properties can degrade. The heater is taken out from the experimental chamber and disassembled. To recover the grown crystals, the whole crucible with the crystals and remained gallium is placed in hydrochloric acid and aqua regia to etch away excess gallium. Although the crucible material, usually graphite, and the $Al_xGa_{1-x}N$ crystals do not dissolve in acids, selective etching of $Al_xGa_{1-x}N$ crystals may occur if the temperature of the acid is too high (∼50 °C).

After and before every experiment the bore of both 30 mm and 40 mm chambers is polished with sand paper and diamond paste with 10-25 μm grain size and subsequently cleaned with a water-free and non corrosive solvent (usually benzene). For longer breaks between experiments, the chamber bores are protected with a thin grease layer. All alumina pieces used in the furnace should be also heated in order to remove the carbon (comes from graphite crucible) and water. During some experiments the W/Re wires recrystallize and the furnace do not work properly. Unfortunately, the re-isolation of the furnace is not possible, because the W/Re heater wires as well as BN isolation break when the furnace is opened.

3.2   Cubic anvil cell

The maximum pressure obtained in our gas pressure autoclave is about 15 kbar. As it was shown in *Chapter 2*, the nitrides can be thermodynamically stabilized at high temperatures under high pressure. The higher the growth temperature, the higher is the solubility of nitrogen in the melt and the quicker the mass transport occurs during the growth. For example, for GaN temperatures up to about 1670 °C can be applied at 20 kbar nitrogen pressure. In order to increase the growth temperature, one should apply pressure higher than 30 kbar. This can be done using the anvil high pressure technique and a solid pressure transmission medium. There are different kinds of anvils such as hemispherical, cubic and octahedral with different sample size and shape. The anvils can be also used together with an x-ray beam facility for the in-situ sample characterisation. In the III-nitrides research a few studies using anvil technology are reported. Karpinski and Porowski [5] used a hemispherical anvil apparatus for the thermodynamic equilibrium studies of GaN in the pressure range of 15 to 70 kbar and temperatures from 1500 to 2300 °C. To study the congruent melting conditions

of GaN, W. Utsumi *et al.* used a multi-anvil apparatus for synchrotron radiation [6]. By slowly cooling the melt under high pressures they could grow GaN crystals up to 100 μm in size. GaN crystal growth up to 0.5 mm in size using hemispherical anvil was also reported by Kelly *et al.* [7]. They used a cell containing pressed GaN powder used as the source of nitrogen upon heating and a metal alloy consisting of Ga (70 at%) and Mn (30 at%) as reactants. Interestingly, Mn was added in order to increase the solubility of nitrogen. Hasegawa *et al.* successed in the growth of nitrides in a laser heated diamond anvil cell [8].
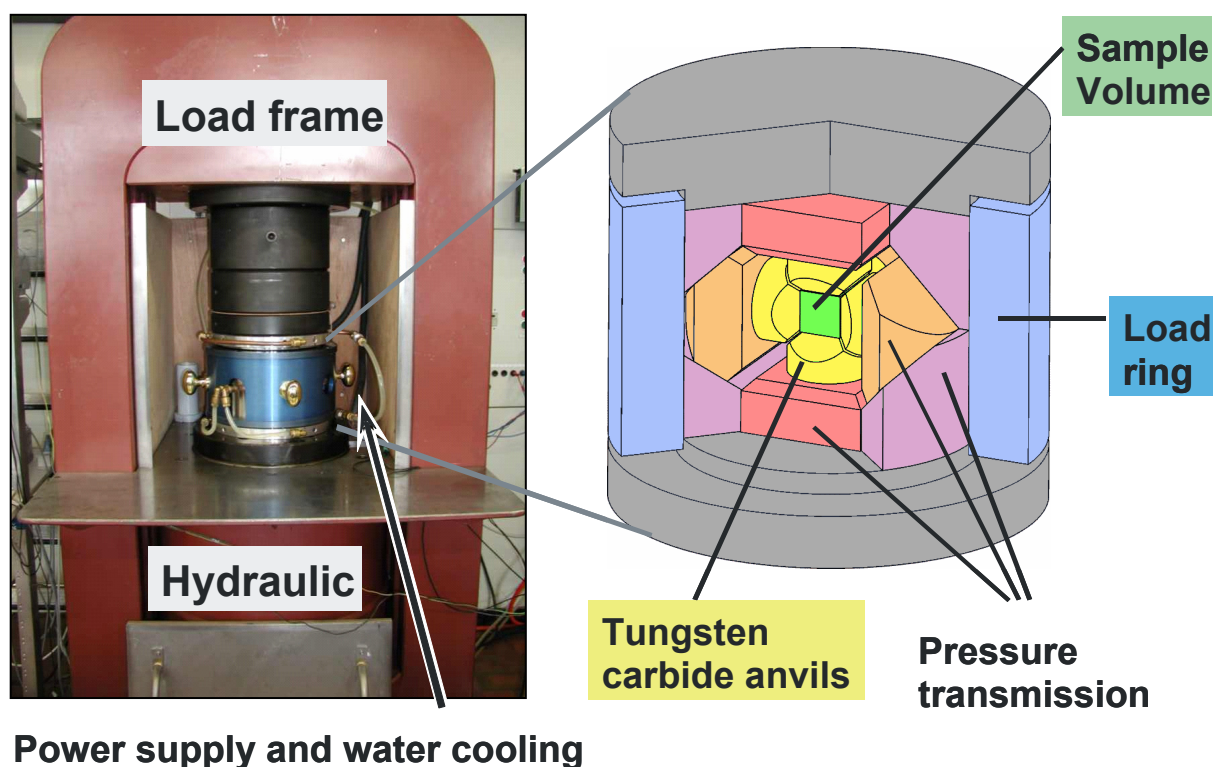
Fig. 5. *Cubic anvil apparatus and schematic setup view [4].*

In this section we focus on use of an anvil apparatus for the $Al_xGa_{1-x}N$ growth. Using cubic anvil cell in our lab [4], Peter Geiser could synthesize $Al_xGa_{1-x}N$ bulk single crystals up to 30% Al from solution in Ga/Al melt. The apparatus is based on a commercially available pressure cell with tungsten carbide anvils as shown in *Figure 5*. The pressure is built up with a 1500 ton oil hydraulic press working perpendicular to the anvil cell, on the two base plates (marked with grey colour in *Figure 5*). The force on the plates is transmitted to a set of eight

large steel dies, which in turn compress the smaller six tungsten carbide anvils, finally applying an amplified pressure on a cubic experimental cell (*Figure 6*). This cell is located at the center of the assembly. The pressure is determined from the measured force of hydraulic press. By applying ∼300 bar oil pressure in the hydraulic press, a pressure of about 30 kbar is generated in the core of cell. The edge length of tungsten carbide anvils is 22 mm. Rubber O-rings serve as spacers between the tungsten carbide anvils. A pyrophylite, alumo-silicate, cube serves as a solid pressure transmitting medium placed in the core of the cell (*Figure* 6). The volume of the cube is about one cubic inch. The assembly has one stage graphite heater placed in the bore of pyrophilite cube. The heater is filled with the BN crucible in the center, and with pyrophilite tablets on the top and bottom. Depending on the dimensions of the cube bore and the graphite heater, the inner diameter of the BN crucible can be chosen between 6.8 and 8.1 mm. The length of the free space in the BN crucible is about 8 mm. This system is capable of applying up to 35 kbar pressure and 2100 °C.
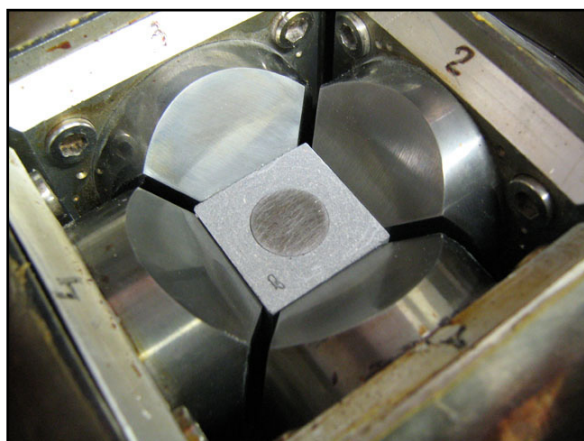
Fig. 6. *Top view on cubic experimental cell: Pyrophilite cube is placed in the core of cell between tungsten carbide anvils.*

In *Figure 7* two types of graphite heaters are shown. Besides the standard graphite heater, a heater with two steel rings on both ends can be used. The latter assembly allows us to reach the desired temperature with electric lower powder applied. For high temperatures, the external load ring and both base plates are water cooled to prevent the anvil from being overheated. If the temperature on the tungsten anvils will be higher than 600 °C the anvils will drastically loose their strength and break. For the pressure calibration, the electrical resistance changes during the phase transitions of Bi, Ba and Tl was used. For heating, a current passes through graphite heater, supplied from outside through the steel parts und two tungsten carbide anvils. The steel parts are isolated with a thin polymer foil. The temperature

is calibrated using B-Type thermocouples and is related to the power dissipated in the pressure cell. Thus, from the applied current and voltage the temperature can be controlled within ±50 °C. In case of a bad connection between graphite heater and tungsten carbide anvils, the resistivity of the cell may increase causing excessive voltage drops and sparks. This leads to the short connection between the steel parts and to the overheating of the tungsten carbide anvils. To avoid this, a water cooling control system is installed that switches off the power supply in case if the current is higher than 550 A and voltage exceeds 5.5 V. The pyrophilite cube should be pre-hardened at 850 °C for 10 hours. The heating/cooling rate is very important due to the possible cube cracking. The pyrophilite cube is typically heated in air up to 400 °C in 4 hours, then to 850 °C at a constant rate of 30 °C/h and after the hardening cooled to room temperature at a constant rate of 100 °C/h. In order to minimize the impurity level in the crystals, the BN crucible was usually heated in vacuum at 1700 °C for several hours.
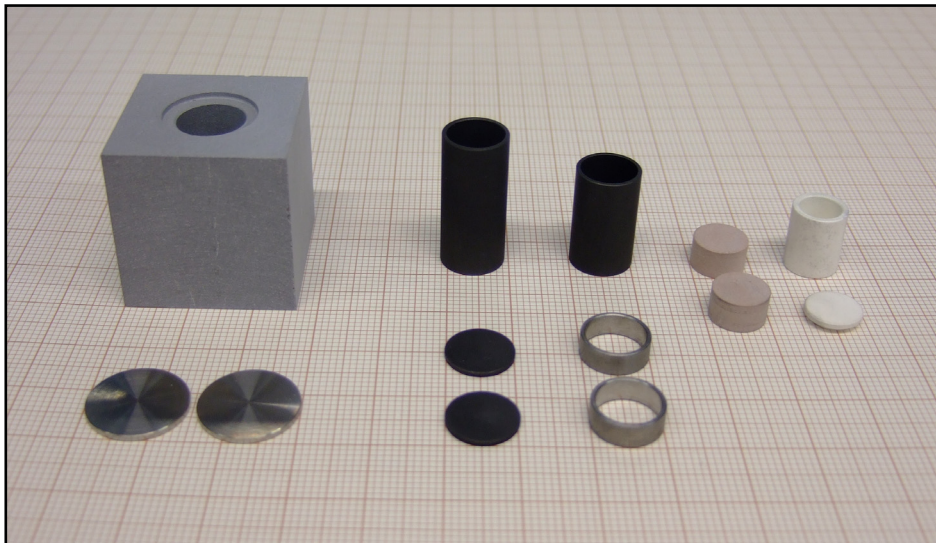
Fig. 7. Sample assembly for the cubic anvil press: Pyrophilite cube, 2 steel disks, two types of graphite heaters, pyrophilite tablets and BN crucible ($\emptyset_{Inn.}$=6.8 mm).

The description of the $Al_xGa_{1-x}N$ growth using this anvil technique was given in the section about $Al_xGa_{1-x}N$ growth from solution. In this study we used the anvil technique to synthesize $Al_yGa_{1-y}N$ powder, similar as reported by H. Saitoh *et al.* [9]. The polycrystalline $Al_yGa_{1-y}N$ samples ($0<y<1$) used as a precursor for $Al_xGa_{1-x}N$ single crystal growth in a gas

pressure autoclave have been synthesized in the cubic anvil press under 30 kbar pressure and 1800 °C. The starting materials were highly pure GaN and AlN (Alfa Ceasar) powders blended with a mortar for suitable compositions (y = 0.2, 0.4, 0.5, 0.9). The samples were filled in boron nitride crucible placed in graphite cylinder that served as a furnace. In the experiments, the pressure was initially increased to 30 kbar at room temperature and then the crucible was heated up to 1800 °C within 1 hour, annealed for 3 hours and finally cooled to room temperature within 1 hour. After the temperature is decreased, the pressure is subsequently released. The pyrophilite cube must be broken apart to get access to the BN crucible and the sintered sample. Sintered samples have a diameter of about 6 mm and are 4 mm height. X-ray measurements show pure $Al_yGa_{1-y}N$ phase.

References:

[1]   J. Karpinski and S. Majorowski, High pressure in research and industry, Proc. of 8th Airapt Conf., Uppsala (1981).

[2]   J. Karpinski, S. Porowski, S. Miotkowska, J. Cryst. Growth **56** (1982) 77-82.

[3]   L. Deffet, L. Lialine, High pressure techniques in general, in A. Van. Itterbeek (editor), Physics of High Pressures and Condensed Phase, North-Holland Publ. Co, Amsterdam (1965) 1-36.

[4]   P. Geiser, Dissertation №16126, ETH Zurich (2005).

[5]   J. Karpinski, S. Porowski, J. Cryst. Growth **66** (1986) 1-10.

[6]   W. Utsumi, H. Saitoh, H. Kaneko, T. Watanuki, K. Aoki and O. Shimomura, Nature Materials **2** (2003) 735-737.

[7]   F. Kelly, D. R. Gilbert, R. Chodecka, R. K. Singh and S. Pearton, Solid-State Electronics **47** (2003) 1027-1030.

[8]   M. Hasegawa, T. Yagi, J. Cryst. Growth **217** (2000) 349-364.

[9]   H. Saitoh, W. Utsumi, H. Kaneko, K. Aoki, Jp. J. Appl. Phys. **43** (2004) L981-983.

Chapter 4

Bulk single-crystal growth of ternary $Al_xGa_{1-x}N$ from solution in gallium under high pressure

4.1 Summary

In this chapter, we report the first growth of (Al,Ga)N crystals with $0.22 \leq x \leq 0.86$ from solution in Ga melt under high nitrogen pressure (up to 10 kbar) and at high temperature (up to 1800 °C) in gas autoclave. A crystal growth rate of up to 0.1 mm/day was achieved, a rate comparable to the growth of GaN from solution, or by the ammonothermal method. For the $Al_{0.86}Ga_{0.14}N$ crystals, the bandgap was determined by the femtosecond two-photon absorption autocorrelation method and is 5.81±0.01 eV. This chapter is published in Journal of Crystal Growth in Priority Communications section, 2009 (see *page 12*). The preliminary studies of the *p-T* equilibrium phase diagram for the growth of $Al_xGa_{1-x}N$ crystals published in this paper were omitted, since the *p-T* diagram was lately explored and published in following paper addressed in the *Chapter 5*.

4.2 Introduction

Due to their particular optical and electrical properties, III-V nitrides, especially GaN, and their ternary alloys are a class of semiconductors of great technical importance. Many GaN-based devices include heterostructures involving alloys of GaN, AlN and InN, with a direct bandgap E_g varying from 0.7 eV for InN to 6.2 eV for AlN [1,2]. Ternary layers such as $Al_xGa_{1-x}N$ are mainly used as electron barriers in power-switching HEMTs, as an active zone in light-emitting structures, or as cladding layers in lasers and as quantum wells in UV LEDs [3-6]. The high optical efficiency of GaN-based devices and, therefore, their potential for

applications are adversely affected by the lattice mismatch to the substrate, by structural defects such as dislocations, and by inhomogeneities in the Al concentration.

(Al,In,Ga)N alloys have been produced as thin films by MBE, MOVPE, and HVPE techniques, mainly on sapphire or silicon carbide substrates [7-9]. Homoepitaxy is strongly preferred and substrates for thin-film deposition would ideally be $Al_xGa_{1-x}N$ single crystals of high crystalline quality. However, growing $Al_xGa_{1-x}N$ crystals poses significant challenges; two of which have been successfully addressed in this study: full control of the growth conditions and proper choice of the solvent. Previously, we have reported the growth of $Al_xGa_{1-x}N$ crystals with up to 30% Al content, using a high-pressure anvil growth technique [10]. In the present study, we have employed a different technique: a high-pressure N_2 gas autoclave for crystal growth from solution. We can precisely control the nitrogen pressure, temperature, temperature gradient, and therefore we can explore the crystal growth conditions in more detail than in the anvil pressure cell. In particular, the gas autoclave provides a thermodynamic equilibrium between the nitrogen gas and $Al_xGa_{1-x}N$ that cannot be established in the anvil pressure cell due to the lack of a gas atmosphere.

The proper choice of the solvent is obviously important. We have used Ga metal as the solvent and have introduced the appropriate amount of Al in the form of previously synthesized polycrystalline $Al_yGa_{1-y}N$. The Al content y has been varied over a wide range. If, instead, Al metal is dissolved in the Ga melt, only a marginal amount of the $Al_xGa_{1-x}N$ phase forms. In addition, alumina crystals can grow or polycrystalline AlN is formed as a result of combustion.

From the solution in Ga melt under high nitrogen pressure, we have been able to grow $Al_xGa_{1-x}N$ bulk crystals with an Al content higher than 22 at%.

4.3   Experimental details

The polycrystalline $Al_yGa_{1-y}N$ precursor material was synthesized by a solid-phase reaction [11] in a cubic anvil at 30 kbar and 1800 °C. The highly pure GaN and AlN (Alfa Ceasar) powders were thoroughly mixed in a ceramic mortar in an Ar atmosphere to yield various compositions ranging from $y = 0.2$ to $y = 0.9$. This starting mixture was placed into a BN crucible which was surrounded by a graphite heater sleeve; the assembly was then placed into the pyrophilite center part of the cubic-anvil high-pressure cell. After the high pressure

was applied, the BN crucible was heated to 1800 °C for 3 hours and, subsequently, cooled to room temperature within one hour. The resulting sintered tablets were ~4-mm thick and ~6-mm in diameter. The polycrystalline precursors were synthesized at all compositions and no miscibility gap was detected. X-ray powder diffraction measurements of the polycrystalline $Al_yGa_{1-y}N$ showed that the peaks shifted according to the Ga-Al content and a slight broadening was observed at intermediate compositions. The full-width at half-maximum (FWHM) for the (002) reflection for all samples did not exceed 0.3° (e.g., 0.26° for $y = 0.35$ and 0.12° for $y = 0.9$).

To grow $Al_xGa_{1-x}N$ single crystals, the precursor material was dissolved in liquid Ga at high temperature and under high nitrogen gas pressure. The high-pressure nitrogen gas system, shown in *Figure 1* of Ref. [12], consists of a compressor and a high-pressure chamber of 40 mm internal diameter with an internal, three-zone furnace. The gas pressure and the temperature were controlled electronically. The combination of the high temperature and pressure provided a substantial technical challenge to the experimental setup. By using BN isolation and W/Re heater wires, a maximum temperature of about 1800 °C could be reached. Such high temperatures are necessary in order to enhance the diffusion of nitrogen into the Ga melt. In order to control both the temperature and the temperature gradient inside the furnace, 3 thermocouples were placed along the graphite crucible and connected to the Eurotherm programming units. The crucible had an internal diameter of 14 mm and was 70 mm long. The previously sintered $Al_yGa_{1-y}N$ pellet was placed in Ga in the upper part of a graphite crucible and this assembly was introduced into the gas pressure chamber (*Figure 1*). By applying a thermal gradient of about 20 K/cm at constant temperature for 6-7 days, $Al_xGa_{1-x}N$ crystals grew in the colder part of the crucible. In order to suppress the formation of GaN crystals, the applied pressure and temperature needed to be kept outside the stability region of the GaN phase. This was especially important during the cooling phase at the end of the growth process.

After the growth procedure, the crystals were etched from the remaining solidified Ga/Al melt using hydrochloric acid and *aqua regia*. The composition of the $Al_xGa_{1-x}N$ crystals was measured by laser ablation inductively coupled plasma mass spectrometry (LA-ICP-MS). For LA-ICP-MS investigations, $Al_xGa_{1-x}N$ crystals were ablated with an ArF excimer laser (193 nm) in a He gas flow. An aerosol was analyzed with a Perkin-Elmer quadrupole mass spectrometer. Ratios of the elements were calculated from the mass spectrometer count rates using standard procedures. In addition, EDX was used for qualitative chemical analysis. The

crystal structure was determined on a four-circle Oxford X-ray diffractometer equipped with a CCD using Mo radiation.
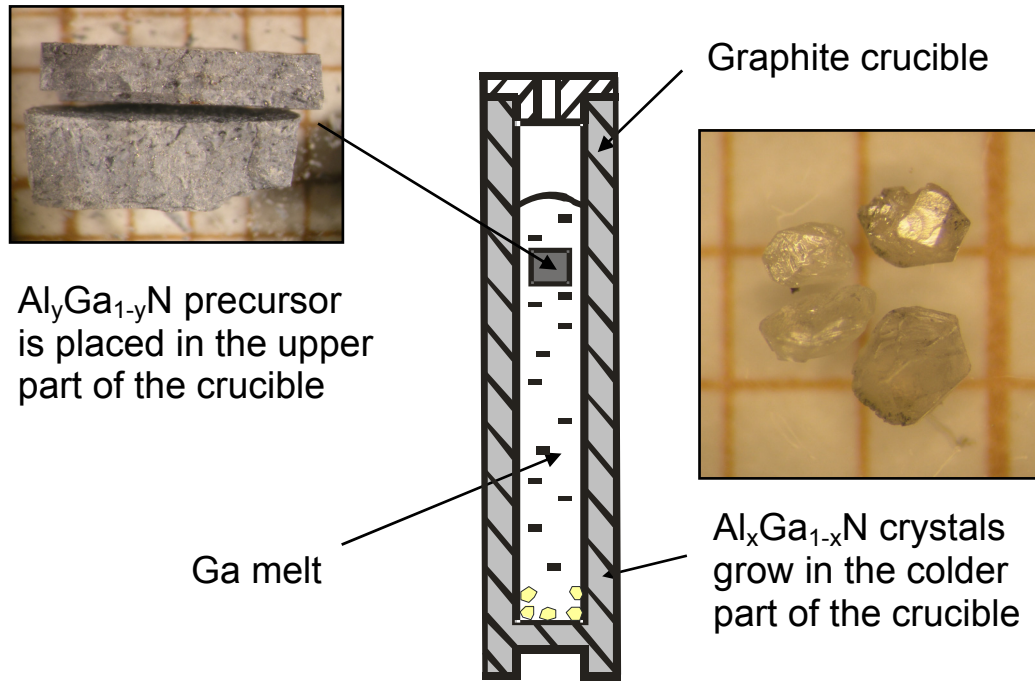
Fig. 1. *Schematic illustration of the $Al_xGa_{1-x}N$ crystal growth crucible. Pre-reacted pellets (left) and $Al_{0.86}Ga_{0.14}N$ crystals, growth run AlGa7, (right) are shown on a 1 mm grid.*

The optical bandgap studies of $Al_xGa_{1-x}N$ ($x = 0.86$) crystals have been also performed using a femtosecond, pump-probe spectrometry technique, based on the two photon absorption (TPA) autocorrelation measurements [13]. The TPA study was performed in the transmission mode, using a commercial Ti:Sapphire mode-locked laser that produced two trains of 100-fs long pulses at a 76-MHz repetition rate. The probe-light wavelength was tuned in the range between 840 nm and 856 nm and had the average power of 5 mW. The pump beam was a frequency-doubled probe light with the average power of 2 mW.

4.4 Results and discussion

Single crystals of $Al_xGa_{1-x}N$ with $x = 0.22, 0.37, 0.5, 0.62, 0.74, 0.78$ and 0.86 were successfully grown using the above procedure. For some of the compositions, more then one experiment was performed. The crystals were up to $\sim 0.8 \times 0.8 \times 0.8$ mm^3 in size and were colorless, of a hexagonal habit, and of wurtzite structure. The morphology of our crystals depends on the process pressure, temperature range, temperature gradient, and nitrogen supersaturation. Crystals grown at lower temperature and otherwise similar conditions tend to be smaller. This trend is likely to be associated with the solubility of nitrogen in the Ga melt at different temperatures: the higher the temperature, the higher the solubility of nitrogen. At the growth temperature of 1500 °C, the $Al_xGa_{1-x}N$ crystals grew slowly and were very small (up to $\sim 0.1 \times 0.1 \times 0.1$ mm^3). Larger crystals were grown at 1800 °C.

In order to study the crystal growth and the pressure-temperature (p-T) equilibrium of the (Al,Ga)N system, several experiments were performed at 5 to 10kbar nitrogen pressure and at a temperature of 1490-1780 °C. The p-T equilibrium diagram is presented in *Chapter 5*. With increasing Al content, growth of $Al_xGa_{1-x}N$ crystals takes place at lower pressures than that required for GaN [14] at the same temperature. By choosing the appropriate pressure and temperature conditions, $Al_xGa_{1-x}N$ crystals with a particular Al composition could be grown. For example, to grow crystals with $x = 0.62$, the required conditions are ~ 8.4 kbar and 1540 °C. By decreasing the pressure to approx. 2.54 kbar and maintaining almost the same temperature of 1550 °C, crystals with $x = 0.85$ could be synthesized.

The *p-T* equilibrium diagram was further supported by monitoring the chemical composition of the polycrystalline $Al_yGa_{1-y}N$ pellets before and after the experiments: the pellets did not decompose during the experiments, but their Al content changed depending on the growth condition. We observed that the pellets and the crystals ended up with a similar composition. In a particular growth run, the starting material had $y = 0.6$ and after keeping the pellet for 168 hours at 1550 °C and 2.54 kbar, its composition changed to $y = 0.85$, as determined by X-ray diffraction measurements.

In *Figure 2*, the relationship between the lattice parameter c and the chemical composition of $Al_xGa_{1-x}N$ crystals is summarized. Two methods have been employed to determine the composition: laser ablation mass spectrometry and a structure refinement based on the X-ray diffraction data. In the latter method, we assumed that Al atoms replaced Ga and the overall occupation of the Ga/Al site was 100 %.

Then, the ratio Al/Ga was refined. No twinning or intergrowth could be detected. The lattice parameter linearly depends on *x*, according to Vegard's law. The *c*-axis lattice constant of $Al_xGa_{1-x}N$, for, e.g., x = 0.86 is 5.015(1) Å and is smaller than that of pure GaN (5.185 Å) [15]. As the laser ablation drilled a small hole into the crystals, the depth profile of the composition was monitored. Accordingly, the Ga/Al ratio was found to be constant (±0.5%) inside the crystals. Overall, there was satisfactory agreement between the compositions determined by two methods. On the surface of our crystals an about 1-μm-thick, inhomogenously substituted $Al_yGa_{1-y}N$ capping layer with varying Al content was formed during the crystal cooling process, depending on the cooling profile. Finally, the EDX measurements did not detect any oxygen or carbon impurities.
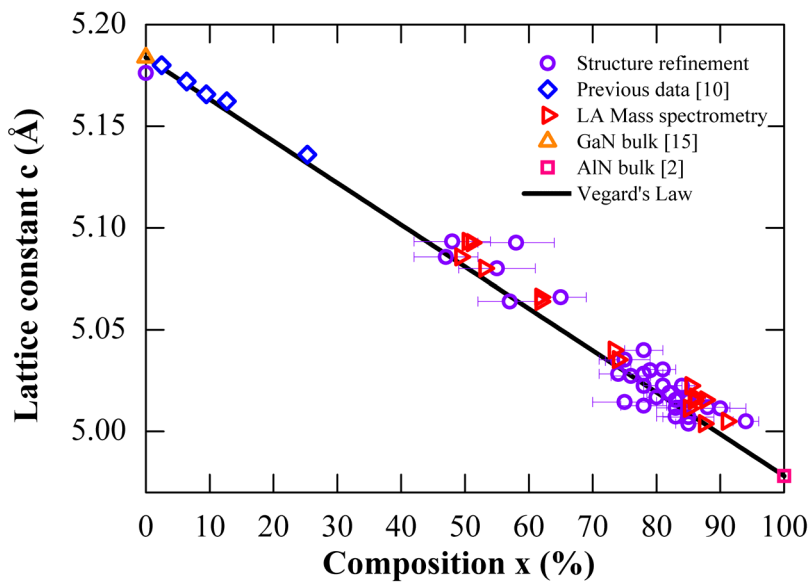
Fig. 2. *The lattice parameter c versus the Al content of the bulk $Al_xGa_{1-x}N$ single crystals. The composition was determined by a full structure refinement of X-ray diffraction and by Laser ablation mass spectroscopy. The solid line represents Vegard's law.*

The results of TPA optical bandgap studies are given in *Figure 3*, where we show the time-resolved normalized change in the transmissivity $\Delta T/T$ waveforms of the probe beam, measured within the above-mentioned tuning range. While a strong autocorrelation-type signal is observed (Gaussian shape with FWHM of 290 fs) for an 840 nm probe wavelength,

the signal completely disappears at 856 nm. The nonlinear autocorrelation response is due to the nonlinearity associated with the bandgap and occurs when the total energy of incident photons [one pump photon and two probe photons (TPA effect)] is greater that the bandgap. Thus, by plotting the autocorrelation signal amplitude, which is proportional to the TPA absorption coefficient [16] (see inset in *Figure 3*), the optical bandgap of $Al_{0.86}Ga_{0.14}N$ was determined to be 5.81±0.01 eV.
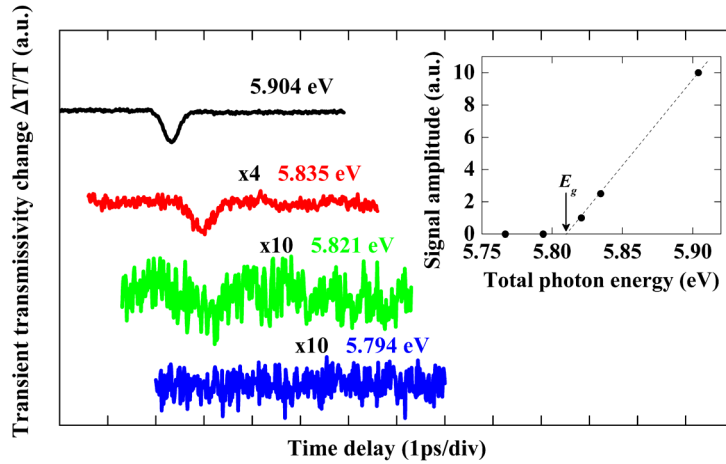

Fig. 3. *Two-photon absorption autocorrelation, ΔT/T, signals versus the time delay for the $Al_{0.86}Ga_{0.14}N$ crystal, measured for different total energy of the incident photons. The increased sensitivity factor is also labeled. The inset shows the TPA signal amplitude dependence on the total photons energy with the optical bandgap absorption edge indicated.*

The compositional dependence of the bandgap of $Al_xGa_{1-x}N$ is a subject of many studies with conflicting results. This dependence is usually described by following empirical expression:

$$E_g^{Al_xGa_{1-x}N}(x) = x \cdot E_g^{AlN} + (1-x) \cdot E_g^{GaN} - b \cdot x \cdot (1-x)$$

where E_g is the bandgap of binary nitrides, 3.4 for GaN and 6.2 for AlN [2], x is the AlN molar fraction, and b is the bowing parameter. The bandgap values for thin films in relation to the Al composition reported by various researches were extracted from photoluminescence or low temperature optical reflectance measurements as well as transmission and photothermal deflection spectroscopy [17,18,19]. The bowing parameters disperse from -0.8 eV (upward bowing) to +2.6 eV (downward bowing) T = 300 K as summarized by Lee *et al.* [20] and later

by Yun *et al.* [17]. This spread emanates mainly from the dispersion in the quality of $Al_xGa_{1-x}N$. It is known that nitride thin films are characterised by the induced strain caused by the difference between thermal expansion of the films and the substrates. If the quality of thin film improves, this may result in a smaller bowing parameter. The theoretically predicted value is 0.53 eV [21]. For comparison the bandgap energies of $Al_{0.86}Ga_{0.14}N$ crystals estimated by TPA absorption as described above and of some $Al_xGa_{1-x}N$ thin films as a function of Al composition are shown in *Figure 4*. The analyzed thin films were prepared by different techniques such as MBE or MOCVD grown on c-plane sapphire. Brunner *et al.* [18] estimated the bowing parameter of 1.3±0.2 eV for $Al_xGa_{1-x}N$ thin films grown by plasma induced molecular beam epitaxy (IPMBE) at temperatures between 810 and 1000 °C. For MBE thin films grown at temperatures 600-670 °C, Yun *et al* [17] reported b=1.0 eV. Shan *et al.* [19] performed the optical absorption studies on $Al_xGa_{1-x}N$ thin films grown by MOCVD and estimated b=1.33 eV. As it can be seen in *Figure 4*, the bandgap value of $Al_{0.86}Ga_{0.14}N$ crystals is on the line for b=0 eV. However, the additional bandgap studies for $Al_xGa_{1-x}N$ crystals over the entire compositional range are needed in order to draw any conclusion.
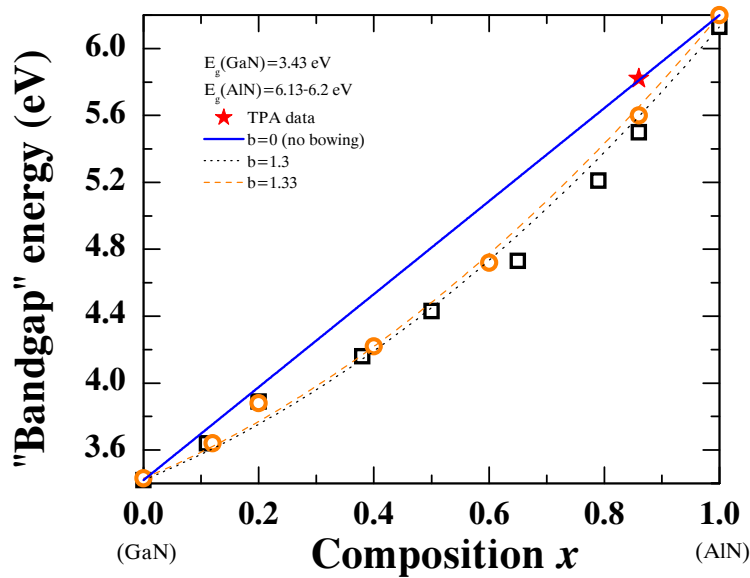
Fig. 4. *Energy bandgap data of $Al_xGa_{1-x}N$ plotted as a function of Al composition:* ★ - *TPA data for $Al_{0.86}Ga_{0.14}N$ crystals,* ○ – *Shan. et al [19] for $Al_xGa_{1-x}N$ thin films grown by MOCVD giving a bowing parameter 1.33 eV,* □ – *Bruner et. al [18] for $Al_xGa_{1-x}N$ thin films grown by MBE giving a bowing parameter b=1.3±0.2 eV. The blue line shows the case of zero bowing.*

References:

[1]   B. Maleyre, S. Ruffenach, O. Briot, B. Gil, and A. Van der Lee, Superlattices and Microstructures **36** (2004) 517-526.

[2]   M. Levinshtein, S. Rumyantsev, and S. Shur, Properties of advanced semiconductors materials: GaN, AlN, InN, BN, SiC, SiGe; John Wiley & Sons, Inc., New York, 2001.

[3]   W. Saito, Y. Takada, M. Kuraguchi, K. Tsuda, I. Omura, T. Ogura, and H. Ohashi, IEEE Transaction on electron devices **50** (2003) 2528-2531.

[4]   S. Nakamura, M. Senoh, S. Nagahama, N. Iwasa, T. Yamada, T. Matsushita, H. Kiyoku, Y. Sugimoto, T. Kozaki, H. Umemoto, M. Sano, and K. Chocho, Appl. Phys. Lett. **72** (1998) 211-213.

[5]   H. X. Jiang and J. Y. Lin, Opto-electronics Rev. **10** (2002) 271-286.

[6]   T. J. Schmidt, X. H. Yang, W. Shan, J. J. Song, A. Salvador, W. Kim, O. Aktas, A. Botchkarev, and H. Morkoc, App. Phys. Lett. **68** (1996) 1820-1822.

[7]   E. Iliopoulos, K. F. Ludwig, T. D. Moustakas, and S. N. G. Chu, Appl. Phys. Lett. **78** (2001) 463-465.

[8]   B. Baranov, L. Däweritz, V. R. Gutan, G. Jungk, H. Neumann, and H. Raidt, Phys. Status Solidi (a) **49** (1978) 629-636.

[9]   Y. Koide, N. Itoh, K. Itoh, N. Sawaki, and I. Akasaki, Jpn. J. Appl. Phys. **27** (1988) 1156-1161.

[10]   P. Geiser, J. Jun, S. M. Kazakov, P. Wägli, L. Klemm, J. Karpinski, and B. Batlogg, Appl. Phys. Lett. **86** (2005) 081908.

[11]   H. Saitoh, W. Utsumi, H. Kaneko, and K. Aoki, Jpn. J. Appl. Phys. **43** (2004) L981-983.

[12]   J. Karpinski, G. I. Meijer, H. Schwer, R. Molinski, E. Kopnin, K. Conder, M. Angst, J. Jun, S. Kazakov, A. Wisniewski, R. Puzniak, J Hofer, V. Alyoshin, and A. Sin, Supercond. Sci. Technol. **12** (1999) R153-181.

[13]   C. Rauscher and R. Laenen, J. Appl. Phys. **81 (6)** (1997) 2818-2821.

[14]   J. Karpinski, J. Jun, and S. Porowski, J. Cryst. Growth **66** (1984) 1-10.

[15]   I. Vurgaftman, J. R. Meyer, and L. R. Ram-Mohan, J. Appl. Phys. **89 (11**) (2001) 5815-5875.

[16]   S. Krishnamurthy, K. Nashold, and A. Sher, Appl. Phys. Lett. **77** (2000) 355-357.

[17] F. Yun, M. A. Reshchikov, L. He, T. King, and H. Morkoc, J. App. Phys. **92** (2002) 4837-4839.

[18] D. Brunner, H. Angerer, E. Bustarret, F. Freudenberg, R. Höpler, R. Dimitrov, O. Ambacher, and M. Stutzmann, J. Appl. Phys. **82** (1997) 5090-5096.

[19] W. Shan, J. W. Ager, K. M. Yu, E. E. Haler, M. C. Martin, W. R. McKinney, W. Yang, and W. Walukiewicz, J. Appl. Phys. **85** (1999) 8505-8507.

[20] S. R. Lee, A. F. Wright, M. H. Crawford, G. A. Petersen, J. Han, and R. M. Biefeld, Appl. Phys. Lett. **74** (1999) 3344-3346.

[21] A. F. Wright and J. S. Nelson, Appl. Phys. Lett. **66** (1995) 3051-3053.

Chapter 5

Al$_x$Ga$_{1-x}$N bulk crystal growth: influence of the growth parameters and structural properties

5.1 Summary

In this chapter, the growth conditions of the single Al$_x$Ga$_{1-x}$N crystals with 0.22<x<0.91 from solution in Ga/Al melt have been determined. The influence of the temperature and the choice of the Al source on the crystal growth are discussed. With increasing growth temperature the solubility of Al$_x$Ga$_{1-x}$N in the liquid gallium is enhanced and therefore the growth of crystals up to 0.8x0.8x0.8 mm^3 in size was achieved.

The *p-T* equilibrium phase diagram of (Al,Ga)N (*s*) + Al/Ga (*l*) + N$_2$ (*g*) system for the various Al content in solid phase is presented. According to the Gibbs rule, the coexistence of these 3 phases (liquid Ga/Al solution, N$_2$ gas and Al$_x$Ga$_{1-x}$N solid) is only possible on the equilibrium curve for particular Al composition *x*. The determined equilibrium lines for particular Al compositions supported by experimental data are shown. By choosing the appropriate pressure and temperature the Al$_x$Ga$_{1-x}$N crystals with a particular Al composition can be grown.

5.2 Introduction

In the last years, the interest in III-nitride materials have become of technical significance due to their optical and electrical properties. In particular, the ternary Al$_x$Ga$_{1-x}$N alloy is a key material in ultra-violet light emitting diodes, power-switching HEMTS and lasers since the band gap energy can be changed from 3.4 to 6.2 eV, depending on the atomic composition. The application of III-nitride materials is still expanding, since the significant progress in

synthesis has been achieved in recent years. Many methods have been developed for depositing $Al_xGa_{1-x}N$ thin films such as MBE [1], HVPE [2] or well-established MOVPE [3,4] and recent research is mostly concentrated on the optimization of the deposition techniques and on the improvement of the structural properties. Although the growth of bulk AlN by sublimation or GaN using ammonothermal method or low/high nitrogen pressure solution methods have been studied by many groups [5-7], a relatively little is known about the growth of bulk $Al_xGa_{1-x}N$ [8].

Recently, we reported on the growth of bulk single $Al_xGa_{1-x}N$ crystals with $0.5<x<0.9$ from solution under high nitrogen pressure (up to 10 kbar) and at high temperature (up to 1800 °C) [9]. We have used Ga metal as the solvent and we have introduced the proper amount of Al in the form of previously synthesized polycrystalline $Al_yGa_{1-y}N$. The high-pressure nitrogen gas autoclave was used which allowed precise control of p-T growth conditions. Several experiments in a wide range of temperatures and pressures were carried out in order to determine optimal p-T conditions for the growth of $Al_xGa_{1-x}N$. We found that by varying the p-T conditions $Al_xGa_{1-x}N$ crystals with a desired Al composition can be grown.

In this paper we report the detailed aspects of the crystal growth, in particular the influence of the amount of aluminum introduced into the melt (up to 1.2 at%) and of p-T conditions on the composition of the grown crystals. We also focus on the crystallographic characterization of the crystals that provide information about their structural quality.

On the basis of the growth experiments and of the calculation of the thermodynamic functions we have derived the equilibrium lines for the $Al_xGa_{1-x}N$ for the whole range of Al content and have updated the experimentally estimated p-T equilibrium phase diagram of (Al,Ga)N compound at high N_2 pressure for various compositions reported previously [9].

5.3   Experimental details

Crystals were grown in a high-pressure nitrogen gas autoclave, in which the maximum working pressure of 12 kbar and the temperature of about 1800 °C can be reached. The high pressure system consists of a compressor, a pressure intensifier and a 40 mm internal diameter high-pressure chamber with an internal, three zone furnace. The nitrogen gas was first pumped up to 3 kbar to the experimental chamber by using a commercial membrane gas compressor (Nova Swiss), and then compressed to the desired value with a pressure

intensifier. The crystal growth has been carried out from the solution in Ga melt under high nitrogen pressure (up to 10 kbar) and at high temperature (up to 1780 °C). Aluminum metal, pre-reacted polycrystalline $Al_yGa_{1-y}N$ or a commercially available AlN powder (Alfa Ceasar) were used as a source of aluminum and nitrogen. Most experiments we have used the pre-reacted polycrystalline $Al_yGa_{1-y}N$ or AlN, because this method led to the best results. Such pre-reacted polycrystalline $Al_yGa_{1-y}N$ in form of a sintered pellet was placed in the Ga melt in the upper part of a graphite crucible and this assembly was introduced into the furnace placed in the experimental chamber as shown previously [9]. The crucible was first heated to 300 °C during 10 min, then to 1000 °C at a constant rate of ~6 °C/min and finally to the desired temperature within 1-2 hours. The crucible was kept at the dwell temperature with a gradient $\Delta T = 15$-35 °C/cm along the 70 mm long crucible. During the dwelling, the nitrogen pressure was kept constant.

$Al_xGa_{1-x}N$ crystals grew in the colder part of the crucible. The temperature was measured by W/Re thermocouples and we estimate it to be correct within ~1 %. In the last stage of the experiment, the crucible was cooled to 1000 °C at a constant rate of ~8-10 °C/min and subsequently to the room temperature at ~6 °C/min. During cool-down the pressure was decreased to follow the calculated p-T equilibrium line of $Al_xGa_{1-x}N$ for the particular composition x (*Figure 4*). Typical duration of the complete growth cycle was 130-170 hours. The crystals were etched from the remaining solidified Ga/Al melt with hydrochloric acid and *aqua regia*.

The crystals were characterized by X-Ray diffraction on a single-crystal diffractometer equipped with a CCD detector (Xcalibur PX, Oxford Diffraction). Data reduction and analytical absorption correction were performed using the software package CrysAlys [10]. The composition of the crystals was measured by laser ablation inductively coupled plasma mass spectrometry (LA-ICP-MS) [11] as well as by structure refinement technique on F^2 using SHELXL [12]. Details of Al composition measurements were published in Ref. [9]. In this method the Al/Ga ratio was measured on various points of the crystals. The variation of the Al/Ga ratio for a particular crystal was up to $\pm$ 0.02. The polycrystalline $Al_yGa_{1-y}N$ pellets were characterized by X-Ray diffraction on a STOE Powder diffractometer and their Al content was estimated from the refined lattice parameters according to the Vegards law.

5.4 Results and discussion

The single $Al_xGa_{1-x}N$ crystals with $0.22<x<0.91$ were synthesized from solution in Ga melt. They grew spontaneously on the wall and bottom of the crucible. The crystals are colorless, up to $0.8 \times 0.8 \times 0.8$ mm^3 in size and of a hexagonal habit (*Figure 1*). The shape of the crystals varies from the platelets to the bulky form depending on the *p-T* conditions. For a given pressure crystals with low Al content were grown at lower temperature and are of smaller size and platelet-shaped. The experiments at small supercooling corresponding to lower supersaturations resulted in slower growth in the *c*-direction in comparison to the growth in perpendicular directions. High temperatures favored bulky shapes following by relatively faster growth in the *c*- axis direction. The *c*-axis of the crystals is perpendicular to
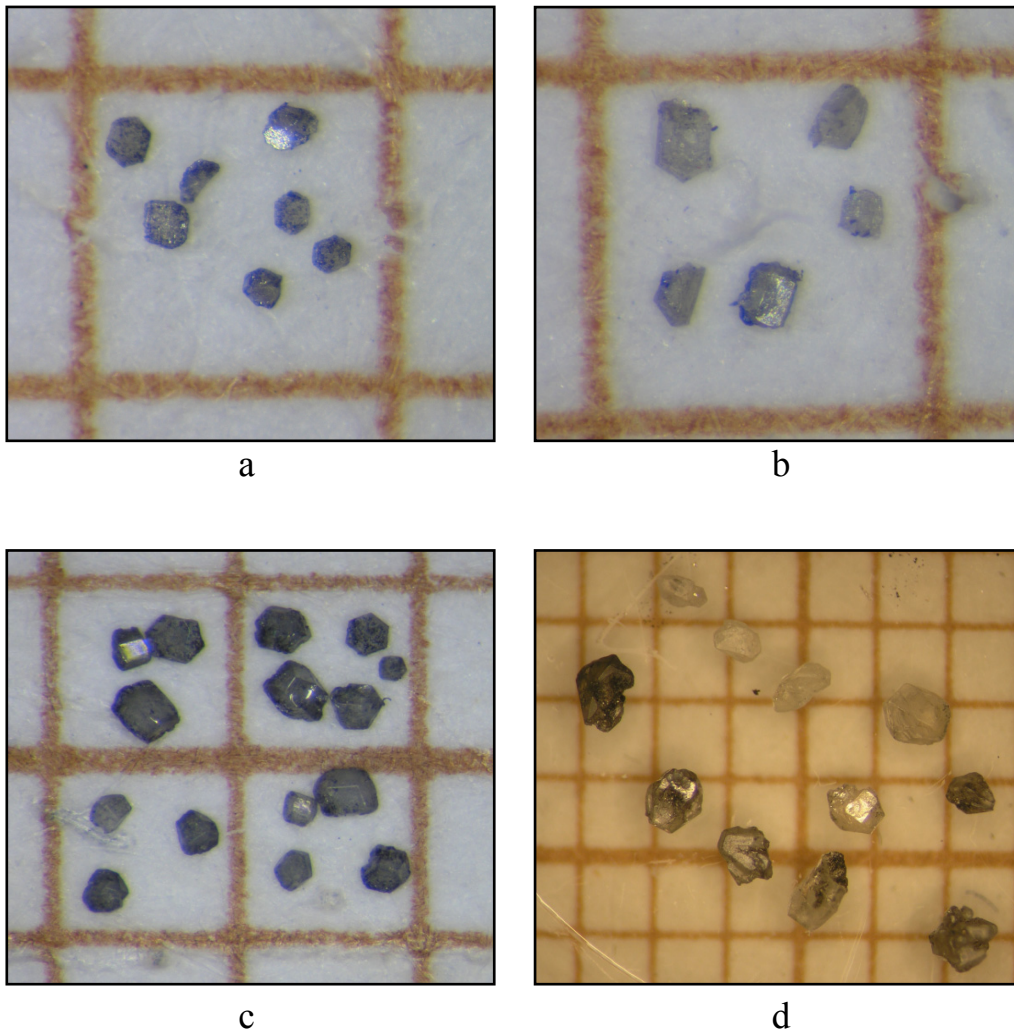
Fig. 1. $Al_xGa_{1-x}N$ crystals with Al composition x: a) 0.37 (AlGa29), b) 0.50 (AlGa25), c) 0.62 (AlGa18) and d) 0.86 (AlGa7). The scale of the square is to 1 mm.

the hexagonal surface of the platelet. The dark appearance is due to the graphite coating on the surface of the crystals, since they were grown in a graphite crucible. We also observed a reaction between liquid Ga and the graphite crucible. This reaction occurs only at high temperature (T~>1600 °C) and does not prevent the growth of the crystals. In *Table I* the *p-T* growth conditions and resulting Al content of the crystals are given for the various runs. For the run AlGa12, crystals with *x*=0.91 and 0.87 were found in the crucible. The Al composition in the precursor before and after experiment is also shown.

Table I. *Growth conditions of $Al_xGa_{1-x}N$ crystals*

Run name	Precursor composition: before	after	Pressure (kbar)	Dwell time (h)	Temperature (°C), (±1% accuracy)	Al composition x
AlGa27	0.6	0.53	9.98-10.15	144	1488	0.22
AlGa29	0.91	0.91	5.00-5.17	166	1426	0.37
AlGa23	0.58	0.55	9.56-9.80	165	1518	0.51
AlGa25	0.6	0.58	9.55-9.73	163	1500	0.50
AlGa18	0.38	0.52	8.32-8.50	166	1542	0.62
AlGa22	0.58	0.66	9.20-9.53	166	1561	0.74
AlGa33	0.62	0.63	4.19-4.28	167.5	1550	0.78
AlGa11	0.53	0.78	4.86-5.41	166	1660	0.84
AlGa30	-	-	6.00-6.16	72	1718	0.85
AlGa15	0.33	0.80	7.57-7.80	50.5	1760	0.85
AlGa28	0.6	0.85	2.50-2.58	168	1546	0.86
AlGa32	-	-	6.00-6.12	336	1720	0.86
AlGa9	-	-	6.40-7.04	136	1760	0.86
AlGa7	0.5	0.81	7.26-7.98	120	1760	0.86
AlGa8	-	-	6.80-7.52	116	1780	0.87
AlGa16	0.33	0.83	7.02-7.16	71	1760	0.87
AlGa12	1	0.88	6.07-7.30	244.5	1760	0.87 and 0.91

In order to investigate the influence of liquid composition on crystal growth in more detail we performed additional growth experiments using Al metal (~0.4 at% in Ga melt) as a source of Al in the melt. This experiment was carried out at 1780 °C with a temperature gradient of 20 °C/cm. In spite of applying the high temperature and temperature gradient only very small crystals grew. The fact that without $Al_xGa_{1-x}N$ pellet as the source of nitrogen and aluminum the efficiency of crystallization was much lower indicates that the enhanced nitrogen access to the solution obtained with $Al_xGa_{1-x}N$ pellet is important for the crystal growth. Moreover, as by-product, Al_2O_3 crystals were observed. Aluminum has an affinity for

oxygen, so all oxygen must be eliminated from the crystal growth zone. Further experiments with a different amount of Al metal (up to 30 at%) in the Ga melt ended up with the so called self-propagating combustion of Al metal and its conversion into AlN powder. The growth of $Al_xGa_{1-x}N$ crystals by this combustion reaction is impossible. M. Bockowski *et al.* [13, 14] investigated this reaction while searching for the possibility to grow the AlN crystal from the solution in Al melt under high nitrogen pressure. While they reported that at pressure higher than 6.5 kbar the AlN combustion can be suppressed, we do not suppressed the AlN combustion reaction even up to 10 kbar nitrogen pressure.


a)   b)
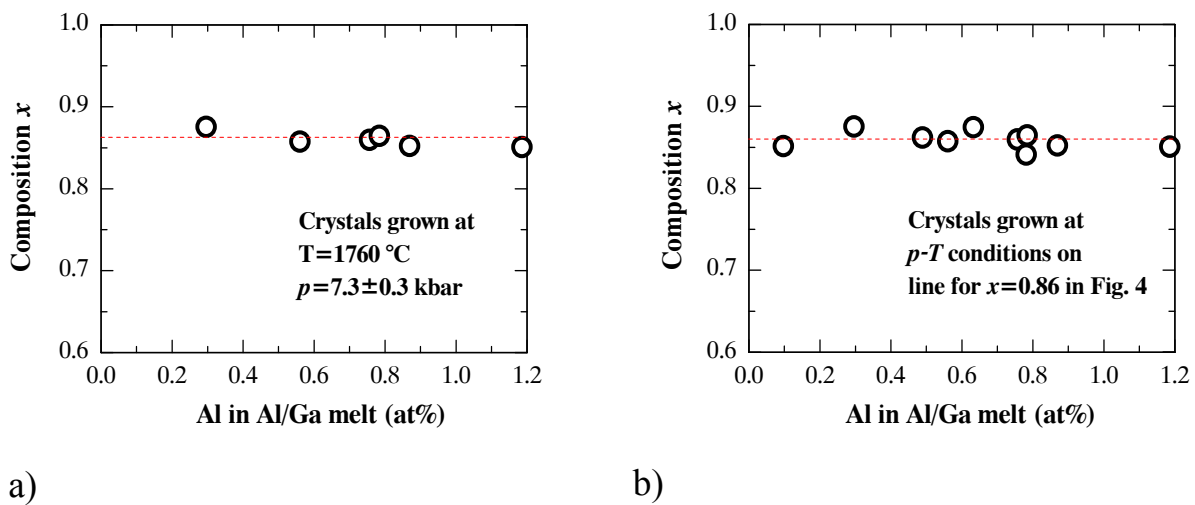
Fig. 2. The Al content x in $Al_xGa_{1-x}N$ crystals as a function of the Al amount introduced into the melt with the pre-reacted polycrystalline $Al_yGa_{1-y}N$ pellet: a) for the crystals grown at constant temperature 1760 °C and p = 7.3 ± 0.3 kbar; b) for the crystals grown at p-T conditions lying on the x=0.86 line in Figure 4.

Instead of Al metal as an Al source we introduced the pre-reacted polycrystalline $Al_yGa_{1-y}N$ nitride or AlN powder for all further experiments. By a proper composition in the pellet the amount of Al introduced into the Ga melt can be controlled. The mass of the pellet for most experiments was kept nearly constant. *Figure 2a* shows the composition of the crystals grown from Ga melt with various amounts of Al. Here, the percentage of Al content relates to Al compared to Ga in the Ga melt (~9-15 g) and in the $Al_yGa_{1-y}N$ pellet (~0.38 g). All experiments were done at the same temperature of 1760 °C and at 7.0-7.6 kbar. The Al composition of the $Al_xGa_{1-x}N$ crystals was $x=0.86\pm0.02$. Obviously, the Al content in the crystals does not depend on the Al content in the Ga melt (up to max. 1.2 at %). We also

observed similar behavior (*Figure 2b*) for all growth experiments of $Al_xGa_{1-x}N$ done at various temperatures and pressures lying on the equilibrium line for *x*=0.86 in *Figure 4*. It should be also mentioned that only the outermost part of the pellet was dissolved. Most remarkably, the Al/Ga composition of the pellet changes during the experiment: its Al/Ga ratio tends to equilibrate towards the value according to the *p-T* phase diagram which also determines the crystals composition (*Figure 3*).
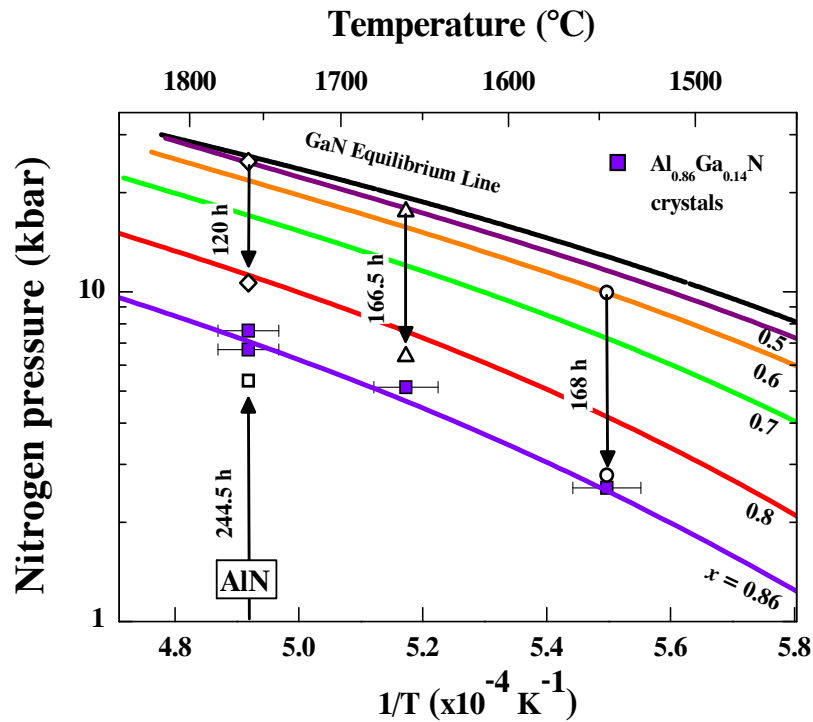
Fig. 3. *Growth of $Al_{0.86}Ga_{0.14}N$ crystals at different temperatures and with different starting compositions of the precursor. Initial and final composition of the polycrystalline $Al_yGa_{1-y}N$ precursor (open symbols connected by arrows) indicate a change of the Al content towards equilibrium. The lines are equilibrium lines calculated for various x (see Chapter 6). The pressure errors are smaller than the size of the symbols.*

In *Figure 3* we indicate the change of the Al content in the pellet, estimated from lattice parameters, before and after the experiment, for runs at which the crystals with *x*=0.86±0.02 were grown (*Table I*: AlGa7, AlGa11, AlGa12 and AlGa28). The dwell time of the experiments varied from 120 to 244.5 h. The composition *y* of the precursor pellets changes

during experiments and shifts after sufficiently long time towards the composition of the crystals. (shown in *Figure 3* by arrows). This indicates equilibration of both precursor and crystals at a given pressure and temperature. The positions of the open symbols correspond to the equilibrium *p-T* conditions for Al content *y* in the pellet. The dynamics of the equilibration process depends on the temperature and dwell time (see *Table I*). For temperatures below ~<1540 °C the equilibrating process is very slow and no significant changes of the Al content in the pellet were observed.

In fact, the final quasi-equilibrium compositions of the pellets should be different (higher Al content) than in the crystals according to the temperature distribution in the crucible (temperature gradient). By the way, this phenomenon is shown in *Figure 3*, where for the longest experiment (>244 h) the composition of the source material (initially AlN) becomes more Al-rich than in the crystal.

More than two dozen experiments in a wide range of temperature and pressure were carried out in order to determine the *p-T* conditions for the growth of $Al_xGa_{1-x}N$. The results of the successful experiments are presented in *Figure 4*. The various symbols correspond to the experimentally observed *p-T* conditions for which the crystals of a particular composition were grown. Inconclusive experiments due to e.g. large *p-T* fluctuations or parasitic chemical reactions with the crucible are not included. We found that $Al_xGa_{1-x}N$ crystals with a particular Al composition could be grown by choosing the appropriate pressure and temperature conditions. For GaN crystal growth the nitrogen pressure during the experiment should be kept higher than the equilibrium pressure over GaN. In case of $Al_xGa_{1-x}N$, the crystals grown at a given pressure and temperature have composition *x* corresponding to equilibrium lines shown in *Figure 4*.

On the basis of the growth experiments the updated *p-T* equilibrium phase diagram for the $(Al,Ga)N(s) + Al/Ga(l) + N_2(g)$ system for various Al compositions is presented. In our previous paper tentative lines for constant composition have been plotted, guided by the shape of the well-established equilibrium line for GaN (*Figure 2* in Ref. [9]). In this report, the lines shown in *Figure 4* are derived using thermodynamic calculations (see *Chapter 6*). Considering the reaction of formation of $Al_xGa_{1-x}N$, one can show that the coexistence of these 3 phases, solid $Al_xGa_{1-x}N$, liquid Ga/Al and gas N_2 is only possible on the equilibrium curves in *p-T* space for certain composition *x*. The solid lines in *Figure 4* are calculated equilibrium curves for various compositions *x*. Based on the experimentally observed *p-T* growth conditions we could derive the pressure-composition dependence for various temperatures.
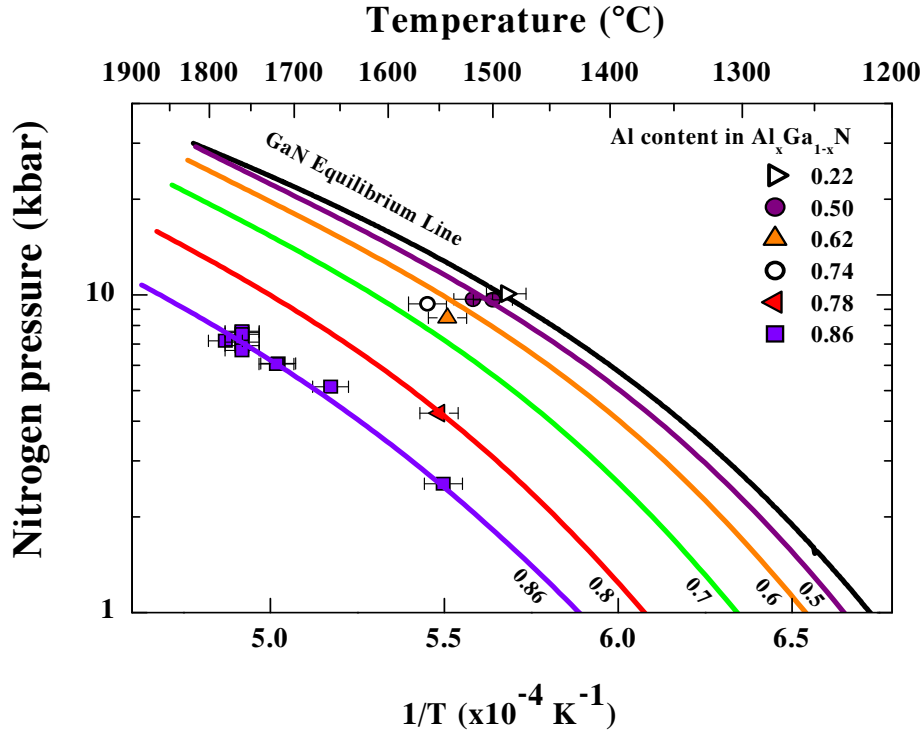
Fig. 4. *Equilibrium pressure of N₂ over Al$_x$Ga$_{1-x}$N +Al/Ga(l) for various Al compositions. Symbols correspond to experimental p-T growth condition for the particular compositions x. Solid lines were calculated using thermodynamic data of nitrogen fugacity. The pressure errors are smaller than the size of the symbols.*

Taking into account the non-ideal behavior of the nitrogen gas, the pressure was converted into the fugacity of nitrogen. This is important because the fugacity of nitrogen is several times higher than the pressure at our experimental conditions. It can be shown that the Gibbs free energy of formation of Al$_x$Ga$_{1-x}$N primarily depends on the Gibbs energy of nitrogen and therefore on the fugacity of nitrogen. Knowing the fugacity-composition dependence for various temperatures the Gibbs free energy as well as the heat and entropy of formation of Al$_x$Ga$_{1-x}$N for various compositions *x* were calculated. In this way we have calculated the *p-T* equilibrium lines for the various Al compositions up to *x*=0.86. Details of thermodynamic calculation will be shown in *Chapter 6*.

According to the *p-T* equilibrium phase diagram, Al$_x$Ga$_{1-x}$N crystals grow at lower pressures, at a given temperature, than GaN crystals [15]. The variation of the temperature during the crystal growth at constant pressure will cause a change of the composition in the

growing crystals. For this reason, the pressure was continuously adjusted during the cool-down after crystal growth, in such way that the equilibrium p-T line for a particular composition x was followed.

Crystals from essentially all runs were characterized by single-crystal X-ray diffraction. The data collection details and the refinement results for some crystals are presented in *Table II*. No additional phases (impurities or intergrown crystals) were detected by examination of the reconstructed reciprocal space sections (*Figure 5*). The average mosaic spread was estimated to be in range of 0.6 - 1.1°. The lattice parameters were determined using all collected reflections. After the analytical X-ray absorption correction, values of R1 indices were within 3.5%. It was assumed that gallium and aluminum ions occupy the same site because the binary AlN and GaN are isostructural compounds with a space group $P6_3mc$. The Al/Ga ratio was refined simultaneously and full occupation of the Al/Ga site was assumed. Positions and atomic displacement parameters of these both ions were held equal. The Al/Ga ratio obtained by structure refinement is in good agreement with the compositions estimated by laser ablation (*Table II* or Ref. 7, *Figure 3*). The composition x shown in the first row was determined by laser ablation mass spectroscopy, while data in the *Table II* were obtained from the structure refinement. $Al_xGa_{1-x}N$ crystals crystallize in the wurtzite (Wz) type structure. The Wz structure can be represented by lattice parameters a in the basal plane, c in the perpendicular direction, and by the internal parameter u, which is defined as the anion-cation bond length divided by the c lattice parameter.
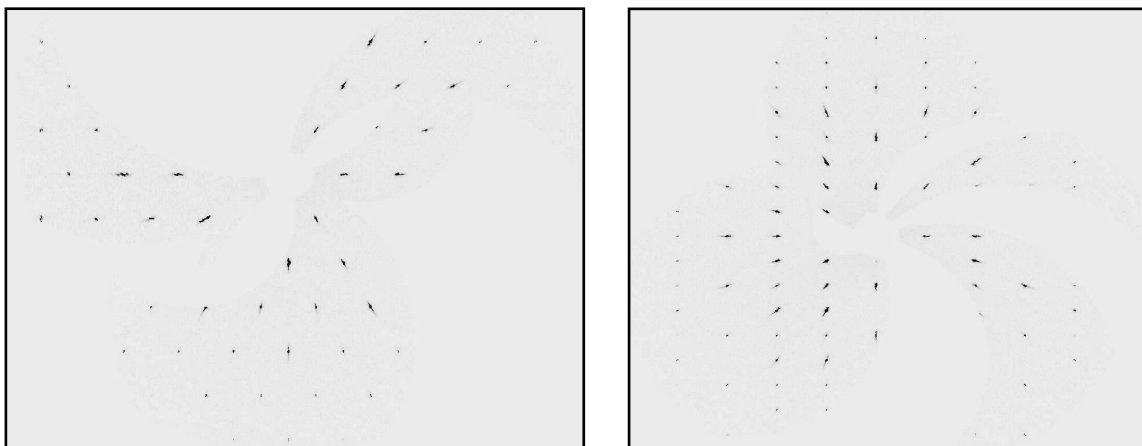
Fig. 5. *Reciprocal space sections of the* $Al_{0.91}Ga_{0.09}N$ *crystal. Left: hk0 and right: h0l sections.*

Table II. Details of the crystal structure refinement of the $Al_xGa_{1-x}N$ crystals. The diffraction study was performed at 295 K using Mo K_α radiation with $\lambda = 0.71073$ Å. The lattice is hexagonal, $P6_3mc$ space group with $Z=2$. The absorption correction was done analytically. A full-matrix least-squares method was employed to optimize F^2.

Chemical formula*	$Al_{0.91}Ga_{0.09}N$	$Al_{0.86}Ga_{0.14}N$	$Al_{0.74}Ga_{0.26}N$	$Al_{0.62}Ga_{0.38}N$	$Al_{0.52}Ga_{0.48}N$	$Al_{0.37}Ga_{0.63}N$
Unit cell dimensions (Å)	a=3.1093(1), c=4.9878(2)	a=3.1126(2), c=5.0033(3)	a=3.1245(2), c=5.0353(3)	a=3.1339(4), c=5.0596(5)	a=3.1422(4), c=5.0842(5)	a=3.1539(2), c=5.1112(3)
Volume (Å³)	41.760(3)	41.979(5)	42.571(5)	43.035(9)	43.473(9)	44.030(5)
Calculated density (g/cm³)	3.498	3.835	4.131	4.219	4.797	5.091
Absorption coefficient (mm⁻¹)	3.326	6.496	9.549	10.630	16.092	19.072
Theta range for data collection (deg)	7.58 to 45.46	7.58 to 37.47	7.55 to 40.44	7.52 to 40.21	7.50 to 39.98	7.48 to 45.72
Index ranges	-5<=h<=6, -5<=k<=6, -10<=l<=9	-5<=h<=5, -5<=k<=5, -8<=l<=6	-4<=h<=4, -5<=k<=4, -2<=l<=9	-3<=h<=4, -5<=k<=4, -7<=l<=9	-4<=h<=5, -3<=k<=5, -9<=l<=4	-5<=h<=3, -4<=k<=5, -10<=l<=6
Reflections collected/unique	432/146 $R_{int.}$=0.0219	600/92 $R_{int.}$=0.0431	447/81 $R_{int.}$=0.0441	280/103 $R_{int.}$=0.0262	168/89 $R_{int.}$=0.0464	273/116 $R_{int.}$=0.0279
Data/restraints/parameters	146/1/9	92/1/9	81/1/9	103/1/9	89/1/9	116/1/9
Goodness-of-fit on F^2	1.212	1.473	1.116	1.206	1.216	1.405
Final R indices [I>2sigma(I)]	R_1 = 0.0277, wR_2 = 0.0704	R_1 = 0.0199, wR_2 = 0.0514	R_1 = 0.0234, wR_2 = 0.0577	R_1 = 0.0247, wR_2 = 0.0600	R_1 = 0.0287, wR_2 = 0.0720	R_1 = 0.0355, wR_2 = 0.0976
R indices (all data)	R_1 = 0.0292, wR_2 = 0.0709	R_1 = 0.0207, wR_2 = 0.0518	R_1 = 0.0267, wR_2 = 0.0594	R_1 = 0.0276, wR_2 = 0.0612	R_1 = 0.0312, wR_2 = 0.0724	R_1 = 0.0380, wR_2 = 0.0980
$\Delta\rho_{max}$ and $\Delta\rho_{min}$ (e/A³)	1.235 and -0.769	0.795 and -0.455	1.508 and -0.894	1.090 and -0.549	0.821 and -0.919	2.817 and -3.358
Absolute structure parameter	0.15(14)	0.19(11)	0.12(12)	0.21(12)	0.31(14)	0.08(14)
Extinction coefficient	2.3(4)	4.5(7)	2.6(5)	0.73(15)	-	0.28(13)
Fractional atomic coordinates*						
Al/Ga: x= 1/3; y= 2/3; z=	0.0002(3)	0.0002(4)	0.0001(6)	0.0017(6)	0.0028(9)	0.0016(10)
N: x = 1/3; y= 2/3 z= u=	0.3816(3)	0.3809(4)	0.3807(6)	0.3801(6)	0.3790(9)	0.3787(10)
Al/Ga occupation	0.93/0.07	0.83/0.17	0.72/0.28	0.68/0.32	0.49/0.51	0.38/0.62
Interatomic distances (Å)						
Al/Ga-N	1.8901(7)	1.8931(9)	1.9001(13)	1.9110(13)	1.912(6)	1.926(2)
	1.902(2)	1.906(3)	1.921(4)	1.915(4)	1.920(2)	1.927(7)
Angles (deg)						
N-Al/Ga-N	110.67(6)	110.59(8)	110.61(11)	110.16(11)	109.14(18)	109.90(19)
N-Al/Ga-N	108.24(6)	108.33(9)	108.30(12)	108.77(12)	109.80(18)	109.0(2)
Al/Ga-N-Al/Ga	0.00(8)	0.00(12)	0.00(16)	0.00(16)	0.0(2)	0.0(3)

*- Composition x was determined by laser ablation mass spectroscopy

Since the structure is non-centro symmetric, the Flack absolute structure parameter [16] was automatically estimated by SHELXL [12]. X-ray studies show that $Al_xGa_{1-x}N$ single crystals form a continuous series of solid solutions between AlN and GaN. This is confirmed by the essentially linear dependence of the lattice parameters on composition x.

In *Figure 6* the lattice parameter a and c as a function of Al composition are shown. The open symbols represent results from this study and closed squares the previously reported results [8]. Reference data for GaN [17] and AlN [18] are also shown. For some experiments AlN crystals synthesized by sublimation method [5] were used as a precursor. Their lattice parameters measured before (closed triangle) and after (open symbols at x=1) high pressure experiment are also presented. The lattice parameters of AlN crystals after the high pressure experiment changed, most probably due to the development of defects at high temperature.
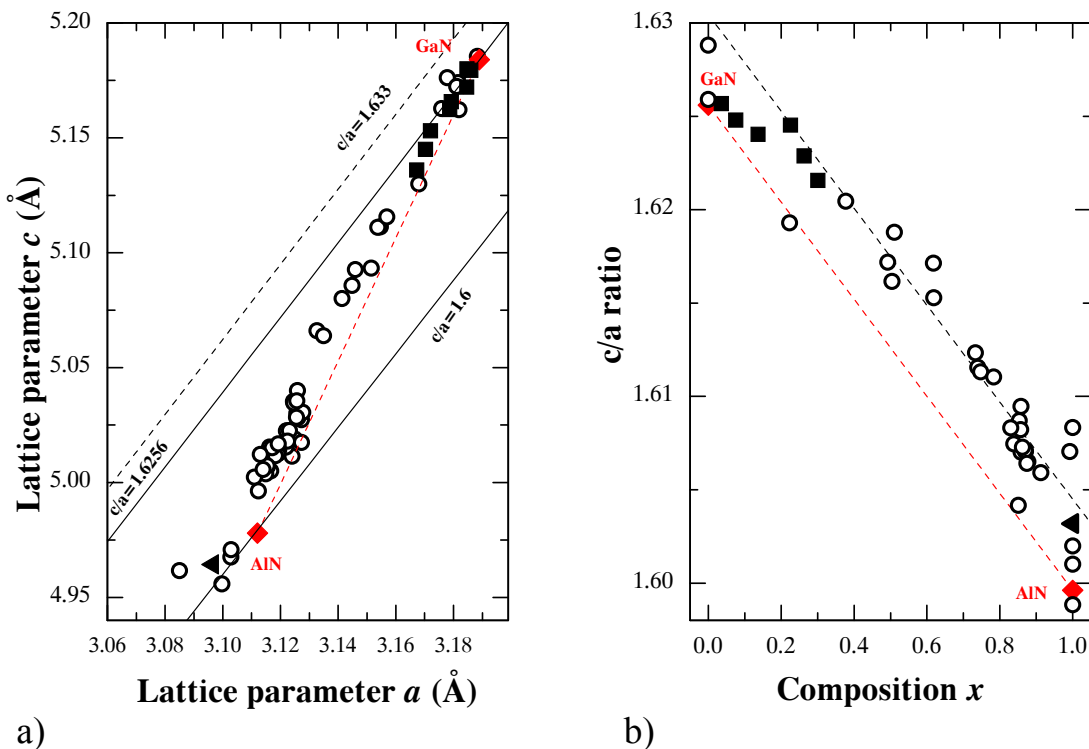
The composition of the crystals was determined by laser ablation mass spectroscopy. While the lattice parameters essentially follow Vegards law (red broken lines), minor, yet

a)   b)
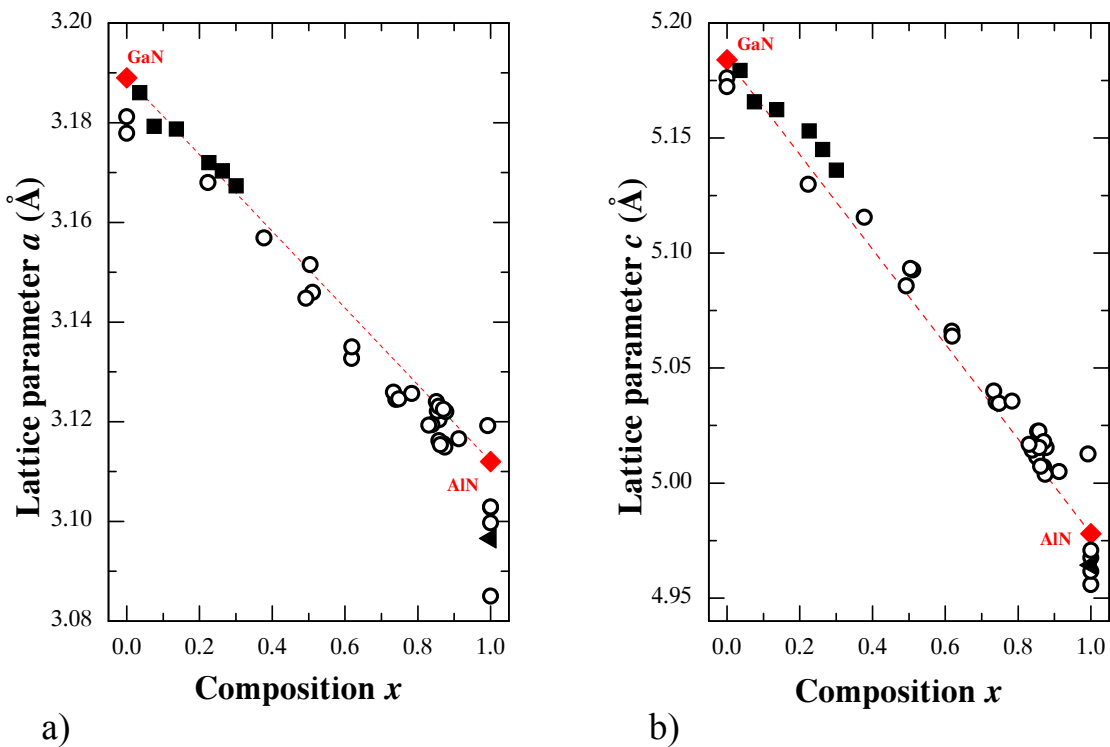
Fig. 6. *Lattice parameters a and c as a function of Al composition: ○ - this study, ■ - previously reported data [8], ◄ - AlN crystal synthesized by sublimation [5] and ♦ - reference data for GaN [17] and AlN [18]. The composition was determined by laser ablation mass spectroscopy. The errors are smaller than the size of the symbols.*

significant, deviations are observed: The lattice parameter *a* tends to be smaller, and *c* slightly larger. Obviously, one would find significant differences in the value of the Al content if the lattice parameters (either *a* or *c*) are used as experimental basis, and both would deviate somewhat from the mass-spectrometrically determined values.

Schottky defects might be expected to produce the observed lattice parameter modifications. Interestingly, however, we do not find significant differences among the crystals grown at different temperatures. Therefore, determining the nature of the defects will remain the subject of future studies. In *Figure 7* the lattice parameters are plotted to focus on the *c/a* ratio. With increasing Al content the *c/a* ratio changes from 1.6256 for GaN to 1.6 for AlN (*Figure 7a* or *7b*). *Figure 7a* represents the *c/a* ratio of all crystals, including those for which the Al content was not measured. For the ideal wurtzite structure the axial ratio *c/a* is 1.633 and the *u* positional parameter (*z* fractional atomic coordinates of the nitrogen atom) is equal to 0.375 [19]. Compounds with the *c/a* larger than 1.633 form stable sphalerite

a)   b)

Fig. 7. *The lattice parameter a vs. c and c/a ratio as a function of Al composition: ○ - this work, ■ - previously reported data [8], ◄ - AlN crystal synthesized by sublimation [5] and ♦ - reference data for GaN [17] and AlN [18]. The composition was determined by laser ablation mass spectroscopy. The errors are smaller than the size of the symbols.*

modification [20]. The parameter *u* increases when *c/a* decreases [21]. *Figure 7b* illustrates that the *c/a* ratio of our crystals (with significant Al content) tends to be systematically larger by ~0.3% than the GaN and AlN values.

References:

[1]   E. Iliopoulos, K. F. Ludwig, T. D. Moustakas, and S. Chu, Appl. Phys. Lett. **78** (2001) 463-465.

[2]   V. Soukhoveev, O. Kovalenkov, L. Shapovalova, V. Ivantsov, A. Usikov, V. Dmitriev, V. Davydov, A. Smirnov, Phys. Stat. Sol. (c) **6** (2006) 1483-1486.

[3]   Y. Koide, N. Itoh, K. Itoh, N. Sawaki, I. Akasaki, Jpn. J. Appl. Phys. **27** (1988) 1156-1161.

[4]   N. Okada, N. Fujimoto, T. Kitano, G. Narita, M. Imura, K. Balakrishnan, M. Iwaya, S. Kamiyama, H. Amano, I. Akasaki, K. Shimono, T. Noro, T. Takagi and A. Bandoh, Jpn. J. Appl. Phys. **45** (2006) 2502-2504.

[5]   B. M. Epelbaum, C. Seitz, A. Magerl, M. Bickermann, A. Winnacker, J. Cryst. Growth **265** (2004) 577-581.

[6]   T. Hashimoto, F.Wu, J. S. Speck, S. Nakamura, Jpn. J. Appl. Phys. **46** (2007) L889-891.

[7]   B. N. Feigelson, R. M. Frazier, M. Gowda, J. A. Freitas, M. Fatemi, M. A. Mastro and J. G. Tischler, J. Cryst. Growth **310** (2008) 3934-3940.

[8]   P. Geiser, J. Jun, J. M. Kazakov, L. Klemm, P. Wägli, J. Karpinski and B. Batlogg, J. Appl. Phys. Lett. **86** (2005) 081908.

[9]   A. Belousov, S. Katrych, J. Jun, J. Zhang, D. Günther, R. Sobolewski, J. Karpinski, and B. Batlogg, J. Cryst. Growth, **311** (2009) 3971-3974.

[10]   Oxford Diffraction Ltd., XCalibur, CrysAlis Software System, Version 1.170 (2003).

[11]   B. Hattendorf, Ch. Latkoczy, D. Günther, Analytical Chemistry (A-pages), **75** (2003) A341-347.

[12]   G. Sheldrick, SHELXL-97. Program for the Refinement of Crystal Structures, University of Göttingen, Germany (1997).

[13]   M. Bockowski, A. Witek, S. Krukowski, M. Wroblewski, S. Porowski, R. M. Marin-Ayral, and J. C. Tedenac, J. Mat. Synth. Process., **5** (1997) 449-458.

[14]   M. Bockowski, B. Łucznik, I. Grzegory, S. Krukowski, M. Wroblewski and S. Porowski, J. Phys: Condens. Matter **14** (2002) 11237-11242.

[15]   J. Karpinski, J. Jun, and S. Porowski, J. Cryst. Growth **66** (1984) 1-10.

[16]   H. D. Flack, Acta Cryst. **39** (1983) 876-881.

[17]   I. Vurgaftman, J. R. Meyer, L. R. Ram-Mohan, J. Appl. Phys. **89** (2001) 5815-5875.

[18]   M. Levinshtein, S. Rumyantsev, S. Shur, Properties of Advanced Semiconductors Materials: GaN, AlN, InN, BN, SiC, SiGe, Wiley, New York, 2001.

[19]   H. Ott, Zeitschrift fuer Physik **22** (1924) 201-214.

[20]   M. E. Fleet, Mat. Res. Bull. **11** (1976) 1179-1184.

[21]   V. A. Zhdanov, L. A. Brysneva, Izvest. Vysshih. Ucheb. Zavedenii Fiz. **3** (1961) 95.

Chapter 6

Thermodynamics in the Al-Ga-N₂ system

6.1 Summary

In this chapter, we reported the results obtained from the studying the thermodynamics of the stability of ternary (Al,Ga)N up to 10 kbar and 1800 °C. The calculation was carried out on the basis of experimentally obtained *p-T* growth conditions presented in *Chapter 5*. The main results can be summarized as follows:

(1)   The equilibrium nitrogen pressure/activity a_{N_2} as a function of composition x shows a non-linear behavior.

(2)   The standard Gibbs free energy ΔG^0 as well as the standard enthalpy ΔH^0 and standard entropy ΔS^0 of formation as a function of composition x are reported.

(3)   The corresponding *p-T* and *x-T* phase diagrams for $Al_xGa_{1-x}N$ are determined.

(4)   Stability of $Al_xGa_{1-x}N$ with particular composition x strongly depends on the pressure and temperature.

6.2 Introduction

Due to the very high melting temperatures of III-V semiconductors, such as GaN with $T_m \approx 2220$ °C [1] and AlN with $T_m \approx 3214$ °C [2] and high partial nitrogen pressure (~60 kbar) above GaN at melting temperature [1], single crystals can not be grown from the stoichiometric melts using typical methods, such as Czochralski or Bridgman. For the growth from solution information on the thermal stability and solubility in liquid Ga or Al are of primary importance. The knowledge about thermal stability is also important for the device application, since they may thermally degrade during device processing or operation. The equilibrium pressure of nitrogen over nitrides was previously reported for GaN at

temperatures up to 1700 °C and for AlN up to 3150 °C [3,4]. More recently we presented the data for the Al-Ga-N$_2$ system up to 1800 °C (see *Chapter 5*).

Al$_x$Ga$_{1-x}$N solid solutions have been produced as epitaxial layers using various growth methods [5,6], and only recently we succeeded in the growth of Al$_x$Ga$_{1-x}$N single crystals using high pressure techniques [7].

Based on the experimental data, the *p-T-x* diagram of the Al-Ga-N$_2$ system has been determined (*Chapter 5*). However, there is lack of information about the basic thermodynamic functions such as the standard Gibbs free energy, the enthalpy and entropy of formation. The stability of AlGaN was also studied theoretically using various methods such as a generalized quasi-chemical approximation (GQCA) or delta lattice-parameter model etc. [8,9]. It was shown that it is possible to have the regular solid solution under normal conditions, in agreement with our observations. Thermodynamic data of the reaction of formation are still missing.

The growth conditions and the extended equilibrium *p-T* phase diagram of Al$_x$Ga$_{1-x}$N were previously published [7]. Here, we present the calculations of the standard Gibbs free energy of formation, the enthalpy and entropy of formation of the AlGaN crystals based on experimental *p-T* growth conditions. The calculations were done for temperatures of up to 1900 °C and up to 30 kbar pressure. Knowing the thermodynamic functions allows us to determine the *p-T* and *x-T* phase diagrams for extended parameter ranges, which is the basis for crystal growth experiments and thermal annealing, and the understanding of interface stability issues.

6.3   The thermodynamic data of AlN and GaN

Published thermodynamic data of the standard enthalpy and entropy of formation for GaN and AlN are summarized in *Table I*. The standard enthalpy of formation was theoretically calculated, measured calorimetrically as well as derived from the experimental high pressure equilibrium experiments. The reported thermodynamic data scatter somewhat. Karpinski and Porowski measured the nitrogen gas pressure over GaN and estimated the standard enthalpy for GaN as -37.7 kcal/mol and the entropy of formation as -32.43 cal/Kmol [3]. For AlN no experimental data of nitrogen partial pressures are available. Instead, the values for AlN were estimated by calorimetric measurements such as carbothermal nitridation of aluminum oxide

or high-temperature oxide melt drop solution. In comparison to the direct measurement of the equilibrium nitrogen pressure over AlN, such methods are, however, highly sensitive to the impurity level in the system. The standard enthalpy of formation -79.5 kcal/mol and standard entropy of formation -28.026 cal/Kmol for AlN were derived from the *p-T* diagram presented by G. Slack and T. F. McNelly [4]. Here one should notice that this diagram was not measured, but calculated using the available thermodynamic data of the constituents of the AlN formation reaction, N_2, Al liquid and Al gas. It was estimated that the pressure of nitrogen necessary to react with Al(l) to form AlN is 1 atm at 2563 °C. At lower temperatures it is less. The temperature of 2493 °C is of particular significance for any experiment as it is the boiling temperature of Al, and reactions with the crucible material leads to the failure of the experiment. The direct measurement of the AlN stability and therefore the determination of the thermodynamic functions are rendered very difficult by the low nitrogen pressure, the high thermal stability of AlN and the high vapor pressure of aluminum.

Table I

Summary of experiments on thermodynamic quantities of AlN (adapted from [10])

Ref. Year [Ref. #]	Temperature range (K)	Method	Enthalpy of formation ΔH^0_{298} (kcal/mol)	Entropy of formation ΔS^0_{298} (cal/Kmol)
1957 [11]	-	Direct nitridation calorimetry	-76.47	-
1961 [12]	-	Oxygen combustion calorimetry	-75.67	-
1963 [13]	1780-1970	Torsion-effusion	-76.10	-
1976 [4]	1750-3200	Derived from *p-T* curves	-79.50	-28.026
1979 [14]	-	Calculation	-76.10	-
1984 [15]	-	Calculation	-76.10	-
1999 [16]	-	Drop solution calorimetry	-74.35	-
2002 [17]	1723-1899	Carbothermal Nitridation	-73.66	-
2006 [18]	-	Calculation	-74.22	-

Table I (continue)

Summary of experiments on thermodynamic quantities of GaN (adapted from [10, 23])

| Ref. Year [Ref. #]	Temperature Range (K)	Method	Enthalpy of formation ΔH^0_{298} (kcal/mol)	Entropy of formation ΔS^0_{298} (cal/Kmol)
1940 [19]	-	Combustion calorimetry	-24.90	-
1975 [20]	1173-1523	Derived from *p-T* curves	-37.70	-
1979 [14]	-	Calculation	--26.19	-
1984 [15]	-	Calculation	-26.20	-
1986 [3]	1343-1913	Derived from *p-T* curves	-37.70	-32.43
1998 [21]	-	Calculation	-27.98	-
2000 [22]	975	Drop solution calorimetry	-37.47	-
2003 [23]	-	Calculation	-33.46	-
2006 [18]	-	Calculation	-38.61	-

Generally, for the III-nitrides the Gibbs free energy of the constituents, i.e. nitrogen and metal, is low and therefore the stability of the system is shifted towards metal and N_2. Accordingly, high nitrogen pressure is necessary to attain the stability condition for III-nitrides, i.e. for GaN and InN. As we mentioned, AlN is considered to be stable even up to 2500 °C at 1 bar nitrogen pressure. No data of nitrogen partial pressure is available for ternary $Al_xGa_{1-x}N$. Moreover, for the ternary compounds, in addition to the equilibrium nitrogen pressure and temperature, the composition x is an additional influential parameter. In this work we use the experimental *p-T* growth conditions in order to calculate the Gibbs free energy of formation depending on the composition x and temperature as well as to explore the stability conditions. We proceed as follows:

1. Convert the experimentally estimated nitrogen equilibrium pressures over $Al_xGa_{1-x}N$ for a particular composition x, to the nitrogen activity a_{N_2} (fugacity).

2. Determine the nitrogen activity-composition dependence for two different temperatures (1550 °C and 1720 °C).

3. Derive the linear activity-temperature dependence for various compositions x using the estimated nitrogen activity-composition dependence.

4. Determine of the Gibbs free energy from the a_{N_2}-T dependence and derive the standard enthalpy and entropy of formation for various compositions x.

5. On the basis of the estimated standard enthalpy and entropy of formation the *p-T* equilibrium lines of $Al_xGa_{1-x}N$ for various Al compositions will be derived and compared with the experimental points.

6.4 The Gibbs free energy, enthalpy and entropy of formation for $Al_xGa_{1-x}N$

The $Al_xGa_{1-x}N$ formation in the $Al\text{-}Ga\text{-}N_2$ system is given by:

$$Al_xGa_{1-x}N \leftrightarrow xAl + (1-x)Ga + \frac{1}{2}N_2 \tag{1}$$
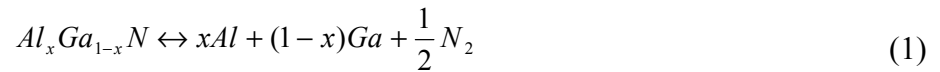
where *x* is Al content in the solid phase.

According to the Gibbs law, the number of degrees of freedom of the system *F* is F=C-P+2, where *C* is the number of independent components and *P* is the number of phases. Thus, if three phases: solid $Al_xGa_{1-x}N$, liquid Ga/Al and gas N_2 exist, F=3-3+2=2, and therefore the coexistence of these 3 phases is only possible on the equilibrium curves in *p-T* space for certain composition *x* of the solid phase. Moreover, it means that, if the pressure of the system is fixed, the composition can be changed by varying the temperature. On the other hand varying the pressure at the fixed temperature should also affect the composition. As illustration one can see the results of our experiments for the growth temperature of 1550 °C (see *Figure 1*).

The Gibbs free energy change of the reaction (1) for constant *p* and *T* is

$$\Delta G = \sum_i \mu_i \upsilon_i \tag{2}$$

where μ_i - is the chemical potential and υ_i denotes the stoichiometric coefficient of the component *i*.

Assuming that solubilities of components are very low, the chemical potential μ_i of *i*-components is equal the molar Gibbs free energy of the component *i*. Therefore, the thermodynamic equilibrium can be described as:

$$\Delta G = G_{Al_xGa_{1-x}N} - (1-x)G_{Ga} - xG_{Al} - \frac{1}{2}G_{N_2} = 0 \tag{3}$$

where ΔG is the Gibbs free energy change of reaction (1).

The pressure dependence of the Gibbs free energy at a constant temperature can be found by integrating the relationship:

$$(\frac{\partial G_i}{\partial p})_T = v_i$$

where v_i is the molar volume of component i.

Varying the pressure from the standard condition of 1 bar to pressure p, we find that

$$G_{Al_xGa_{1-x}N}(p,T) = G^0_{Al_xGa_{1-x}N}(T) + \int_1^P v_{Al_xGa_{1-x}N}(p,T)dp \qquad (4a)$$

$$G_{Ga}(p,T) = G^0_{Ga}(T) + \int_1^P v_{Ga}(p,T)dp \qquad (4b)$$

$$G_{Al}(p,T) = G^0_{Al}(T) + \int_1^P v_{Al}(p,T)dp \qquad (4c)$$

$$G_{N_2}(p,T) = G^0_{N_2}(T) + \int_1^P v_{N_2}(p,T)dp \qquad (4d)$$

where $G_i^0(T)$ is the standard Gibbs free energy of component i at 1 bar pressure.

Inserting (4) into (3) we get:

$$\Delta G^0(T) = G^0_{Al_xGa_{1-x}N} - (1-x)G^0_{Ga} - xG^0_{Al} - \frac{1}{2}G^0_{N_2} =$$
$$= \int_1^{P_{eq.}} \left[\frac{1}{2}v_{N_2}(p,T) + xv_{Al}(p,T) + (1-x)v_{Ga}(p,T) - v_{Al_xGa_{1-x}N}(p,T) \right] dp$$

Solids and liquids are not very compressible, so to first approximation, we can regard their molar volume v_i as constant. (as long as the pressure range is not too large). Equation (4) for the solid components simplifies to:

$$G(p,T) = G^0(T) + v(T)(P_{Eq.} - 1) \qquad (5)$$

The second part is small compared to the first one (e.g. ~66.38 kcal/mol for Ga and ~79.25 kcal/mol for Al [24]), and more importantly, it is negligible compared to the correspond *p*-depend part of the gas component N_2. The equilibrium pressure P_{Eq} depends on temperature and for ternary $Al_xGa_{1-x}N$ is in order of 10^4 bar ~ 10^9 Pa (N/m^2) (see Ref [7], *Figure 2*). The values for GaN are similar [3]. For AlN lower pressure is required. The molar volume of a typical metal υ_i is ~ 10 cm^3/mol or 10^{-6} m^3/mol. The Gibbs free energy change will be 10^{-6} m^3/mol x 10^9 N/m^2 = 10^3 Nm/mol = 1000 J/mol ≈ 240 cal/mol. Thus, the Gibbs energy change of the metal caused by pressure does not exceed ~ 10^2 cal/mol.

As Karpinski and Porowski [3] showed, the value of

$$\int_1^{P_{eq.}} \left[\upsilon_{Ga}(p,T) - \upsilon_{GaN}(p,T) \right] dp$$

is less than 170 cal/mol, calculated from the compressibility and thermal expansion data.

The value $\int_1^P \upsilon_{Al_xGa_{1-x}N}(p,T)dp$ is not known, but one can estimate it to be similar to that of GaN.

As we discuss below, the present study yields the equilibrium pressure $P_{Eq.}(x, T)$ in the Al-Ga-N_2 system. Accordingly, the contribution (4d) to ΔG^0 from the N_2 component is calculated to be in range of 21.4 kcal/mol (for *x*=0) to 15.1 kcal/mol (for *x*=0.86). Therefore, the Gibbs free energy change is dominated by the contribution from N_2.

Introducing the activity a_{N_2} $(P_{Eq.},T)$, ΔG^0 is given by:

$$\Delta G^0(T) \cong \frac{1}{2}\int_1^{P_{eq.}} \upsilon_{N_2}(p,T)dp = \frac{1}{2}RT\ln a_{N_2}(p_{ep},T)$$

(6)

where a_{N_2} $(P_{Eq.},T)$ is the activity of gaseous nitrogen (dimensionless) and P_{eq} is the equilibrium pressure of nitrogen for the temperature *T*. The activity of nitrogen, defined as nitrogen fugacity over the nitrogen fugacity at the reference state of 1 bar, describes the non-ideal behaviour of the nitrogen gas. This is important because the fugacity of nitrogen is several times higher than the pressure at our experimental conditions.

We assumed that the solubilities of the component are very low. However, in general solubilities can influence the Gibbs free energy. It was shown for GaN that the change of Gibbs free energy of gallium resulting from the solubility of nitrogen in gallium at 1500 °C and 16 kbar is 72 cal/mol [3]. This value is negligible compared to the term connected to the nitrogen activity. As in our case the solvent is also metallic Ga with very small amounts of Al we can assume that it is also valid for our system.

6.5   The results of the calculation

In this section the thermodynamic functions are calculated on the basis of the experimentally obtained equilibrium temperature and pressure P_{eq}. *Figure 1* shows the dependence of the activity of nitrogen over $Al_xGa_{1-x}N$ versus reciprocal temperature for the experimentally obtained growth pressure and temperature.
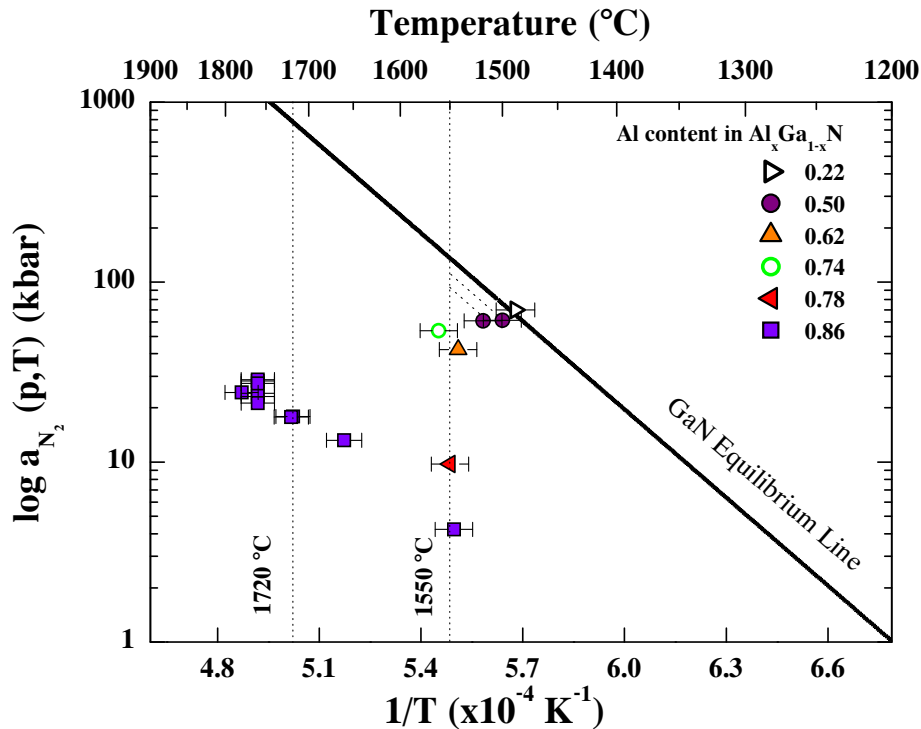
Fig. 1. *Activity of nitrogen a_{N2} over $Al_xGa_{1-x}N$. The symbols are calculated from the experimental pressure for particular compositions x. The activity errors are smaller than the size of the symbols.*

The nitrogen pressure was converted to activity a_{N_2} according to the equation (7) reported by J. Unland *et al.* [23]. They calculated and extrapolated the nitrogen fugacity coefficient on the basis of an equation of state reported by Jacobsen *et al.* [25] using the program ALLPROPS [26] up to 3000 K and 20 kbar.

$$\ln(\frac{a_{N_2}}{P}) = (\frac{2800}{T^3} - \frac{39.23}{T^2} + \frac{0.3926}{T}) \cdot P + (-\frac{0.07}{T^3} + \frac{0.00113}{T^2} - \frac{3.805 \cdot 10^{-6}}{T}) \cdot P^2 \qquad (7)$$

where a_{N_2} – is the nitrogen activity and P - is the pressure, given in bar.
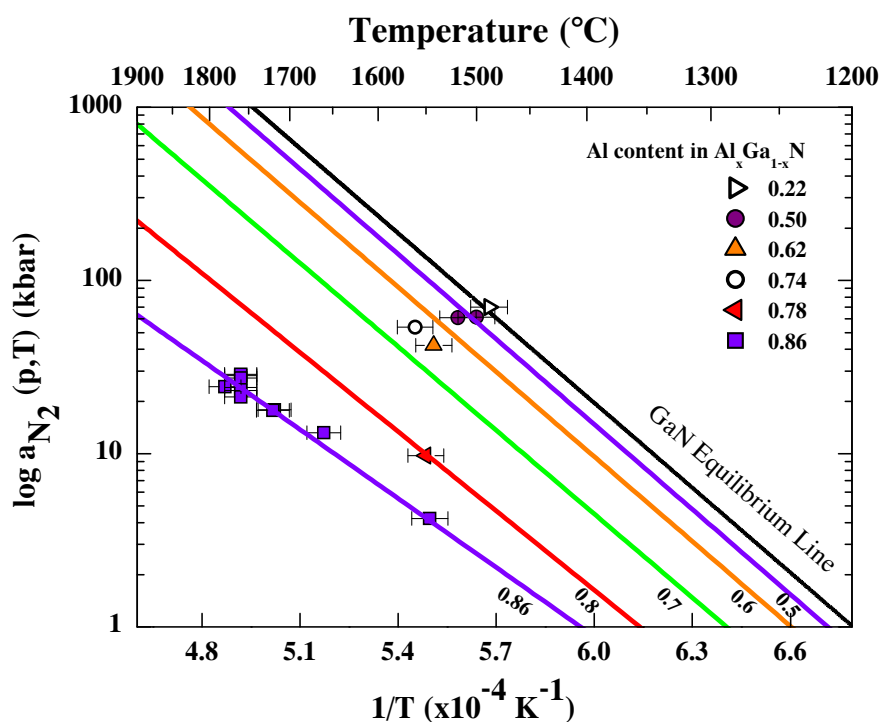
From equation (6):

$$\ln a_{N_2}(p_{eq}, T) = \frac{2\Delta G^0(T)}{R} \cdot \frac{1}{T} \qquad (8)$$

Thus, equilibrium lines for $Al_xGa_{1-x}N$ with various Al compositions should be linear in a *ln a_{N_2} -1/T* plot. In order to plot such dependences we need to have at least two points at difference temperatures for a particular composition *x*. We cut the a_{N_2}-*T* plot in *Figure 1* at T= 1550 °C and 1720 °C and plot the nitrogen activity as a function of Al composition (*Figure 2*).
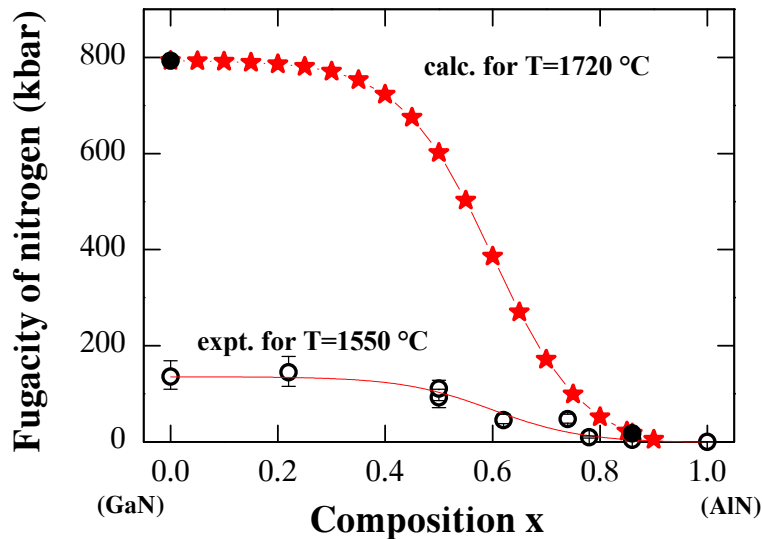

Fig. 2. *Nitrogen activity as a function of Al composition at the temperatures, 1550 °C and 1720 °C. The open circles represent the experimental data at 1550 °C approximated by the red line and the red stars were calculated for 1720 °C according to the fitting function.*

The red line in *Figure 2a* is a smooth fit to the experimental points (open circles). The points at x=0.22 and x=1 (derived from [4]) were not considered. The point x=0.22 is at higher pressures than for GaN and therefore it is obviously unreliable. Thus, the curve was fitted only in a range of the experimental and reliable composition, up to x=0.86 and the resulting fit is in a good approximation of the experimental points. The errors of the activity are estimated to be up to 28% of the value. Especially, one can see it for the values at x<0.6. Since the equilibrium p-T (or a_{N_2}-T) points for x<0.5 are at higher pressures, close to the GaN equilibrium line (*Figure 1*), the temperature deviation of 1% can lead to large errors in the fugacity estimation at T= 1550 °C and 1720 °C. We assumed that the shape of the a_{N_2}-x curve does not depend on the temperature and we have calculated the a_{N_2}-x dependence for 1720 °C using the polynomial function. For comparison the experimental point at x=0.86 (closed circle) is also shown in *Figure 2b*. Knowing the activity-composition dependence for two different temperatures the activity-temperature dependence of $Al_xGa_{1-x}N$ for various compositions can be determined. The calculated plots are shown in *Figure 3*.

Fig. 3. *Equilibrium nitrogen activity lines over $Al_xGa_{1-x}N$ for various Al compositions. The lines were calculated according to the procedure described in text. The activity errors are smaller than the size of the symbols.*

From equation (8) the standard Gibbs free energy of formation $\Delta G^0(T)$ as a function of the composition x was calculated (*Figure 4*). The data are presented for several temperatures. The solid points are $\Delta G^0(T)$ values of the pure AlN, which were derived from the *p-T* equilibrium curve published by Slack *et al.* [4]. $\Delta G^0(T)$ is almost constant up to certain x value and decreases at larger x. The slope of the $\Delta G^0(T)$ decrease is steeper for higher temperature isotherms. For x close to 1 $\Delta G^0(T)$ values are negative. If the $\Delta G^0(T)>0$ for reaction (1), then the reverse reaction will be spontaneous at $p=1$ bar and it will produce Ga/Al metal und nitrogen gas. For our case at 1 bar pressure, the $Al_xGa_{1-x}N$ phase with Al content up to 0.9 seems to be unstable and decompose. This is in a good agreement with the experimental data. To stabilize $Al_xGa_{1-x}N$ with Al content at least up to 0.86 pressures in a range of several kbar are required. E.g. for $Al_{0.86}Ga_{0.14}N$ crystal growth at the 1550 °C the nitrogen pressure will be about 5 kbar [7]. For $\Delta G^0(T)=0$ the reaction (1) is at equilibrium and $Al_xGa_{1-x}N$ is stable. From *Figure 4* we conclude that at 1 bar pressure $Al_xGa_{1-x}N$ with Al content $x>0.9$ is stable.
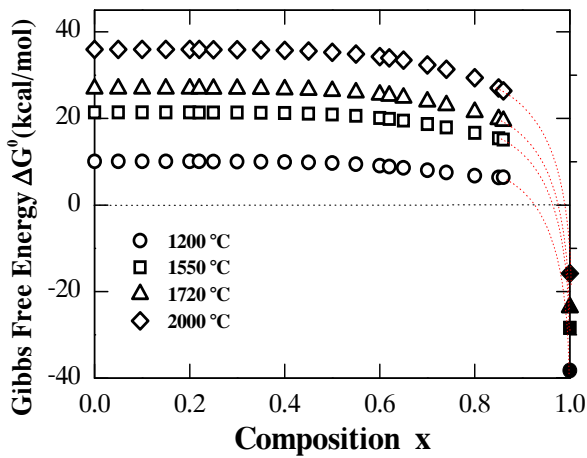
Fig. 4. The standard Gibbs free energy $\Delta G^0(T)$ dependence on the composition x for several temperatures.

The change in the standard Gibbs free energy of reaction $\Delta G^0(T)$ is given by the simplified Gibbs-Helmholtz equation:

$$\Delta G^0(T) = \Delta H^0 - \Delta S^0 \cdot T \tag{9}$$

From equations (8) and (9) the standard enthalpy ΔH^0_{298} and standard entropy ΔS^0_{298} of formation for various compositions x have been calculated (*Table II*). Both ΔH^0 and ΔS^0 were found to be independent of the temperature up to 1800 °C. The dependence of the standard

Table II. *Thermodynamic quantities of $Al_xGa_{1-x}N$ calculated from the thermodynamic description in the text.*

Composition x	Enthalpy of formation ΔH^0_{298} (kcal/mol)	Entropy of formation ΔS^0_{298} (cal/Kmol)
0	-37.53	-32.32
0.05	-37.53	-32.32
0.10	-37.53	-32.32
0.15	-37.52	-32.31
0.20	-37.52	-32.31
0.22	-37.52	-32.31
0.25	-37.52	-32.30
0.30	-37.52	-32.29
0.35	-37.52	-32.26
0.40	-37.51	-32.22
0.45	-37.49	-32.14
0.50	-37.46	-32.01
0.55	-37.41	-31.81
0.60	-37.32	-31.50
0.65	-37.15	-31.06
0.70	-36.83	-30.45
0.74	-36.36	-29.79
0.80	-34.88	-28.27
0.85	-31.60	-25.79
0.86	-30.36	-24.95

enthalpy ΔH^0_{298} and standard entropy ΔS^0_{298} of formation on the compositions x is shown in *Figure 5*. Similar to the dependence of the standard Gibbs free energy the ΔH^0_{298} and ΔS^0_{298} slightly decrease with increasing x and their change becomes significant for $x>0.6$ (open points). Some additional experiments are needed for the region $0.86<x<1$. The solid points indicate the values for AlN derived from [4]. The experimental values of ΔH^0_{298} for AlN measured by different techniques are also shown as crosses. Taking those values of ΔH^0_{298} and value of ΔG^0_{298} for AlN derived from the *p-T* dependence [4], the standard entropy ΔS^0_{298} of formation for AlN can be estimated (cross symbols). The small changes of ΔH^0_{298} result in significant scatter of the ΔS^0_{298} values.

The values of ΔH^0_{298} for the end compositions are rather well established, both experimentally (*Table I*) and from electronic structure calculations (e.g. Ref. [27]), and reflect, among another factors, the larger cohesive energy for AlN [27, 28]. In any case, the region for $x{\geq}0.8$ is of particular interest and further studies will need to address the apparent difference between the various measured values of ΔH^0_{298} for AlN, and the trend suggested by the present results in *Figure 5*.
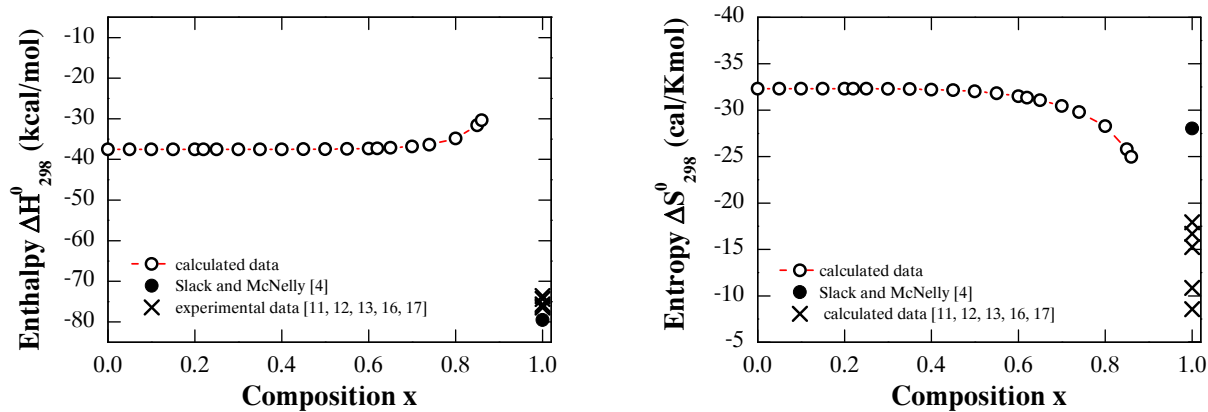

Fig. 5. *The standard enthalpy ΔH^0_{298} and entropy ΔS^0_{298} of formation of $Al_xGa_{1-x}N$ as a function of composition x. Open circles represent the calculated data and closed circles are according to Slack and McNelly [4]. The crosses are experimental data taken from Table I, whereas the points for the standard entropy ΔS^0_{298} were calculated as described in text.*

Table III. *Equilibrium temperatures for $Al_xGa_{1-x}N$ with various compositions x at 1 bar nitrogen pressure.*

Composition x	T (K)	Composition x	T(K)
0	1160.9[*]	0.50	1170.1
0.10	1161.0	0.60	1184.6
0.20	1161.2	0.70	1209.4
0.30	1161.9	0.80	1233.5
0.40	1164.0	0.86	1216.7
0.45	1166.3		

[*]- Ref. [3].
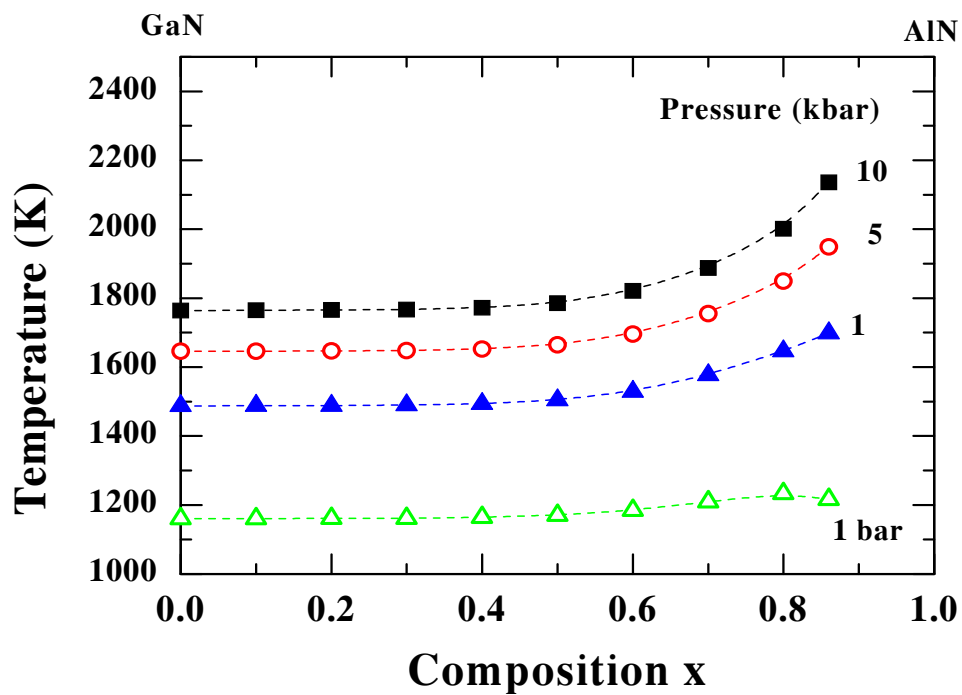
Fig. 6. *x-T phase diagram of $Al_xGa_{1-x}N$ at various nitrogen pressures.*

The stability of $Al_xGa_{1-x}N$ with a particular composition x strongly depends on pressure and temperature. In *Table III* the equilibrium temperatures for $Al_xGa_{1-x}N$ are presented for $p=1$ bar. Using the thermodynamic functions calculated in this study we determinated the pressure-temperature and temperature-composition phase diagrams for $Al_xGa_{1-x}N$. The *p-T* equilibrium phase diagram was discussed in our early studies (*Chapter 5* or [7]).

Here we present the *x-T* phase diagram of $Al_xGa_{1-x}N$ for different pressures (*Figure 6*). For 1 bar the equilibrium isobar of the temperature seem to depend linearly on the composition x. However, with increasing pressure the isobars have a tendency to bend to the higher temperatures, particularly for the higher Al content, $x>0.6$. Accordingly, the nitride is more stable at higher pressures. For e.g. $Al_xGa_{1-x}N$ with $x=0.5$, the equilibrium temperature at 1 kbar is 1503 K. An increase of the pressure up to 5 or 10 kbar will lead to a higher stability and the equilibrium temperature has been calculated to be 1665 K and 1786 K respectively.

References:

[1]   W. Utsumi, H. Saitoh, H. Kaneko, T. Watanuki, K. Aoki and O. Shimomura, Nature Materiale **2** (2003) 735-737.

[2]   J. A. Van Vechten, Phys. Rev. B **7** (1973) 1479-1507.

[3]   J. Karpinski, S. Porowski, J. Cryst. Growth **66** (1986) 11-20.

[4]   G. A. Slack, T. F. McNelly, J. Cryst. Growth **34** (1976) 263-279.

[5]   E. Iliopoulos, K. F. Ludwig, T. D: Moustakas, and S. Chu, Appl. Phys. Lett. **78** (2001) 463-465.

[6]   Y. Koide, N. Itoh, K. Itoh, N. Sawaki, and I. Akasaki, Jpn. J. Appl. Phys. **27** (1988) 1156-1161.

[7]   Andrey Belousov, S. Katrych, J. Jun, J. Zhang, D. Günther, R. Sobolewski, J. Karpinski, and B. Batlogg, J. Cryst. Growth, **311** (2009) 3971-3974.

[8]   L. K. Teles, J. Furthmüller, L. M. R. Scolfaro, J. R. Leite, and F. Bechstedt, Phys. Rev. B **62** (2000) 2475-2485.

[9]   V. G. Deibuk, A. V. Voznyi, Semiconductors **39** (2005) 623-628. (and references inside).

[10]   V. P. Vasilev and J. C. Gachon, Inorganic Materials **42** (2006) 1176-1187.

[11]   C. A. Neugebauer and J. L. Margrave, Z. Anorg. Allgem. Chem. **290** (1957) 82-86.

[12]   A. D. Mah, E. G. King, W. W. Weller, and A. U. Christensen, **RI 5716**, U. S. Bureau of Mines, Berkeley, CA (1961) 8.

[13]   D. L. Hildebrand, W. F. Hall, J. Phys. Chem. **67** (1963) 888-893.

[14]   O. Kubaschewski, C. B. Alcock, Metallurgic Thermochemistry, Pergamon Press., London, 1979.

[15]   R. D. Jones, K. Rose, R. D. Jones and K. Rose, CALPHAD **8**, (1984) 343-354.

[16]   J. M. McHalle, A. Navrotsky, and F. J. DiSalvo, Chem. Mater. **11** (1999) 1148-1152.

[17]   W. Nakao, H. Fukuyama, K. Nagata, J. Am. Ceram. Soc. **85** (2002) 889-896.

[18]   D. Sedmidubsky, J. Leitner, J. Cryst. Growth **286** (2006) 66-70.

[19]   H. Hahn, R. Juza, Z. Anorg. Allgem. Chem. **244** (1940) 111-124.

[20]   R. Madar, G. Jacob, J. Hallais, R. Fruchart, J. Cryst. Growth **31** (1975) 197-203.

[21]   A. V. Davydov, T. J. Anderson, III-V Nitride Materials and Processes III, ECS, Boston, PV 98-18 (1998) 38-49.

[22]   M. R. Ranade, F. Tessier, A. Navrotsky, V. J. Leppert, S. H. Risbud, F. J. DiSalvo, C. M. Balkas, J. Phys. Chem. B **104** (2000) 4060-4063.

[23]   J. Unland, B. Onderka, A. Davydov, and. R. Schmid-Fetzer, J. Cryst. Growth **256** (2003) 33-51.

[24]   L. V. Gurvich, I. V. Veyts and C. B. Alcock, Thermodynamic properties of individual substances, 4th edition, V. 1, part 2, Hemisphere Publishing Corp., 1989.

[25]   R. T. Jacobsen, R. B. Stewart and M. Jahangiri, J. Phys. Chem. Ref. Data **15** (1986) 735-908.

[26]   E. W. Lemmon, R. T. Jacobsen, S. G. Penoncello, S. W. Beyerlein, Computer programs for calculating thermodynamic properties of fluids of engineering interest, version 6/4/1996, CATS University of Idaho, Moscow, USA (1996).

[27]   A. Zoroddu, F. Bernardini, P. Ruggerone, V. Fiorentini, Phys. Rev. B **64** (2001) 045208.

[28]   W. A. Harrison, Electronic Structure and Properties of Solids, San Francisco (1980).

Chapter 7

Conclusions and Outlook

The work presented in this thesis demonstrates the progress in the synthesis of ternary (Al,Ga)N compounds by the solution growth method under high pressure. It is known that, in comparison to other growth methods such as thin film deposition, high pressure solution growth (HPSG) leads to the excellent quality, nearly dislocation free crystals, in particular for GaN crystals [1]. Availability of the bulk (Al,Ga)N crystals permits to address some of current deficiencies in understanding of the synthesis of such compound, its thermodynamic stability and therefore to expand the potential for application.

7.1 Crystal growth

The main results demonstrated and addressed in this thesis are the growth of polycrystalline (Al,Ga)N by solid-state reaction [2] and of (Al,Ga)N bulk single crystals from solution in Ga melt. Using the anvil techniques (see *Section 3.2*) the polycrystalline (Al,Ga)N samples covering the whole compositional range were synthesized at 30 kbar and 1800 °C. X-ray powder diffraction measurements proved the homogenous composition of the nitride compound and lack of a miscibility gap between AlN and GaN. Though the single (Al,Ga)N crystals with up to 30% Al content were grown using an anvil technique as reported previously [3,4], the main goal set in this work and finally achieved was to explore the possibilities of crystal growth in a gas autoclave. The advantage of this technique is that temperature, temperature gradient and nitrogen pressure can be well controlled. Moreover, it allows the use of lager crucibles than in the anvil technique. Most of the (Al,Ga)N crystal growth experiments were performed using our self-constructed high pressure gas autoclave (*Section 3.1*).

Al$_x$Ga$_{1-x}$N single crystals with 0.22≤x≤0.91 were synthesized from solution in Ga melt under high nitrogen pressure (2.5-10 kbar) and at high temperature (1425-1780 °C). A growth rate of up to 0.1 mm/day, a rate comparable to the growth of GaN from solution under high pressure [5] or by the ammonothermal method [6], was achieved. The growth process was optimized, yielding (Al,Ga)N crystals up to 0.8x0.8x0.8 mm^3 in size. Numerous successful experiments prove the reproducibility of the crystal growth. The (Al,Ga)N growth from solution under high nitrogen pressure poses a significant challenge which could be successfully overcome in this thesis. In particular, the major hurdles in growing (Al,Ga)N bulk crystals from solution in Al/Ga melt were previously established as follows [4]: the formation of AlN capping layer on the Al/Ga melt surface and self-propagating AlN combustion reaction when nitrogen is present in gas form. The proper choice of the solvent is obviously important. Adding Al metal to the melt (up to 0.4 at%) resulted in the growth of very small (Al,Ga)N crystals accompanied by Al$_2$O$_3$ crystals as by-product. Further experiments with larger amount of Al (up to 30 at%) ended up with so called self-propagating AlN combustion. It was found that using pure Ga metal as a solvent and introducing an appropriate amount of Al in form of the pre-reacted polycrystalline (Al,Ga)N or AlN pellet helps to avoid the formation of AlN capping layer on the melt surface and the AlN combustion reaction. The detailed study with different Al compositions in the (Al,Ga)N pellet showed that the presence of the pellet enhances also the nitrogen supersaturation in the melt and does not affect the Al content in the grown crystals (at least by up to 1.2 at% Al content in the melt).

To extent the capacities of the high pressure experiments some modifications of the heater construction and plug connection were made. It brought several advantages such as an increasing of the maximum working temperature up to 1800 °C or more accurate temperature measurements thanks to the additional Type T thermocouple placed in the plug as a reference for the cold point of the three thermocouples placed inside the furnace.

One of the important issues in HPSG method is the unwanted oxygen contamination. If some oxygen is present in the growth zone, Al$_2$O$_3$ crystal growth dominates because of the high affinity of aluminium for oxygen. It was argued that the most probable oxygen source in our system is the BN crucible partially containing boron oxide traces. Indeed, if the BN crucible was used for the crystal growth, the (Al,Ga)N growth was mostly suppressed. The (Al,Ga)N growth was carried out in a graphite crucible which acts as oxygen purifier. EDX measurements did not detect any oxygen or carbon impurities in the crystals.

The key question also concerns the equilibrium conditions required to thermodynamically stabilize the (Al,Ga)N phase. More than two dozen experiments in a wide range of temperature and pressure were carried out in order to determine the p-T conditions for the $Al_xGa_{1-x}N$ growth. First, we found that $Al_xGa_{1-x}N$ crystals could be grown by choosing the appropriate pressure and temperature conditions selected below the GaN p-T equilibrium line [7]. Second, the composition x in the growing $Al_xGa_{1-x}N$ crystals can be selected by the proper choice of the p-T conditions according to the estimated $Al_xGa_{1-x}N$ equilibrium phase diagram established in this study. Thus, summarizing the conclusions, proper p-T conditions are the *sine qua non* conditions for successful (Al,Ga)N crystal growth.

The composition of the crystals was measured by laser ablation inductively coupled plasma mass spectrometry (LA-ICP-MS) [8] as well as by structure refinement. The variation of the Al/Ga ratio for one crystal measured on various points by LA-ICP-MS was up to ± 0.02. Overall, there was a satisfactory agreement between the compositions determined by those two methods. Importantly, it was demonstrated that an about 1-μm-thick, inhomogenously substituted (Al,Ga)N capping layer with various Al composition was formed on the surface of the crystals. It was noted that the Al composition of this layer strongly depends on the cooling profile.

7.2 Thermodynamics

The study of p-T-x equilibrium phase diagram is an important pillar of (Al,Ga)N research towards applications and for basic research, particularly for exploring the thermodynamic data of the reaction of formation. Basic studies on the thermodynamics of ternary (Al,Ga)N are rather scarce and this work was aimed at expanding this knowledge and to motivate other researchers.

For the first time, some attempts, described in *Chapter 6* of this work, were made to estimate the standard Gibbs free energy, the enthalpy and entropy of formation of the (Al,Ga)N system on the basis of experimental p-T growth conditions. These calculations were done for temperatures of up to 1800 °C and up to 30 kbar pressure. The standard enthalpy ΔH^0_{298} and entropy ΔS^0_{298} of formation, as a function of Al composition x, slightly decrease with increasing x and their change becomes significant for the region x=0.6. However, the

trend of the values, particularly for the end composition AlN, raises some questions to be discussed in the future.

In essence, knowing the thermodynamic functions allowed us to determine the *p-T* and *x-T* phase diagrams for extended parameter ranges, which is the basis for crystal growth experiments and thermal annealing, and the understanding of interface stability issues. Furthermore, on the phase diagram, for instance in *p-T* space, the equilibrium lines between (Al,Ga)N(s) and Al/Ga(l) + N_2(g) for various Al composition in the crystals were defined. Polycrystalline (Al,Ga)N pellets tend to equilibrate with the crystals at a given pressure and temperature. The Al composition of the precursor pellets changes during experiments and shifts after sufficiently long time towards the composition of the crystals.

7.3 Outlook

So far the experiments have been concentrated on the crystal growth at different *p-T* conditions for the phase diagram studies. However, there is a clear need for experiments which can provide information on – how to grow bigger size crystals. The fact that GaN can be synthesized as plates of a size up 100 mm^2 [9] without internal seeding augurs well for the possible chance to increase the size of (Al,Ga)N crystals. However, it still remains a huge challenge. The limited crystal size in our study seems to be a result of kinetically controlled complicated process. The experiments done with different dwell time showed that even sufficiently long dwell time (10 days) almost does not affect the crystal size. The reaction between liquid Ga and the graphite crucible at higher temperature (T~>1600 °C) was observed which may be taken as possible limiting-size reason, since the Ga melt is filled up with a graphite. Thus, one promising way may be the search of the suitable crucible materials which do not contaminate the crystals and do not cause the uncontrolled secondary reactions. For instance, pyrolytic BN or TaC are promising candidates. They are compatible with (Al,Ga)N growth temperatures (TaC is successfully used in AlN bulk crystal growth [10]) and characterized by low oxygen impurity.

A series of experiments should be also performed in order to address the apparent difference between the values of ΔH^0_{298} for AlN measured by various independent methods and the aforementioned trend suggested by our thermodynamic studies. In any case, the region for $x \geq 0.86$ is of particular interest and further studies are desirable.

Alternatively, the (Al,Ga)N synthesis can be performed also in a double atmosphere autoclave (DAA), available in our lab. Our experiments showed that the (Al,Ga)N crystals can be also grown at lower pressure and temperature conditions, for instance at 1 kbar and 1550 °C, which are technically feasible for DAA. This system can be used up to 3 kbar and, more importantly, allows works with much larger crucible size (up to 10-15 cm^3) than ones used in HPSG.

The (Al,Ga)N single crystals form also the basis for extended investigations of optical and electrical properties. However, in many cases it required larger crystals. Preliminary studies [11] on the optical bandgap of $Al_{0.86}Ga_{0.14}N$ crystals (on our largest crystals) using femtosecond pump-probe spectrometry technique based on two photon absorption autocorrelation measurements were already performed and large crystals of various Al content are necessary for the further instigation of the optical bandgap and its evolution with Al content as well as time-resolved dynamics of conduction electrons in (Al,Ga)N.

As mentioned in *Chapter 5*, more should be learned about the defects in the crystals and their relation to growth parameters, crystal morphology etc. Many well-known techniques can be applied. In particular, positron annihilation measurements (PAS) will contribute to the knowledge about the nature and charge of defects, even for small-sized defects at low concentration, or PL spectroscopy measurements will provide information about deep impurity transitions.

Finally, besides an obvious advantage of the measurements of the physical properties of the compositionally homogeneous and unstrained (Al,Ga)N compound , the understanding of the crystal growth of ternary (Al,Ga)N, in a gas autoclave, is a novel and useful knowledge that can be also explored for the growth of other ternary compounds.

Alternatively, the HPSG technique can be used for the growth of ternary (In,Ga)N compounds. Adding even a small amount of In to GaN leads to an enhancement of light emission in LEDs and Laser diodes. This phenomenon relates an enhancement effect is of particular interest of many research groups and measurements on the strain-free (In,Ga)N bulk crystals may substantial contribute to interpretation of such mechanism.

References:

[1] S. Porowski, I. Grzegory, M. Bockowski, B. Lucznik and P. Perlin, „High Pressure GaN crystals on HVPE GaN seeds as substrates for laser diodes", 6th International Workshop on Bulk Nitride Semiconductors", August 23-28 (2009), Galindia, Poland.

[2] H. Saitoh, W. Utsumi, H. Kaneko, and K. Aoki, Jpn. J. Appl. Phys. **43** (2004) L981-983.

[3] P. Geiser, J. Jun, S. M. Kazakov, P. Wägli, L. Klemm, J. Karpinski, and B. Batlogg, Appl. Phys. Lett. **86** (2005) 081908.

[4] P. Geiser, Dissertation №16126, ETH Zurich (2005).

[5] I. Grzegory, J. Phys. Condens. Matter. **14** (2002) 11055-11067.

[6] T. Hashimoto, E. Letts, M. Ikari, and Y. Nojima, „Improvement of crystal quality in ammonothermal growth of bulk GaN", 6th International Workshop on Bulk Nitride Semiconductors", August 23-28 (2009), Galindia, Poland.

[7] J. Karpinski, J. Jun, and S. Porowski, J. Cryst. Growth **66** (1984) 1-10.

[8] B. Hattendorf, Ch. Latkoczy, D. Günther, Analytical Chemistry (A-pages), **75** (2003) 341A-347.

[9] S. Krukowski, C. Skierbiszewki, P. Perlin, M. Leszczyński, M. Bockowski, S. Porowski, Acta Physica Polonia B **37** (2006) 1265-1311.

[10] R. Schlesser, R. Dalmau, D. Zhuang, R. Collazo, Z. Sitar, J. Cryst. Growth **281** (2005) 75-80.

[11] J. Zhang, A. Belousov, J. Karpinski, B. Batlogg, R. Sobolewski, Femtosecond optical spectroscopy of high-pressure grown $Al_xGa_{1-x}N$ single crystals, EDISON16 Proceedings, Monpellier (2009), to be published in Journal of Physics.

Acknowledgements

Many people have contributed to this thesis, both, by making this an unforgettable chapter of my life and, of course, in many cases scientifically, for which I hereby would like to thank all of them.

First and foremost, I would like to thank my advisors Bertram Batlogg and Janusz Karpinski, who encouraged me to grow, personally as well as academically, and shared their great and worthwhile experience. Thank you both, Janusz, for your continuing guidance, support and teaching on the crystal growth at high pressure and Bertram, for advising, sharing a subtle knowledge and understanding in writing papers and substantial support in the final stage of the work. Cordial thank to my co-examiner Dr. hab. Isabella Grzegory for the time and effort it takes to referee my PhD thesis and her interest in this work.

I also would like to express my deepest gratitude to Jan Jun, whom I particularly indebt and who enormously contributed experimentally to make this thesis possible.

Furthermore, I am extremely thankful to my collaborators from the "High Pressure Materials Synthesis Group", namely Nikolai Zhigadlo for his continuing help, encouraging and support during this work, Sergiy Katrych for X-ray measurements on crystals (*Chapter 4 and 5*), Zbigniew Bukowski for fruitful discussions and exchanging of experiences. Moreover, I would like to express my gratitude to our guests and friends, Krzysztof Rogacki, Roman Puzniak and Andrey Mironov, who always teach me and helped to satisfy my greed for knowledge and experience.

A very special thanks to Jie Zhang and Roman Sobolewski (Laboratory for Laser Energetics, University of Rochester) for their fruitful collaboration, hospitality in Rochester and performing the optical bandgap studies using a femtosecond, pump-probe spectrometry technique discussed in *Chapter 4*. Furthermore, I would like to thank Kathrin Hametner and Prof. Detlef Günther (Laboratory of Inorganic Chemistry, ETH Zurich) for the chemical characterisations of my crystals using laser ablation inductively coupled plasma mass spectrometry (*Chapter 4* and *5*). For the EDX measurements I am tremendously grateful to Peter Wägli (Electron Microscopy ETH Zurich). The mechanical workshop staff of D-Phys, Andreas Stuker, Bernhard Morath, Willy Staubli, Roy Hunziker, Kurt Jacob, Andreas Mathys, Marcel Wachter are gratefully acknowledged for their excellent work and technical support as well as Pierrot Dekumbis, Pierre Cohn for reliable and in time gas supply.

List of publications

[1]   Andrey Belousov, S. Katrych, J. Jun, J. Zhang, D. Günther, R. Sobolewski, J. Karpinski, and B. Batlogg, J. Cryst. Growth, **311** (2009) 3971-3974.

[2]   Andrey Belousov, S. Katrych, K. Hametner, D. Günther, J. Karpinski and B. Batlogg, $Al_xGa_{1-x}N$ bulk crystal growth: crystallographic properties and *p-T* phase diagram, (2010) submitted to J. Cryst. Growth.

[3]   Andrey Belousov, J. Karpinski and B. Batlogg, Thermodynamics of the Al-Ga-N_2 system, (2010) submitted to J. Cryst. Growth.

[4]   S. Wu, J. Zwang, A. Belousov, J. Karpinski, R. Sobolewski, Ultra-Long-lived coherent acoustic phonons oscillations in GaN single crystals, Phonons 2007, Journal of Physics: Conference Series **92** (2007) 012021.

[5]   S. Wu, J. Zwang, A. Belousov, J. Karpinski and R. Sobolewski, Dynamics of intervalley transitions and propagation of coherent acoustic phonons in GaN single crystals studied by femtosecond pump-probe spectroscopy, Gallium Nitride Materials and Devices III, ed. by H. Morkoc, C. W. Litton, J.I. Chyi, Y. Nanishi, and E. Yoon, Proc. of SPIE, **6894**, San Jose (2008), 68940K.

[6]   J. Zhang, A. Belousov, J. Karpinski and Roman Sobolewski, Propagation of multiple coherent-acoustic-phonon transients in GaN single crystals, 1st International Symposium on Laser Ultrasonics: Science, Technology and Applications, Montreal, Canada (2008).

[7]   J. Zhang, A. Belousov, S. Katrych, J. Jun, J. Karpinski, B. Batlogg and R. Sobolewski, Femtosecond pump-probe characterization of high-pressure grown $Al_xGa_{1-x}N$ single crystals, Gallium Nitride and Devices IV, edited by H. Morkoc, Proc. of SPIE, Vol. **7216**, San Jose (2009) 721623-1.

[8] J. Zhang, <u>A. Belousov</u>, J. Karpinski, B. Batlogg, R. Sobolewski, Femtosecond optical spectroscopy of high-pressure grown $Al_xGa_{1-x}N$ single crystals, EDISON16 Proceedings, Monpellier (2009), to be published in Journal of Physics.

[9] J. Zhang, <u>A. Belousov</u>, J. Karpinski, B. Batlogg, R. Sobolewski, Femtosecond optical spectroscopy studies of high-pressure-grown $Al_xGa_{1-x}N$ single crystals, in progress, (2010) will be submitted to APL.